NATIONAL ADVISORY COMMITTEE FOR AERONAUTICS

APR 1 1949

REPORT No. 862

AN INVESTIGATION OF A THERMAL ICE-PREVENTION SYSTEM FOR A TWIN-ENGINE TRANSPORT AIRPLANE

DTIC ELECTE SEP 0 6 1995 F

By ALUN R. JONES

LIBRARY OF CONGRESS TO BE RETURNED

DISTRIBUTION STATEMENT A
Approved for public release
Distribution Unlimited

1946

For sale by the Superintendent of Documents, U. S. Government Printing Office, Washington 25, D. C. - - - - Price 25 cents

19950831 113

DTIC QUALITY INSPECTED 5

AERONAUTIC SYMBOLS

1. FUNDAMENTAL AND DERIVED UNITS

	Symbol	Metric		English	
		Unit	Abbreviation	Unit	Abbreviation
Length	l	meter	m	foot (or mile)	ft (or mi)
Time	t	second	s	second (or hour)	sec (or hr)
Force	F	weight of 1 kilogram	kg	weight of 1 pound	lb
Power	P	horsepower (metric)		horsepower	hp
Speed	V	kilometers per hour	kph	miles per hour	mph
		meters per second	mps	feet per second	fps

2. GENERAL SYMBOLS

W Weight$=mg$

g Standard acceleration of gravity$=9.80665$ m/s^2 or 32.1740 ft/sec^2

m Mass$=\frac{W}{g}$

I Moment of inertia$=mk^2$. (Indicate axis of radius of gyration k by proper subscript.)

μ Coefficient of viscosity

ν Kinematic viscosity

ρ Density (mass per unit volume)

Standard density of dry air, 0.12497 kg-m^{-4}-s^2 at 15° C and 760 mm; or 0.002378 lb-ft^{-4} sec^2

Specific weight of "standard" air, 1.2255 kg/m^3 or 0.07651 lb/cu ft

3. AERODYNAMIC SYMBOLS

S Area

S_w Area of wing

G Gap

b Span

c Chord

A Aspect ratio, $\frac{b^2}{S}$

V True air speed

q Dynamic pressure, $\frac{1}{2}\rho V^2$

L Lift, absolute coefficient $C_L=\frac{L}{qS}$

D Drag, absolute coefficient $C_D=\frac{D}{qS}$

D_0 Profile drag, absolute coefficient $C_{D_0}=\frac{D_0}{qS}$

D_i Induced drag, absolute coefficient $C_{D_i}=\frac{D_i}{qS}$

D_p Parasite drag, absolute coefficient $C_{D_p}=\frac{D_p}{qS}$

C Cross-wind force, absolute coefficient $C_C=\frac{C}{qS}$

i_w Angle of setting of wings (relative to thrust line)

i_t Angle of stabilizer setting (relative to thrust line)

Q Resultant moment

Ω Resultant angular velocity

R Reynolds number, $\rho\frac{Vl}{\mu}$ where l is a linear dimension (e.g., for an airfoil of 1.0 ft chord, 100 mph, standard pressure at 15° C, the corresponding Reynolds number is 935,400; or for an airfoil of 1.0 m chord, 100 mps, the corresponding Reynolds number is 6,865,000)

α Angle of attack

ϵ Angle of downwash

α_0 Angle of attack, infinite aspect ratio

α_i Angle of attack, induced

α_a Angle of attack, absolute (measured from zero-lift position)

γ Flight-path angle

REPORT No. 862

AN INVESTIGATION OF A THERMAL ICE-PREVENTION SYSTEM FOR A TWIN-ENGINE TRANSPORT AIRPLANE

By ALUN R. JONES

Ames Aeronautical Laboratory
Moffett Field, Calif.

Accesion For
NTIS CRA&I ☑
DTIC TAB ☐
Unannounced ☐
Justification .....
By .....
Distribution /
Availability Codes
Dist | Avail and / or Special
A-1

National Advisory Committee for Aeronautics

Headquarters, 1500 New Hampshire Avenue NW., Washington 25, D. C.

Created by act of Congress approved March 3, 1915, for the supervision and direction of the scientific study of the problems of flight (U. S. Code, title 49, sec. 241). Its membership was increased to 15 by act approved March 2, 1929. The members are appointed by the President, and serve as such without compensation.

JEROME C. HUNSAKER, Sc. D., Cambridge, Mass., *Chairman*

THEODORE P. WRIGHT, Sc. D., Administrator of Civil Aeronautics, Department of Commerce, *Vice Chairman*.

Hon. WILLIAM A. M. BURDEN, Assistant Secretary of Commerce.

VANNEVAR BUSH, Sc. D., Chairman, Joint Research and Development Board.

EDWARD U. CONDON, PH. D., Director, National Bureau of Standards.

R. M. HAZEN, B. S., Chief Engineer, Allison Division, General Motors Corp.

WILLIAM LITTLEWOOD, M. E., Vice President, Engineering, American Airlines System.

EDWARD M. POWERS, Major General, United States Army, Assistant Chief of Air Staff–4, Army Air Forces, War Department.

ARTHUR W. RADFORD, Vice Admiral, United States Navy, Deputy Chief of Naval Operations (Air), Navy Department.

ARTHUR E. RAYMOND, M. S., Vice President, Engineering, Douglas Aircraft Co.

FRANCIS W. REICHELDERFER, Sc. D., Chief, United States Weather Bureau.

LESLIE C. STEVENS, Rear Admiral, United States Navy, Bureau of Aeronautics, Navy Department.

CARL SPAATZ, General, United States Army, Commanding General, Army Air Forces, War Department.

ALEXANDER WETMORE, Sc. D., Secretary, Smithsonian Institution.

ORVILLE WRIGHT, Sc. D., Dayton, Ohio.

GEORGE W. LEWIS, Sc. D., *Director of Aeronautical Research*

JOHN F. VICTORY, LL.M., Executive Secretary

HENRY J. E. REID, Sc. D., Engineer-in-charge, Langley Memorial Aeronautical Laboratory, Langley Field, Va.

SMITH J. DEFRANCE, B. S., Engineer-in-charge, Ames Aeronautical Laboratory, Moffett Field, Calif.

EDWARD R. SHARP, LL. B., Manager, Aircraft Engine Research Laboratory, Cleveland Airport, Cleveland, Ohio

CARLTON KEMPER, B. S., Executive Engineer, Aircraft Engine Research Laboratory, Cleveland Airport, Cleveland, Ohio

---

TECHNICAL COMMITTEES

AERODYNAMICS
POWER PLANTS FOR AIRCRAFT
AIRCRAFT CONSTRUCTION
OPERATING PROBLEMS
MATERIALS RESEARCH COORDINATION
SELF-PROPELLED GUIDED MISSILES
SURPLUS AIRCRAFT RESEARCH
INDUSTRY CONSULTING COMMITTEE

Coordination of Research Needs of Military and Civil Aviation
Preparation of Research Programs
Allocation of Problems
Prevention of Duplication
Consideration of Inventions

LANGLEY MEMORIAL AERONAUTICAL LABORATORY, Langley Field, Va.

AMES AERONAUTICAL LABORATORY, Moffett Field, Calif.

AIRCRAFT ENGINE RESEARCH LABORATORY, Cleveland Airport, Cleveland, Ohio

Conduct, under unified control, for all agencies, of scientific research on the fundamental problems of flight

OFFICE OF AERONAUTICAL INTELLIGENCE, Washington, D. C.

Collection, classification, compilation, and dissemination of scientific and technical information on aeronautics

REPORT No. 862

AN INVESTIGATION OF A THERMAL ICE-PREVENTION SYSTEM FOR A TWIN-ENGINE TRANSPORT AIRPLANE

By ALUN R. JONES

SUMMARY

Several previously published reports on a comprehensive investigation of a thermal ice-prevention system for a typical twin-engine transport airplane are correlated with some unpublished data to present the entire investigation in one publication. The thermal system investigated was based upon the transfer of heat from the engine exhaust gas to air, which is then caused to flow along the inner surface of any portion of the airplane for which protection is desired. The investigation consisted of (1) the analysis of the heat requirements for ice protection of the wings, empennage, and windshield; (2) the design, fabrication, and installation of the thermal system in the test airplane; (3) performance tests of the system in clear air and in natural icing conditions, at various altitudes and engine operating conditions; and (4) the evaluation of the effects of the system on the airplane cruise performance and the structural integrity of the wings.

For the determination of the thermal performance of the system, venturi meters and thermocouples were installed to measure the heated-air-flow rates throughout the system and the resultant temperature rise of the surfaces to be protected. Flight tests were made in clear air to obtain data for comparison with the design analysis, supplemented by actual performance tests in natural-icing conditions during which both thermal data and observations of the ice-prevention and removal capabilities of the thermal system were recorded.

To determine the effects of the thermal ice-prevention installation on the airplane cruise performance, comparative flight tests were undertaken with the airplane in the original and the revised conditions. The possible deleterious effects of the system on the wing structure were considered to be (1) reduction in the strength of the wing structural material at elevated temperatures, (2) thermal stresses generated by temperature gradients in the wing, and (3) corrosion. The first two effects were evaluated by flight tests in which structure temperatures and stresses were measured. A metallurgical examination of the wing leading edge provided information concerning the third factor, corrosion.

The surface-temperature rises measured in the performance tests of the thermal system were greater than those predicted by the design analysis, indicating the analysis method is conservative but requires refinement. The system provided satisfactory protection in all of the icing conditions encountered which, in some instances, were sufficiently severe to produce ice accretions from 2 to 4 inches thick on unprotected surfaces.

The change in the airplane cruising performance resulting from the installation of the thermal system was about 6 miles per hour indicated airspeed at 10,000 feet, and was considered to be almost entirely caused by the parasite drag of the primary heat exchanger-installations. The maximum structure temperatures recorded during operation of the thermal system indicated that sizable reductions in strength could be expected in an unregulated system. These losses, however, could be reduced to an acceptable value by regulating the system to supply only the surface temperatures required for ice prevention.

The operation of the wing leading-edge thermal system produced thermal stresses which may be negligible for regions aft of the heated leading edge, but should be considered during design for the leading-edge region. The metallurgical examination of the wing leading edge indicated that no corrosive effects were noted which could be attributed to the basic principle of employing free-stream air (heated by an exhaust-gas-to-air heat exchanger) as the heat-transfer medium in an internal circulatory system.

INTRODUCTION

For several years the NACA has been engaged in a research program to investigate the feasibility of utilizing the waste heat of airplane engine exhaust gases for the protection of the airplane from ice accretion. The initial stages of this research were conducted in wind tunnels and in flight, utilizing heated models and simulated icing conditions (references 1, 2, 3, and 4). The results of these tests indicated that the heating requirements for the wings, empennage, and windshield were of a magnitude which one could reasonably expect to extract from the exhaust gases, and that the structure temperatures required would not be excessive. As a result of these encouraging conclusions, the NACA exhaust-heat system was installed in a small transport airplane and in two four-engine bombers and successfully tested in natural-icing conditions (references 5, 6, and 7).

As a continuation of this general research program, the Ames Aeronautical Laboratory has completed a comprehensive investigation of the development of a thermal ice-prevention system for a typical twin-engine transport air-

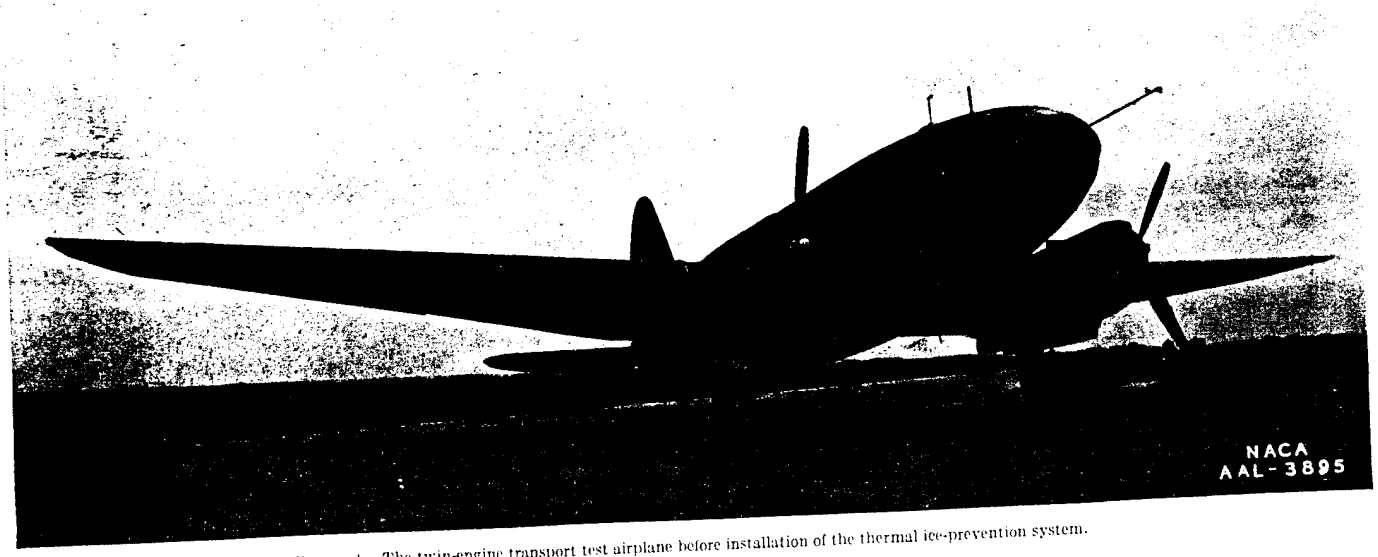

FIGURE 1.—The twin-engine transport test airplane before installation of the thermal ice-prevention system.

plane. (See fig. 1.) The investigation consisted of (1) a design analysis for the thermal system, (2) the design and installation of the system in the airplane, (3) performance tests of the thermal system in clear air and in icing conditions at various airplane operating conditions, (4) observations of the effect of the thermal system on the cruising speed of the airplane, (5) measurement of the thermal stresses in the wing resulting from operation of the system, and (6) a metallurgical examination of the wing interior to determine if any corrosive or high-temperature effects were present.

Seven reports (references 8 to 14, inclusive) have been published on the various phases of the investigation. This report comprises a summary of those references together with some previously unpublished data, and has been prepared to present the entire scope of the research in one publication. The investigation was undertaken in cooperation with the Air Matériel Command of the Army Air Forces, and extended from approximately February 1943 to October 1945. Valuable assistance was provided by the Curtiss-Wright Corp. throughout the project. The flight tests were made at the Ames Aeronautical Laboratory, Moffett Field, Calif., and at the Army Air Forces Ice Research Base, Minneapolis, Minn.

DESIGN ANALYSIS OF THE THERMAL SYSTEM

The basic principle of the NACA exhaust-heat ice-prevention system consists of the removal of heat from the exhaust gas and the transfer of this heat to the surfaces to be protected. The transfer medium employed is free-stream air, which receives heat in heat exchangers located in the exhaust-gas stream and releases the heat to the protected regions while passing between a double-surface arrangement provided to increase the rate of heat transfer.

WING, EMPENNAGE, AND WINDSHIELD HEAT REQUIREMENTS

For the test airplane, the inner surface at the wing and empennage leading edges (fig. 2) extends to 10 percent of the chord, is corrugated to form chordwise air passages, and is separated at the leading edge to allow entrance of the

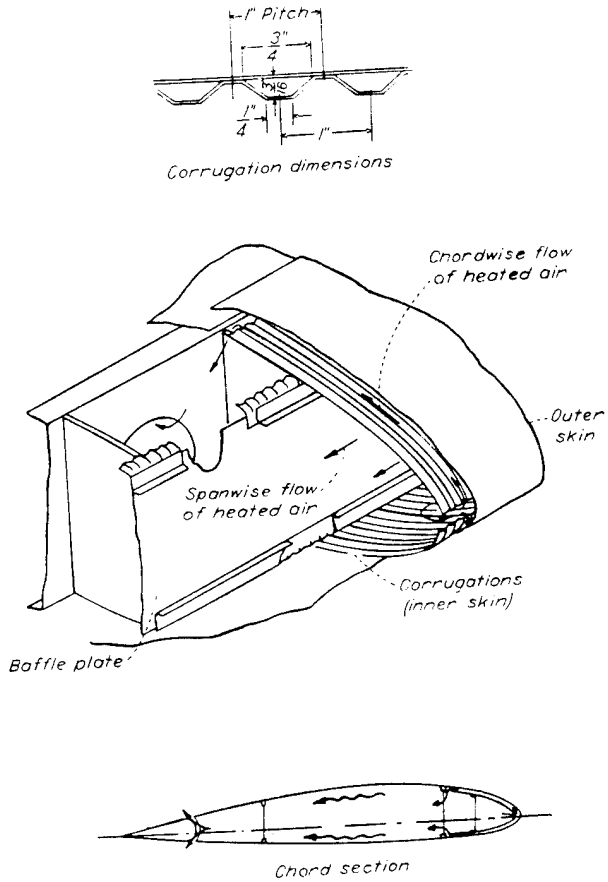

FIGURE 2.—Structural details of a typical wing or empennage thermal ice-prevention system employing heated air.

heated air. Spanwise distribution of the heated air to the corrugation passages is effected by a baffle plate located about 5 percent chord. After passage through the double-surface region, the heated air circulates freely in the wing interior and is discharged at the flap or aileron slot. To provide a double-surface system for the windshield, an inner

transparent panel was installed. The complete design analysis of the thermal system is presented in detail in reference 8, and only the general procedure followed and principal results obtained will be presented here.

Wing and empennage analysis.—The design specification selected for the wing and empennage surfaces, based on past experience, was the maintenance of the airfoil surface forward of the 10-percent-chord point at a temperature of approximately 100° F above free-stream temperature during flight in clear air. The temperature rise just specified was calculated for flight at a pressure altitude of 18,000 feet and at engine power corresponding to maximum range. The free-stream air temperature was taken as 0° F.

Because of structural temperature limitations, a value of 300° F was selected as the maximum temperature of the heated air entering the wing or empennage. In the general case, the design analysis consists of the determination of the external-surface heat-transfer coefficients and the adjustment of the double-surface gap and the heated-air-flow rate to provide the required surface-temperature rise. For this investigation, however, it was expedient to utilize the same corrugated inner-surface dimensions as employed for the airplanes of references 6 and 7, hence the only controllable variable remaining was the heated-air-flow rate. This was not a serious restriction because of the similarity in performance, and hence heating requirements, of the airplanes concerned.

In order to provide basic data for the calculation of the external-surface heat-transfer coefficients, pressure belts (reference 15) were installed over the forward 20 percent of the chord on the wing and empennage surfaces. Transition from laminar to turbulent flow was considered to take place at the theoretical laminar separation point which, based on calculations from the flight pressure distribution data, always occurred well aft of the double-surface region (10 percent chord). The method of reference 16 was used for the computation of the surface-heat-transfer coefficients. This method applies only to laminar flow, and is based on a derived relation between boundary-layer thickness and heat-transfer coefficient. A typical curve of the variation of heat-transfer coefficient with chord position for the wing is presented in figure 3.

The next step was the determination of the spanwise distribution of heated-air-flow rate which would provide the desired surface temperature rise. Since the corrugation passages were of constant cross section, the exact design value of 100° F surface temperature could not be established at all points on the leading edge. The procedure followed was to assume 100° F rise for the surface from 0 to 3 percent chord, calculate the required heated air flow, and then determine the temperature rise aft of 3 percent chord produced by that flow. After the desired air flow for several representative corrugation passages was established, it was found that location of the baffle at 5 percent chord provided a spanwise-flow pressure drop which would cause the air to distribute itself properly in the corrugations. Considerable trial-and-error and compromise was involved and the surface temperatures varied as a consequence. The calculated surface-temperature rises for the double-surface regions of the

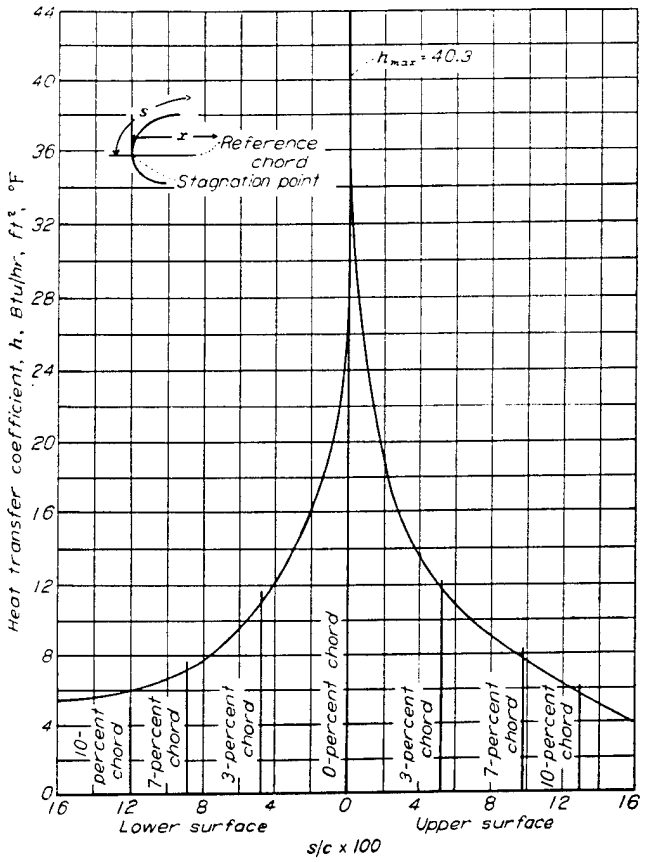

FIGURE 3.—Calculated external heat-transfer coefficient from pressure-belt data for wing station 157.

wing and empennage are presented in figures 4, 5, and 6. The wing-surface-temperature rises were all in reasonable agreement with the design requirement of 100° F. In the case of the empennage, the temperatures from 0 to 3 percent chord were of the specified magnitude, but the values from 3 to 10 percent chord were considerably higher than the design requirement. This effect could have been alleviated by varying the corrugation passage area, but the anticipated improvement did not justify the shop work required.

Windshield analysis.—The determination of the heat required for windshield protection differed from the general procedure used for the airfoil surfaces because no data were available for the calculation of the surface-heat-transfer coefficient. The method of reference 17 was used, which is based on the selection of a heat flow through the windshield outer panel considered satisfactory for ice protection. This specified heat flow was taken as 1,000 Btu per hour per square foot, with the outer-surface temperature assumed to be 50° F, as recommended in reference 17.

The heated air for the windshield was supplied from a secondary exchanger and discharged into the cockpit, for heating purposes, after passing through the windshield gap. The secondary exchanger was required in order to avoid the possible danger of carbon monoxide in the primary air from the exhaust-heat gas exchangers being discharged into the cockpit.

Calculations, using the charts of reference 17, indicated that no practical double-panel design which would give the

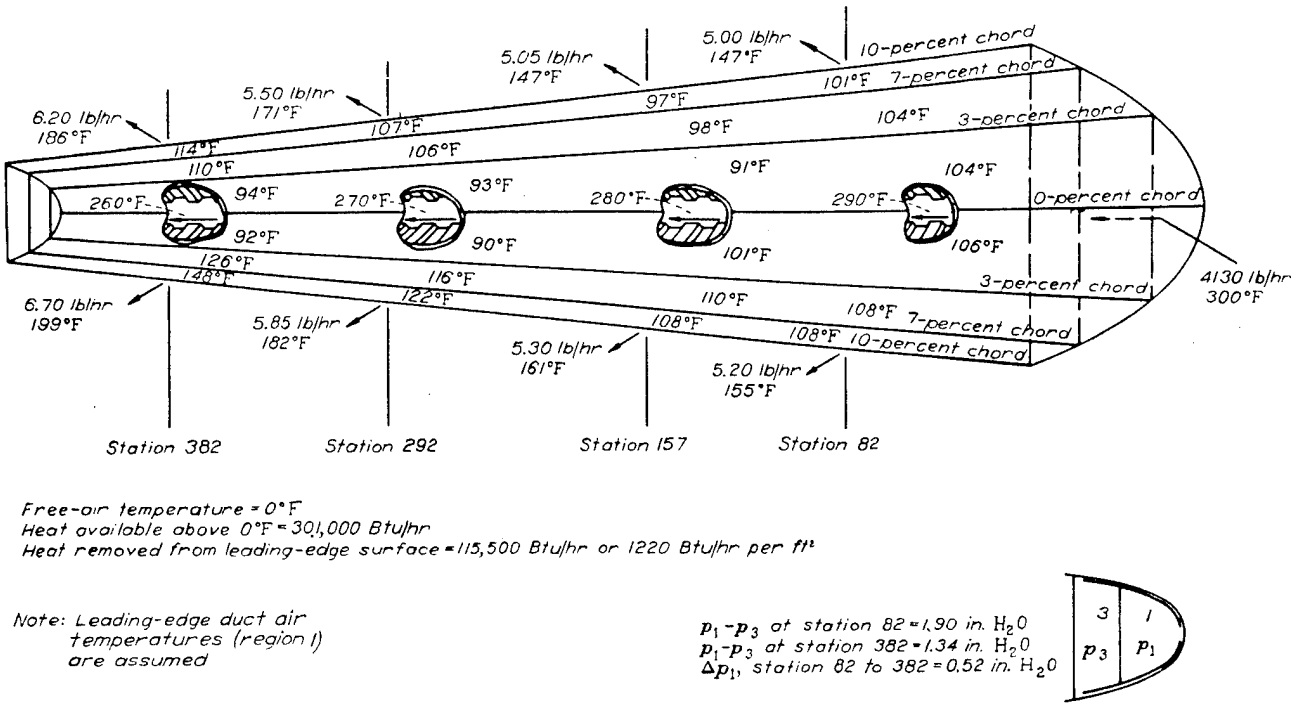

FIGURE 4.—Calculated heat and air-flows and leading-edge skin temperature rises for the wing thermal ice-prevention system.

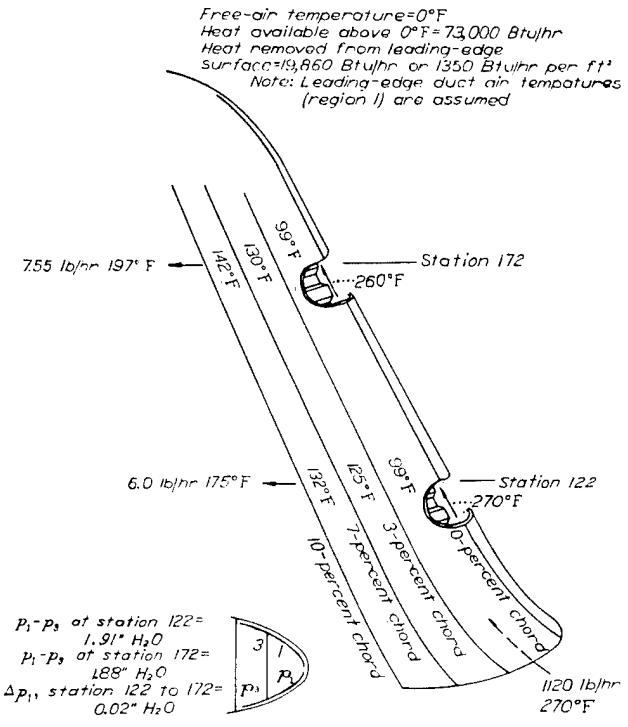

FIGURE 5.—Calculated heat and air-flows and leading-edge temperature rises for the vertical fin thermal ice-prevention system.

required heat flow was possible with the heat available from the secondary exchanger. The windshield installation finally adopted consisted of (1) the double-panel arrangement which would provide the most heating for the allowable pressure drop through the gap, and (2) a means for discharging the primary air from the secondary exchanger over the outer surface of the windshield. The windshield gap was established as three-sixteenths inch.

EXHAUST GAS-AIR HEAT EXCHANGER DESIGN

Requirements.—The results of the analysis of the wing and empennage heat requirements (figs. 4, 5, and 6) show a design heated air flow of 4,130 pounds per hour for each wing and 6,148 pounds per hour for the empennage. The exhaust-collector installation on the test airplane provided an exhaust stack on each side of the two nacelles. The two outboard stacks were selected to provide wing heat and the two inboard stacks, empennage and windshield heat. The heat requirement for one wing (4,130 lb/hr at a temperature of 300° F, or about 300,000 Btu/hr) was selected as the required output for each of the four exchangers at the design flight condition.

In order to avoid auxiliary air pumps in the thermal ice-prevention system, it was necessary that the design over-all pressure loss of the heated air, from induction in the heat-exchanger scoop to discharge from the wing, be no greater than free-stream dynamic pressure.

At the design conditions of maximum range cruising at 18,000 feet, the indicated airspeed was about 155 miles per hour, or approximately 60-pounds-per-square-foot dynamic pressure. The allowable loss was arbitrarily divided equally between the heat-exchanger installation and the system after the exchangers. The pressure loss in the wing and empennage heating systems was computed during the wing and empennage analysis and is discussed in reference 8. The allowable heat-exchanger-installation pressure loss of 30 pounds per square foot was divided into three equal parts of 10 pounds per square foot each for the inlet header, exchanger core,[1] and outlet-header losses.

[1] The exchanger core is the portion of the exchanger installation in which the heat is transferred from the exhaust gas to the air.

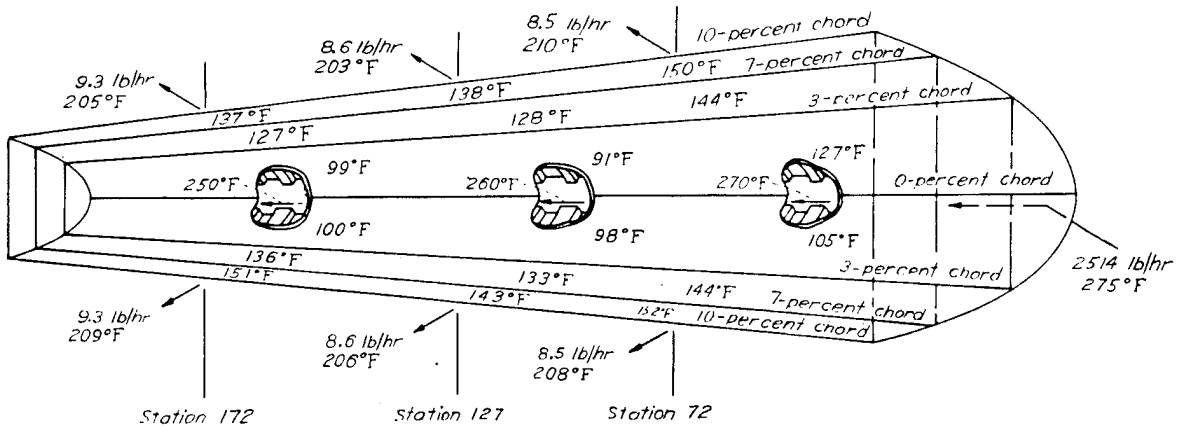

Free-air temperature = 0°F
Heat available above 0°F = 167,000 Btu/hr
Heat removed from leading-edge surface = 32,640 Btu/hr or 1730 Btu/hr per ft²

Note: Leading-edge duct air temperatures (region 1) are assumed

$p_1 - p_3$ at station 72 = 2.39 in. H_2O
$p_1 - p_3$ at station 172 = 1.88 in. H_2O
Δp_1, station 72 to 172 = 0.49 in. H_2O

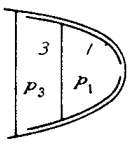

FIGURE 6.—Calculated heat and air-flows and leading-edge skin temperature rises for the horizontal stabilizer thermal ice-prevention system.

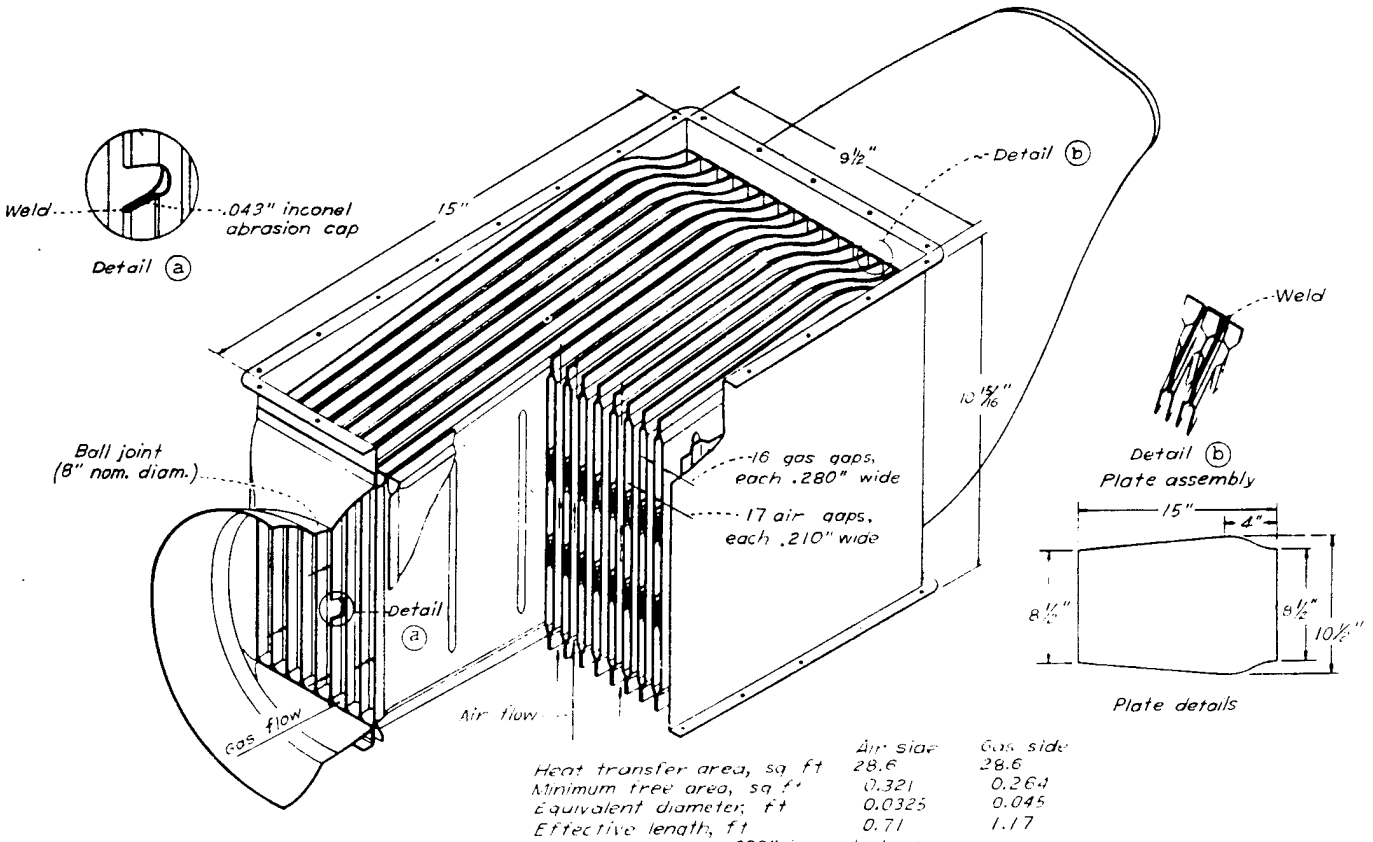

	Air side	Gas side
Heat transfer area, sq ft	28.6	28.6
Minimum free area, sq ft	0.321	0.264
Equivalent diameter, ft	0.0325	0.045
Effective length, ft	0.71	1.17
Material	.032" inconel sheet	
Fabrication	Core-overlapping spotwelds Headers-gas welded	
Weight of core	52.5 lb	

FIGURE 7.—Details of primary heat exchangers for the test airplane.

Core design.—Flight tests of several exhaust gas-air heat exchangers at the Ames Aeronautical Laboratory (reference 18) and an extensive laboratory investigation by the University of California (reference 19) indicated several advantages of the flat-plate-type cross-flow exchanger selected for this investigation. These were (1) a high ratio of useful to nonuseful pressure loss, (2) ease of design and fabrication, (3) a favorable ratio of heat output to core weight and volume, (4) service life as satisfactory, if not better, than other available types.

The calculations, which were undertaken to establish the size of the exchanges are presented in detail in reference 9, and the final exchanger configuration is shown in figure 7.

Header design.—The fixed location of the heat-exchanger core, and the necessity for maintaining the heated-air outlet outside the nacelle in order to avoid extensive nacelle alterations, restricted to a large extent the choice of inlet and outlet header shape. To these difficulties was added the lack of information on the design of converging and diverging bends. Consequently, the headers were built, rather than designed and the over-all isothermal pressure drop was measured for various air-flow rates supplied by a blower. These pressure losses obtained at approximately constant-temperature, sea-level pressure conditions were extrapolated to the design flight conditions, and the pressure drops for the header configurations were about 4 pounds per square foot for the inlet and 11 pounds per square foot for the outlet. The over-all pressure drop for the exchanger installation would then be approximately 25 pounds per square foot, as compared to the value of 30 allowed for design.

DESCRIPTION OF THE ICE-PREVENTION SYSTEM

The test airplane (Air Forces designation C–46) is a twin-engine low-wing monoplane of the heavy cargo type powered by two Pratt & Whitney Model R–2800–51 engines having a sea-level rating of 2,000 horsepower each. The general

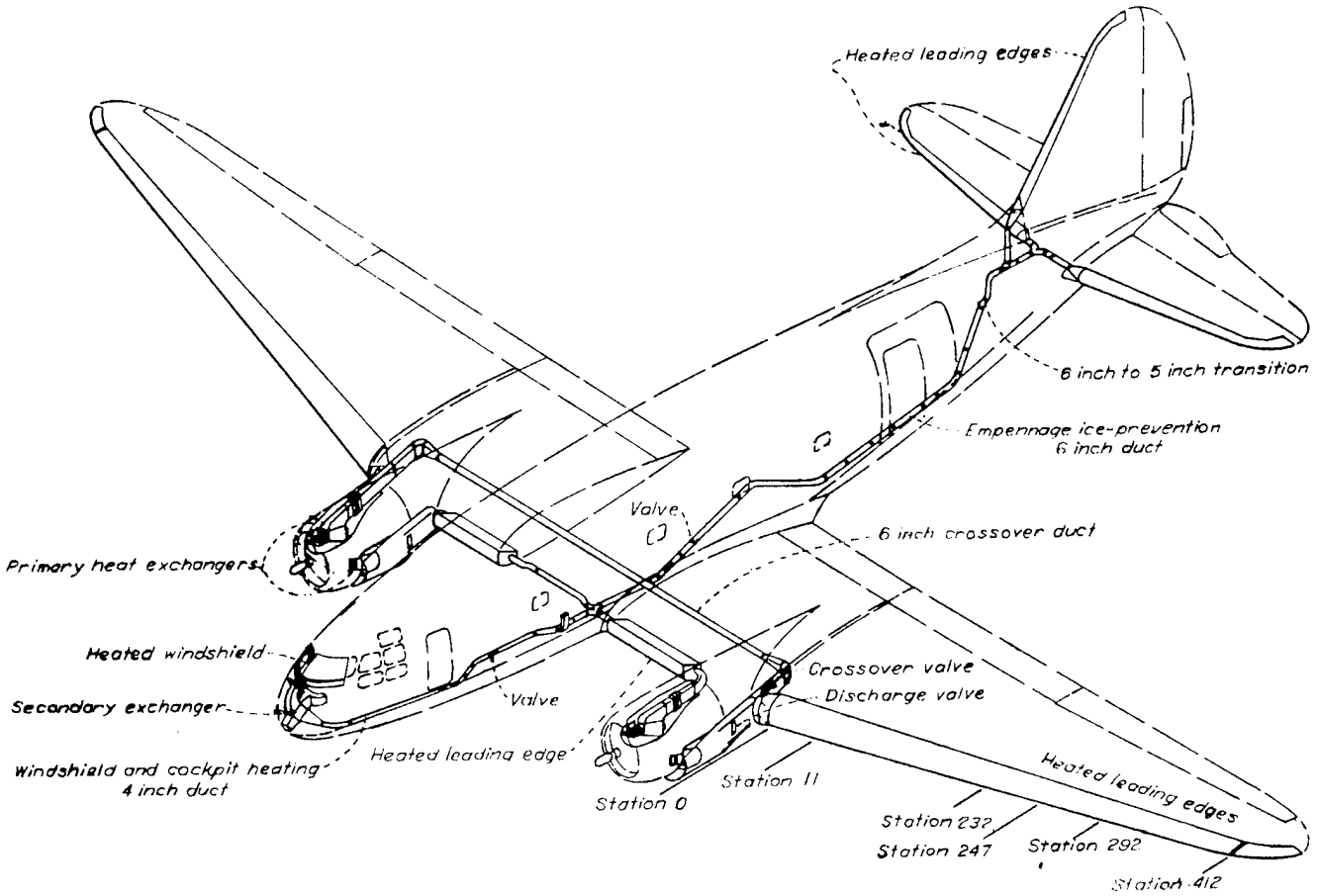

FIGURE 8.—General arrangement of thermal ice-prevention equipment in the test airplane.

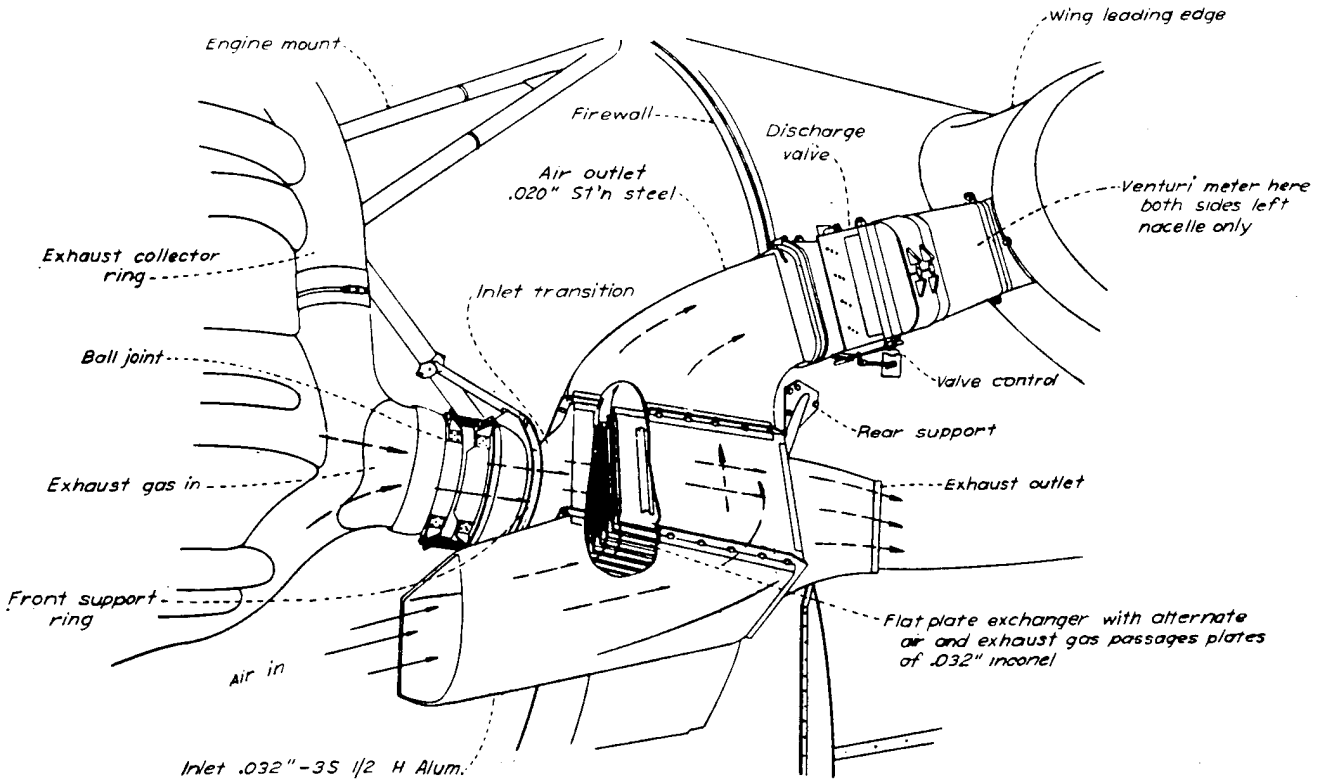

FIGURE 9.—Location of the heat exchangers on the test airplane.

arrangement of the thermal ice-prevention system installed for this investigation is shown in figure 8. A detailed description of the system is presented in reference 10, and only the major items will be discussed in this report.

PRIMARY HEAT EXCHANGERS

The final heat-exchanger design and the installation in the nacelle are presented in figures 7, 9, and 10. The exchangers are of the flat-plate cross-flow type, incorporating alternate exhaust-gas and air passages. Provisions were made in the installation for such factors as expansion of the exchanger longitudinally and relative motion between the exchanger and the exhaust collector. Valves for the purpose of directing the heated air to the ice-prevention system or discharging it to the free stream were installed immediately

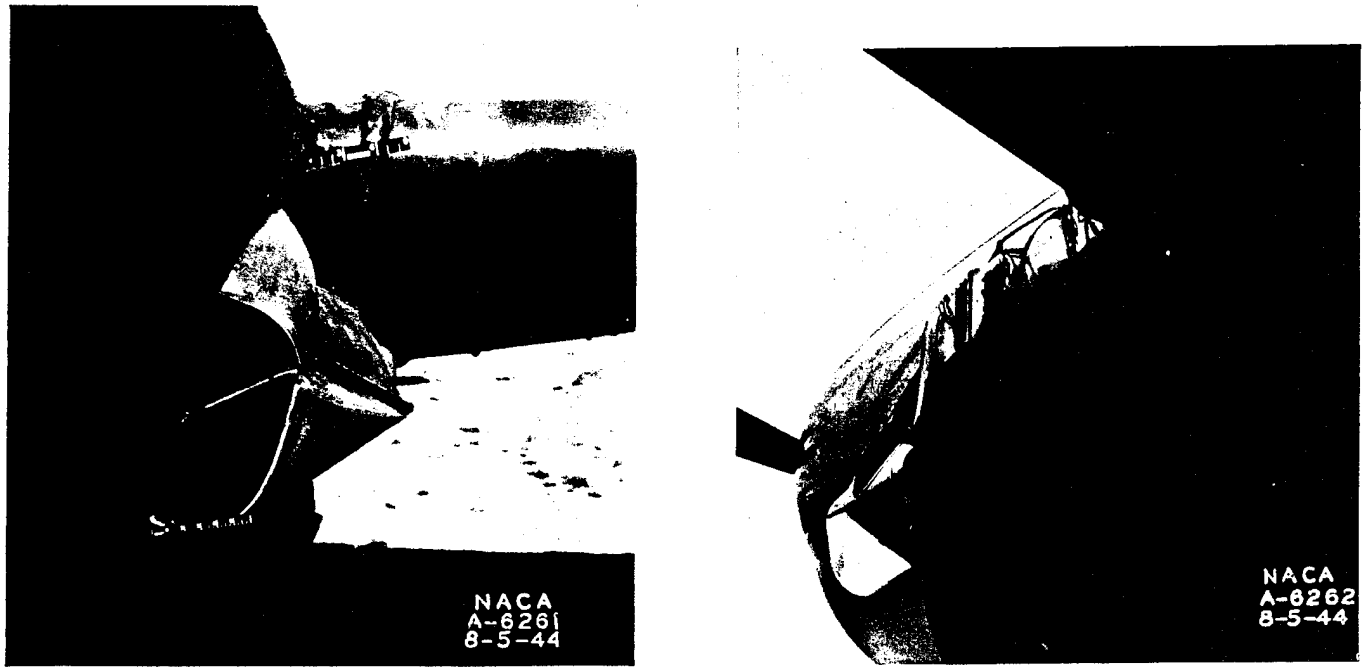

(a) Front view. (b) Rear view.

FIGURE 10.—Typical heat exchanger installation, without fairing, on the test airplane.

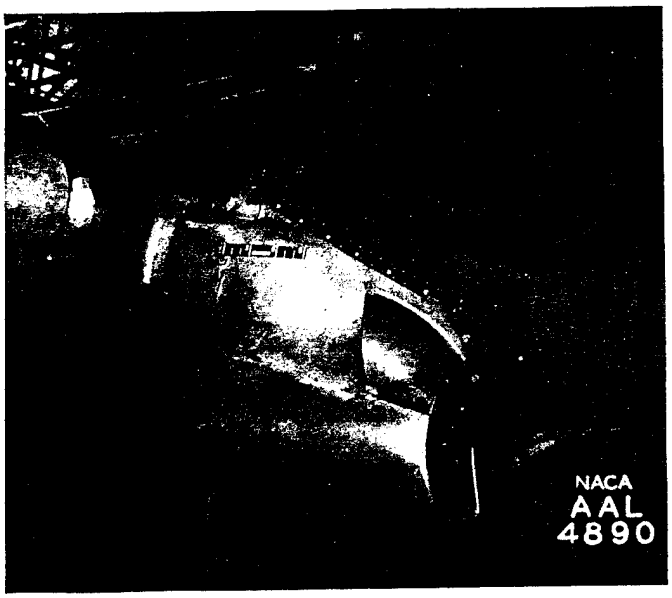

FIGURE 11.—Typical heat exchanger installation with fairing.

after the exchanger air outlets. For the left nacelle, the heated-air ducts from the discharge valves to the leading edge of the wing were formed as venturi meters in order to provide means for evaluating the rate of air flow. The fairing provided for the exchanger installation is shown in figure 11 and incorporated a scoop for cooling the universal ball-joint between the exchanger and the collector.

HEATED-AIR DISTRIBUTION SYSTEM

The heated-air distribution system is shown in figure 8. In the case of the outboard exchangers, the heated air is admitted to the wing outer-panel ice-prevention system at a point just outboard of the nacelles. For single-engine operation of either engine, the heated air can be divided between the right and the left wing outer-panel systems by operation of crossover valves located as shown in figure 8. The heated air from the inboard exchangers passes through the leading edge of the inboard panels in 6-inch-diameter ducts to a common junction on the left side of the fuselage. A portion of the air is diverted from the ducts in the inboard panels to supply the inboard-panel leading-edge ice-prevention system. From the junction in the fuselage, the heated air is directed forward through a 4-inch duct to the secondary-exchanger in the airplane nose, and aft through a 6-inch duct to the empennage. These supply ducts were all insulated with asbestos paper and a rock-wool-type covering. Several valves, usually of the butterfly type, were located throughout the heated-air supply system in order to control the distribution of the air flow.

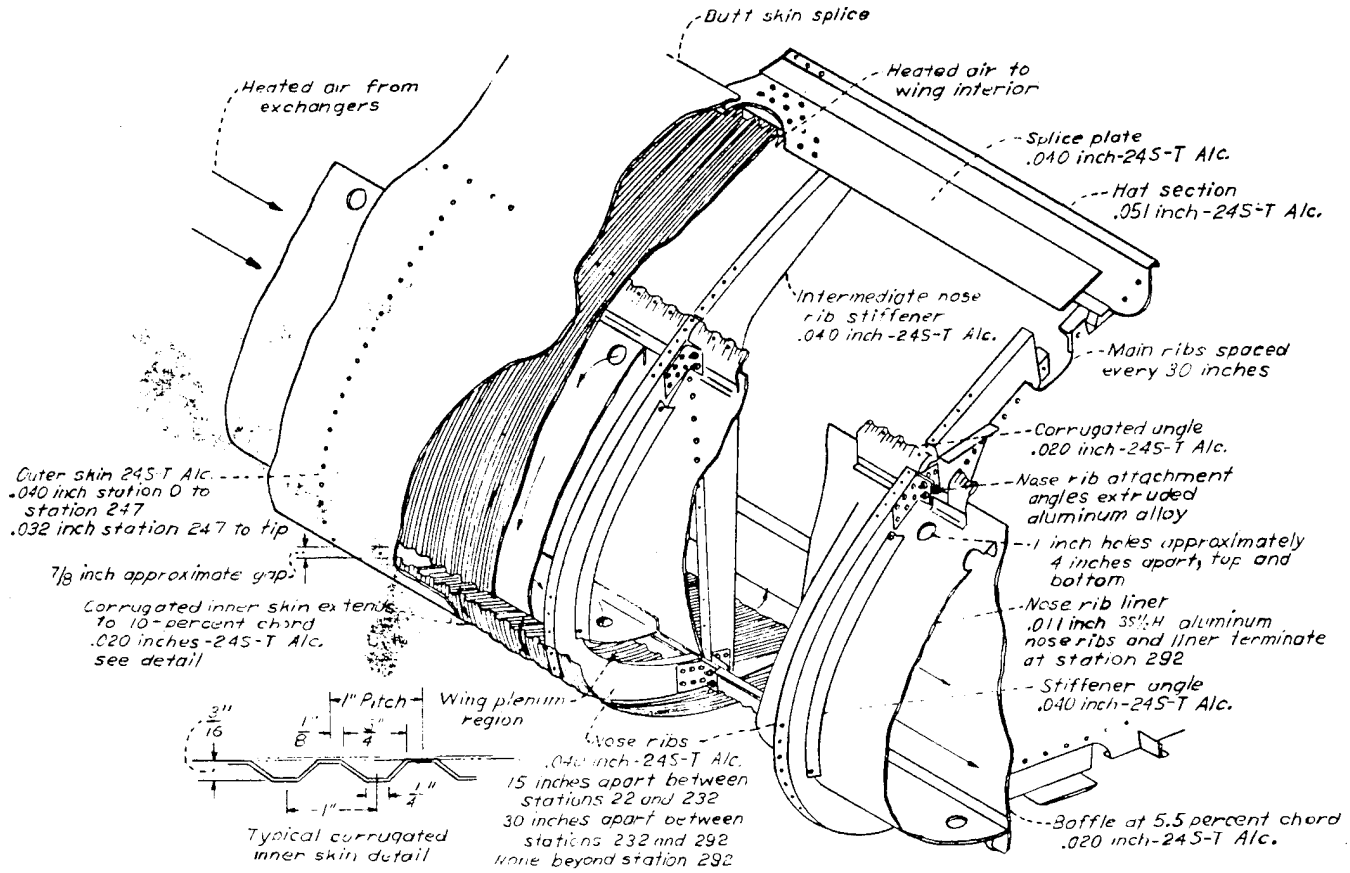

FIGURE 12.—Typical wing outer-panel leading-edge section as revised for thermal ice prevention.

WINGS

A typical section of the wing outer-panel leading edge as revised for thermal ice-prevention is shown in figure 12. The construction is basically the same as that presented in the analysis section (fig. 2) with the exceptions that the nose ribs are shown and a nose rib liner has been added. This liner was found to be required in order to reduce the pressure drop in the spanwise distribution duct caused by the nose ribs. The corrugated inner skin extends to the 10-percent-chord point and the heated air enters the chordwise passages through a gap at the leading edge between the upper and lower segments of the inner skin. After leaving the corrugation passages, the heated air circulates throughout the wing interior, passing through reinforced holes in the spar webs, and is discharged through the aileron and flap slots. For the wing tips, the type of leading-edge construction is similar to that employed for the outer panel with the exception that the corrugated inner skin was replaced by a dimpled type which was more adaptable to the double-contour forming necessary. In the case of the wing inboard panels, the corrugated inner skin extends in a continuous sheet from 5 percent chord on the wing lower surface to 10 percent chord on the upper surface. The heated air flows from bottom to top around the leading edge.

EMPENNAGE

The general arrangement of the thermal ice-prevention equipment in the empennage is shown in figure 13. Distribution of the heated air is controlled by adjustment of the three butterfly valves shown in the figure. The revisions to the stabilizer and fin leading edges are identical and a typical section is shown in figure 14. The corrugated inner skin extends to 10 percent of the airfoil chord and the corrugation passages are identical in size to those for the wing. After leaving the leading-edge region, the heated air circulates in the stabilizer or fin interior and is discharged at the elevator or rudder slot. The dimpled skin type of construction employed in the wing-tip revisions was also used for the stabilizer and fin tips.

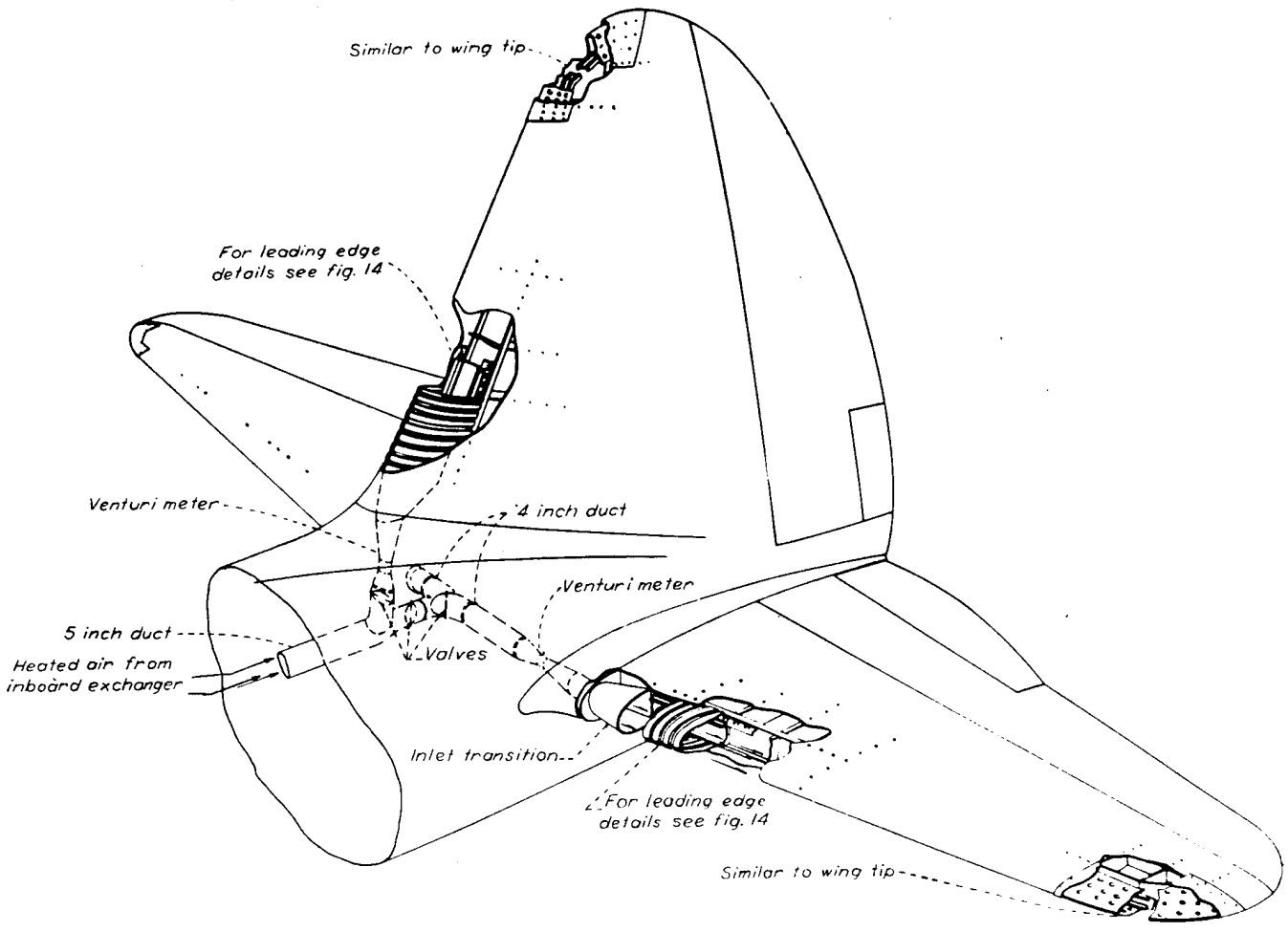

FIGURE 13.—General lay-out of thermal ice-prevention equipment in the empennage of the test airplane.

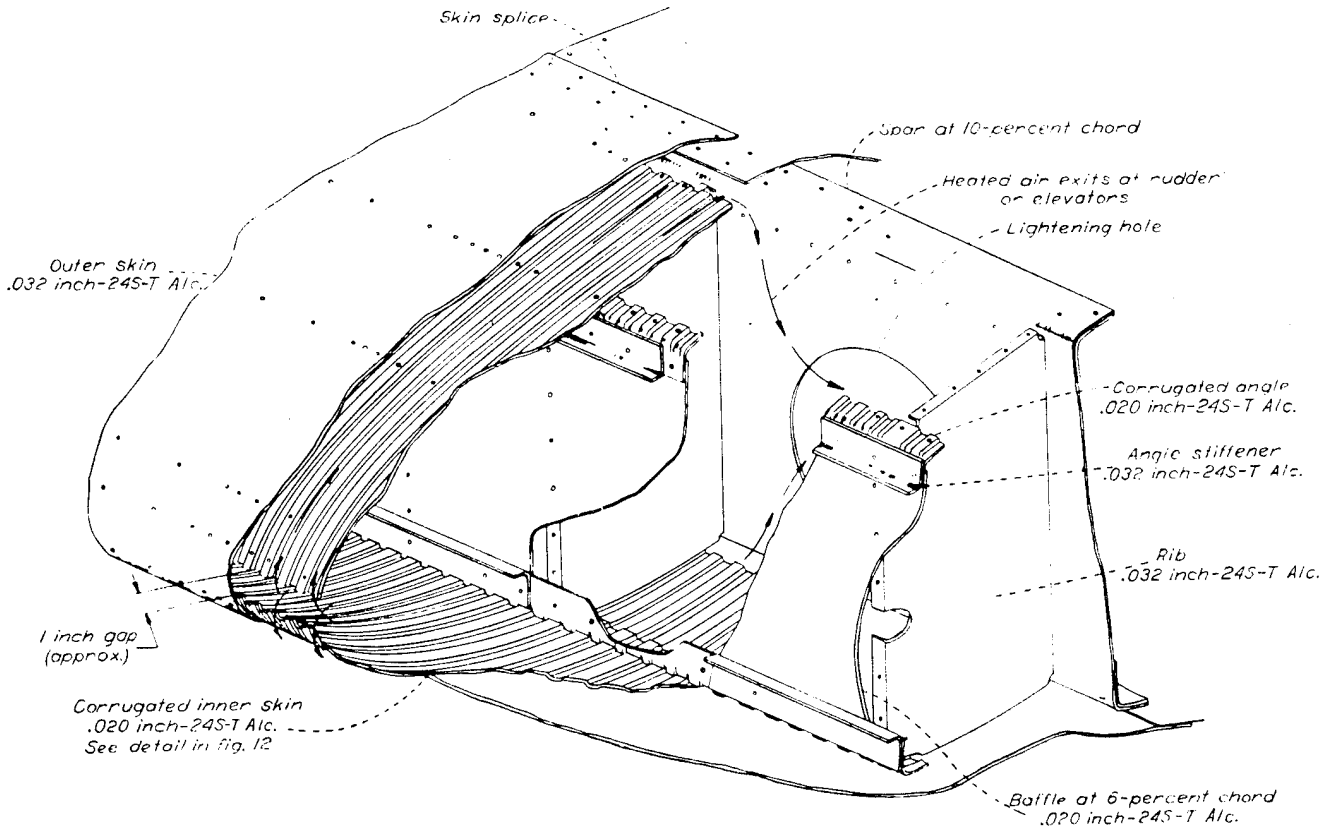

FIGURE 14.—Details of test airplane stabilizer and fin leading edges as revised for thermal ice prevention.

SECONDARY HEAT EXCHANGER AND WINDSHIELD

A secondary heat exchanger was installed in the nose of the airplane to provide carbon-monoxide-free heated air for cockpit and windshield heating as shown in figure 15. The design analysis of the windshield heating requirements indicated that the secondary air would not have sufficient heat capacity for windshield protection and, therefore, provision was made to discharge the primary air for the secondary exchanger over the outer surface of the windshield to provide additional heating. This air was discharged along the lower edge of the windshield through a slot. The secondary air enters the system at the airplane nose and, by means of valves located behind the exchanger, the mixture temperature of the cockpit ventilating air can be controlled. When windshield heating is desired, further manipulation of these same valves deflects the heated secondary air to a blower, which, in turn, boosts the air through the windshield system. Inner removable panels, spaced three-sixteenths inch from the existing outer panels, were installed on both the pilot's and copilot's windshields. Heated air is supplied to the three-sixteenths inch gap at the bottom and is discharged into the cockpit at the top.

CONTROLS

The four discharge valves at the primary exchanger air outlets are operated by electric motors controllable from the cockpit. Various degrees of valve openings can be obtained by intermittent operation of the motor switches, and a cam on the motor automatically opens the circuit at the end of the valve travel. The cross-over valves (fig. 8) and the valves at the secondary heat-exchanger outlet (fig. 15) are adjustable in flight by means of push-pull cable controls. All of the remaining valves of the system are normally adjusted on the ground, although some can be reached in flight if necessary.

PROPELLER PROTECTION

The propellers were provided with a standard alcohol distribution system consisting of slinger rings and grooved rubber shoes cemented to the blades to aid in the removal of ice accretions during the flight tests in natural-icing conditions.

PERFORMANCE TESTS OF THE THERMAL ICE-PREVENTION SYSTEM

In order to establish the thermal performance of the ice-prevention system, flight tests were undertaken in clear air and in natural-icing conditions. The clear air flights included tests at the design conditions, and also at several twin- and single-engine operating conditions at various altitudes. The flights in icing conditions were made at various engine powers, and at altitudes up to 13,000 feet.

In initial flight tests, the quantity of free-stream air entering the secondary exchanger from the opening in the airplane nose was excessive. For all tests reported herein, the nose inlet was sealed and holes were made in the side of the duct forward of the exchanger, thus allowing cabin air to be drawn through the exchanger by the windshield blower.

Clear-air flights were conducted at the Ames Aeronautical Laboratory, Moffett Field, Calif., and clear-air and icing flights at the Air Matériel Command Ice Research Base.

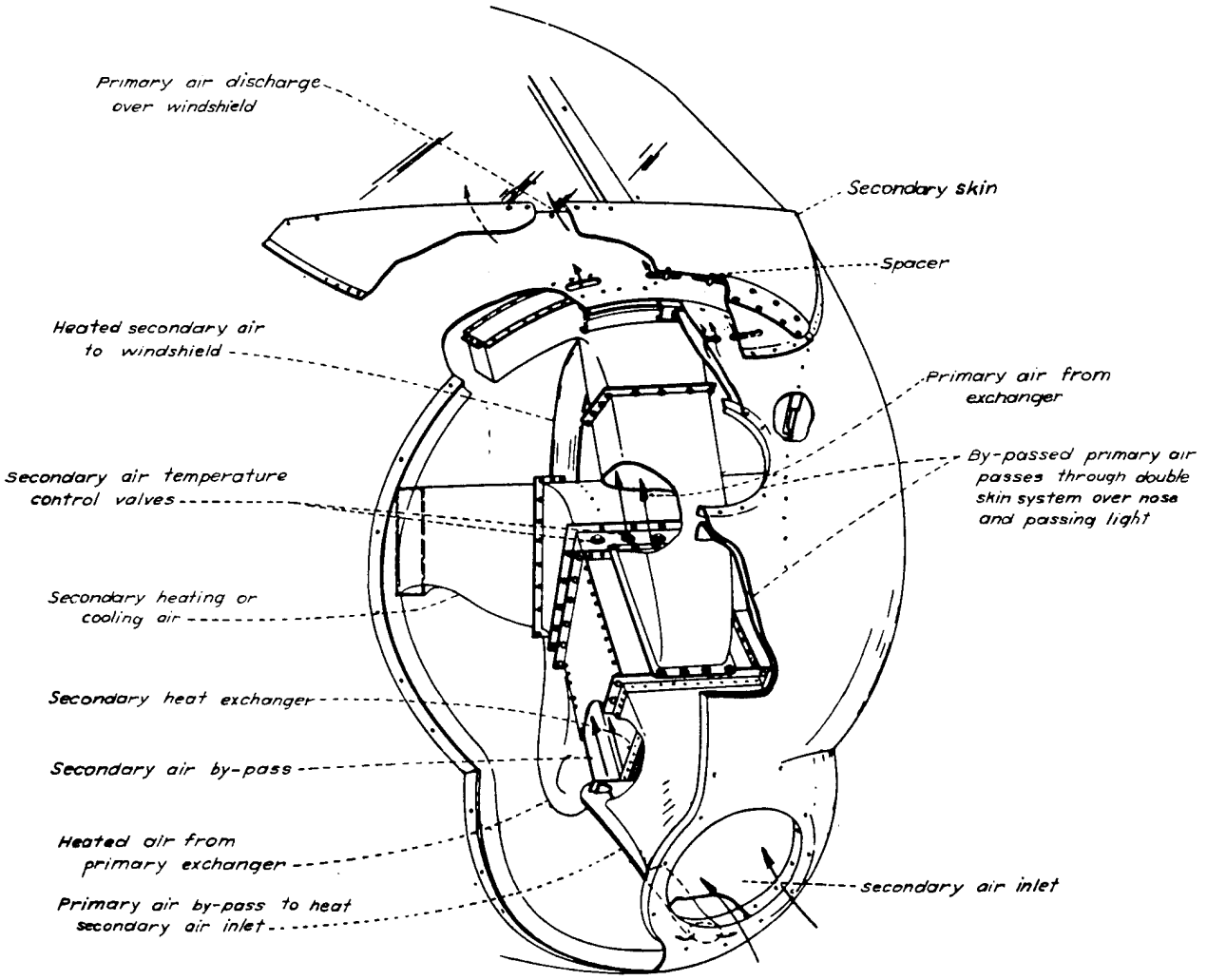

FIGURE 15.—Details of heat-exchanger installed in nose of the airplane to provide secondary heated air for windshield and cockpit heating.

Minneapolis, Minn. During all of these tests the airplane gross weight was about 40,000 pounds.

DESCRIPTION OF INSTRUMENTATION

The principal factors measured, upon which the evaluation of the performance was based, were (1) weight rate of heated air flow to all parts of the system, (2) temperatures of the heated air, (3) temperature rise of components of the airplane exposed to the heated air, and (4) operating condition of the airplane. The air-flow rates were determined by venturi meters installed in the supply ducts and the temperatures were determined with thermocouples. The thermocouples (about 200 in number) were connected to a switching arrangement which provided either manual selection and temperature indication or automatic recording in sequence. The specific locations of all points of pressure and temperature measurement are presented in reference 11. The airplane operating conditions (altitude, airspeed, and engine speed and manifold pressure) were measured with standard aircraft indicating instruments. To reduce the possibility of errors in airspeed indication as a result of ice accumulations on the airspeed mast, the indicators at the copilot's station and the engineer's station in the cabin utilized vents in the fuselage as a source of static pressure. The position error of these vents was determined with a trailing airspeed head. Free-stream air temperature was indicated by a glass-stem thermometer, shielded from the accretion of ice, located outside one of the fuselage windows.

During the analysis of the test results, some question arose concerning the accuracy of the data obtained from the thermocouple installation used to measure surface temperatures. The installation consisted of attaching the thermocouple wires to a small washer which, in turn, was attached to the inner surface of the skin by a rivet through the washer. In the case of the double-surface region, the rivets attaching the inner, corrugated skin to the outer skin served to secure the washers. The washer and the flattened end of the rivet provided an obstruction to heated air flowing along

the inner surface, resulting in a local over-heating of the region and temperature values too large.

In order to compare the data from this type of thermocouple with a more delicate but probably more accurate type of installation, eight special thermocouples (hereinafter called surface thermocouples) were installed at wing outer-panel station 159 at 0, 1.5, 3.5, 7, 9, 30, 50, and 85 percent chord on the lower surface and a few flight checks were undertaken. Each installation was placed immediately adjacent to a washer-type thermocouple for comparative purposes. The surface-type thermocouples were made from 0.005-inch-diameter manganin and constantan wires which were butt-welded together and rolled to a flat strip approximately 0.002 inch thick.

The limited tests conducted indicated appreciable differences between the washer- and surface-type-thermocouple readings whenever the internal structural configuration was such as to promote increased surface velocities. Thus, in all flight conditions at full heated air flow, the washer thermocouples forward of the baffle plate indicated temperatures from 20° to 30° F above the surface thermocouples. This increase in temperature was probably the result of installing the nose rib liner, which certainly could be expected to increase the heat transfer from the heated air to the washer thermocouples. The differences between the washer and surface thermocouple temperatures aft of the baffle plate were much less than the values forward of the baffle, and are probably representative of conditions outboard of station 292 where the nose rib liner ceases to exist. The limited comparative data obtained were not considered an adequate basis for correction of all of the surface-temperature data, hence, the values are presented herein as measured, except where noted.

CLEAR AIR TESTS

The thermal performance of the wing and the empennage ice-prevention systems was determined during twin-engine operation in clear air at the following flight conditions:

Flight condition	Approximate pressure altitude (ft)
1. Level flight, engines operated at 1,900 rpm, with—	
(a) Full throttle	25,000 18,000 10,000 14,000 6,000 4,000
(b) 55-percent maximum continuous power	
2. Level flight, engines operated at 2,050 rpm, throttles at about 55-percent maximum continuous power.	4,000 18,000
3. Level flight, engines operated at 2,400 rpm and full throttle	20,000 18,000 25,000 14,000 6,000
4. Climb at 400 feet per minute, 2,050 rpm, throttle for normal climb	4,000 10,000 6,000 18,000
5. Climb at approximately 130 mph, engines operated at 40 in. Hg manifold pressure and 2,400 rpm (rated power climb)	15,000 10,000 5,000
6. Descent at 400 feet per minute, 2,050 rpm, throttle for normal descent.	18,000 10,000 14,000 6,000 4,000

In addition, performance data were obtained during single-engine operation at the following conditions:

Flight condition	Approximate pressure altitude (ft)
7. Approximately 115 mph indicated airspeed, single engine operated at maximum continuous power, flight attitude adjusted to give desired indicated airspeed	18,000 [1] 13,000 14,000 10,000 5,000
8. Descent at about 400 feet per minute and approximately 140 mph indicated airspeed, single engine operated at 1,900 rpm, manifold pressure as required	18,000 10,000 6,000
9. Level flight at approximately 130 mph, single engine operating at 2,400 rpm, manifold pressure as required	10,000 5,000
10. Descent at approximately 130 mph indicated airspeed, single engine operated at 30 in. Hg manifold pressure and 1,900 rpm	10,000

[1] Single-engine ceiling.

The single-engine tests were conducted at all of the foregoing conditions with the right propeller feathered, and were repeated at all these conditions except No. 7, with the left propeller feathered. For the tests with the left propeller feathered, the venturi meter in the crossover duct was reversed in order to measure the heated airflow rates from the right outboard heat exchanger to the left-wing outer panel.

ICING TESTS

Flights were made in natural icing conditions whenever such conditions were available during the period from January 10 to April 1, 1944, in a 500-mile radius area surrounding Minneapolis, Minn. Flight data were taken at the 1,900 rpm cruise condition (condition 1 (b) of clear air tests) and, to a limited extent, at the maximum-range-cruise condition. Tests were made both at full heat capacity for the system and at reduced heat air-flow rates. Data were taken when conditions were of sufficient extent and intensity to obtain a complete set of readings and observations.

The extent to which frost was removed from the heated surfaces when the airplane was at rest on the ground was observed. The extent to which ice was removed during the take-off operation was also investigated. For these tests, artificial icing conditions which simulated a freezing rain were provided by the use of a water spray. The ice was applied in chordwise strips one-sixteenth inch thick and 2 feet wide to the wing outer panels at station 159. The strips covered the entire chord. The tests were conducted on an overcast day to reduce the solar radiation effects.

RESULTS OF THE CLEAR-AIR TESTS

The performance of the thermal ice-prevention system in clear air is presented in tables I and II. Table I presents the test results for the twin-engine conditions, and table II presents the single-engine results. These tables present the basic performance of the thermal system in terms of calculated values of heat flow based on recorded temperatures and air-flow rates. Further data can be found in reference 11.

TABLE I.—THERMAL PERFORMANCE OF THE WING AND THE EMPENNAGE ICE-PREVENTION SYSTEMS DURING TWIN-ENGINE OPERATION IN CLEAR AIR

PART 1.—OPERATING CONDITIONS

Flight condition (see text)	Flight No.	Run No.	Pressure altitude (ft)	Correct indicated airspeed (mph)	Ambient air temp. (° F)	Engine operating conditions			Airplane attitude
						Manifold pressure (in. of Hg)	Rpm	Blower	
1 (a)	70	4	24,700	133	−17	22	1,900	High	Level
1 (b)	22	12	3,900	187	36	31	1,900	Low	Level
	22	8	6,000	184	30	31	1,900	Low	
	37	1	13,760	152	8	31	1,900	Low	
	60	1	10,403	154	10	29.5	1,900	Low	
	61	3	18,000	138	−12	30	1,900	High	
2	22	13	4,000	187	36	30	2,050	Low	Level
	61	5	18,000	153	−12	29	2,050	High	
3	70	2	20,150	117	−37	25	2,400	High	Level
	70	3	24,800	148	−17	28	2,400	High	
	70	5	18,100	170	13	32	2,400	High	
	70	7	14,300	198	31	43	2,400	High	
	70	9	6,275	212	50	43	2,400	Low	
4	22	16	4,000	169	32	29	2,050	Low	Climb
	22	17	6,150	159	30	28	2,050	Low	
	22	18	10,000	163	23	27	2,050	Low	
	61	1	18,000	133	−12	25	2,050	Low	
5	71	1	5,000	135	41	39.5	2,400	Low	Climb
	71	2	10,000	128	29	40	2,400	High	
	71	3	15,000	126	15	40	2,400	High	
6	22	19	10,000	199	23	29.5	1,900	Low	Descent
	22	20	5,950	203	36	31	1,900	Low	
	22	21	5,960	198	37	31	1,900	Low	
	37	3	14,000	192	8	27	2,050	Low	
	61	2	18,000	179	−11	28	2,050	High	

PART 2.—HEAT DISTRIBUTION

Flight condition (see text)	Flight No.	Run No.	Exchanger heat flows (1,000 Btu/hr)			Heat flows to heated surfaces (1,000 Btu/hr)			
			Left outboard	Left inboard	Right inboard	Left wing outer panel	Right stabilizer	Fin	To secondary exchanger
1 (a)	70	4	284	265	136	284	62	100	75
1 (b)	22	12	392	395	205	392	102	136	95
	22	8	373	396	207	374	102	136	92
	37	1	329	344	140	329	90	113	70
	60	1	356	338	153	356	84	132	85
	61	3	323	263	129	323	69	113	78
2	22	13	391	412	231	391	111	149	102
	61	5	362	322	147	362	73	122	83
3	70	2	273	261	124	273	52	86	72
	70	3	337	346	144	337	72	114	86
	70	5	393	401	156	393	82	132	84
	70	7	446	422	193	446	97	138	104
	70	9	521	445	236	521	127	123	122
4	22	16	388	411	223	388	107	142	100
	22	17	347	364	217	347	103	137	94
	22	18	350	356	211	350	118	131	98
	61	1	407	332	193	407	88	145	99
5	71	1	399	378	123	399	85	75	94
	71	2	369	348	109	369	79	68	88
	71	3	342	277	102	342	75	62	83
6	22	19	352	356	209	352	102	110	91
	22	20	360	343	240	360	101	138	93
	22	21	362	363	218	362	100	134	90
	37	3	370	352	181	370	79	128	83
	61	2	402	364	178	402	86	140	88

TABLE I.—Concluded

PART 3.—SURFACE HEATING VALUES

Flight condition (see text)	Flight No.	Run No.	Average heat delivered per square foot of double skin leading edge surface (Btu/hr)			Average heat flow through skin surface per square foot of double skin surface (Btu/hr)			Ratio of heat flow through heated skin surface to heat delivered (%)			Average temperature rise of wing outer panel 0% chord (°F)[4]
			Left wing outer panel	Right stabilizer	Vertical fin	Left wing outer panel[1]	Right stabilizer[2]	Vertical fin[3]	Left wing outer panel	Right stabilizer	Vertical fin	
1 (a)	70	4	-------	-------	-------	-------	-------	-------	------	------	------	-------
1 (b)	22	12	3,700	4,750	7,560	1,470	2,270	3,660	40	48	48	120
	22	8	3,540	4,760	7,570	1,330	2,150	3,660	38	45	48	129
	37	1	3,120	4,200	6,280	1,320	1,490	3,090	42	35	49	125
	60	1	3,370	3,940	7,390	1,230	1,760	3,840	36	45	52	143
	61	3	3,060	3,220	6,280	1,130	1,410	3,260	37	44	52	153
2	22	13	3,700	5,170	8,310	1,470	2,300	3,970	40	44	48	124
	61	5	3,430	3,420	6,800	1,240	1,520	3,560	36	44	52	155
3	70	2	2,580	2,420	4,800	1,000	1,000	2,480	39	41	52	195
	70	3	3,190	3,350	6,350	1,250	1,200	3,280	39	36	52	180
	70	5	3,720	3,820	7,350	1,490	1,520	3,900	40	40	53	163
	70	7	4,220	4,520	7,700	1,720	2,020	4,110	41	45	53	152
	70	9	4,960	5,920	6,860	1,940	2,560	3,740	39	43	54	136
4	22	16	3,680	4,990	7,940	1,390	2,220	2,670	38	44	34	137
	22	17	3,290	4,820	7,650	1,300	2,100	2,660	40	44	35	142
	22	18	3,310	5,500	7,320	1,330	2,500	2,670	40	45	37	148
	61	1	3,860	4,080	8,060	1,410	1,720	2,720	37	42	34	150
5	71	1	3,780	3,950	4,180	1,420	1,690	2,220	38	43	53	151
	71	2	3,500	3,680	3,790	1,290	1,540	2,000	37	42	53	167
	71	3	3,240	3,490	3,450	1,200	1,460	1,860	37	42	54	171
6	22	19	3,340	4,750	6,120	1,330	2,120	2,460	40	45	40	120
	22	20	3,420	4,730	7,670	1,410	2,160	2,490	41	46	31	106
	22	21	3,430	4,670	7,490	1,360	2,040	2,350	40	43	31	106
	37	3	3,500	3,680	7,160	1,490	1,630	2,260	43	44	32	125
	61	2	3,810	3,990	7,820	1,110	1,570	2,760	29	39	35	146

[1] Calculated on basis of average temperature drop of the heated air in the corrugations at stations 24, 84, 159, 290, and 380 and the total air-flow rate from the left outboard exchanger.
[2] Calculated on basis of average temperature drop of the heated air in the corrugations at stations 69, 125, and 171 and the total heated-air-flow rate to the right stabilizer.
[3] Calculated on basis of average temperature of the heated air in the corrugations at stations 124 and 170 and the total heated-air-flow rate to the vertical fin.
[4] Average percent chord leading-edge temperatures at stations 24, 84, 159, 290, and 380.

TABLE II.—THERMAL PERFORMANCE OF THE WING ICE-PREVENTION SYSTEM DURING SINGLE ENGINE OPERATION IN CLEAR AIR

PART 1.—OPERATING CONDITIONS

Flight condition (see text)	Flight No.	Run No.	Pressure altitude (ft)	Corrected indicated airspeed (mph)	Manifold pressure (in. Hg)		Rpm		Ambient air °F	Super charger blower setting	Flight altitude
					Left	Right	Left	Right			
7	104	2	18,000	118	35.3	------	2,400	0	23	High	Descent.
	104	3	14,000	117	39.9	------	2,400	0	41	High	Descent.
	104	4	13,000	114	40	------	2,400	0	45	High	Level.
	104	5	10,240	116	40	------	2,400	0	52	High	Climb.
	104	1	5,000	117	40	------	2,400	0	75	Low	Climb.
8	103	1	18,000	137	29.2	------	1,900	0	22	High	400 ft/min descent.
	103	2	10,000	142	23.8	------	1,900	0	50	Low	
	103	3	6,000	140	24.0	------	1,900	0	59	Low	
9	103	4	10,000	128	35.7	------	2,400	0	50	High	Level flight.
	104	8	6,000	131	37.2	------	2,400	0	74	Low	
10	104	6	9,500	130	30	------	1,900	0	57	Low	Descent.
8	105	1	18,000	138	------	28.8	0	1,900	21.5	High	400 ft/min descent.
	105	2	10,000	137	------	30.6	0	1,900	51	High	
	105	3	6,000	138	------	27.1	0	1,900	64	Low	
9	105	6	9,900	127	-----	40.0	0	2,400	55	High	Level flight.
	105	4	6,000	127	------	35.3	0	2,400	65	Low	
10	105	5	10,000	127	------	30.0	0	2,400	51	Low	Descent.

TABLE II—Concluded

PART 2.—HEAT DISTRIBUTION

Flight No.	Run No.	Heat flows, 1,000 Btu/hr			Heat flows per square foot of double skin leading edge surface Btu/hr		Average [1] 6% chord left wing temperature rise
		Left outboard exchanger	To right outer wing	To left outer wing	Right outer wing	Left outer wing	
104	2	283	135	137	1,270	1,290	70
104	3	262	139	107	1,310	1,010	74
104	4	306	144	147	1,360	1,390	79
104	5	314	140	153	1,320	1,440	68
104	1	354	170	169	1,600	1,590	74
103	1	287	135	135	1,270	1,270	77
103	2	298	140	130	1,320	1,310	70
103	3	296	137	141	1,290	1,330	66
103	4	325	152	156	1,430	1,470	78
104	8	357	168	168	1,580	1,580	71
104	6	292	170	105	1,600	990	68
105	1	.....	.....	136	.....	1,290	80.5
105	2	.....	.....	142	.....	1,340	71
105	3	.....	.....	147	.....	1,390	69
105	6	.....	.....	159	.....	1,505	80
105	4	.....	.....	153	.....	1,450	78
105	5	.....	.....	144	.....	1,360	72

[1] Average of 0% chord temperatures at stations 159, 380, and 455.

A comparison of the experimental test results and the design analysis of reference 8 introduces the opportunity for considering the heat-transfer relationships discussed in the analysis (reference 8) and the indications of actual heat-transfer phenomena resulting during the tests. A graphical comparison of experimental and analytical air and skin temperatures above ambient-air temperature is presented for the four wing outer-panel stations analyzed in figures

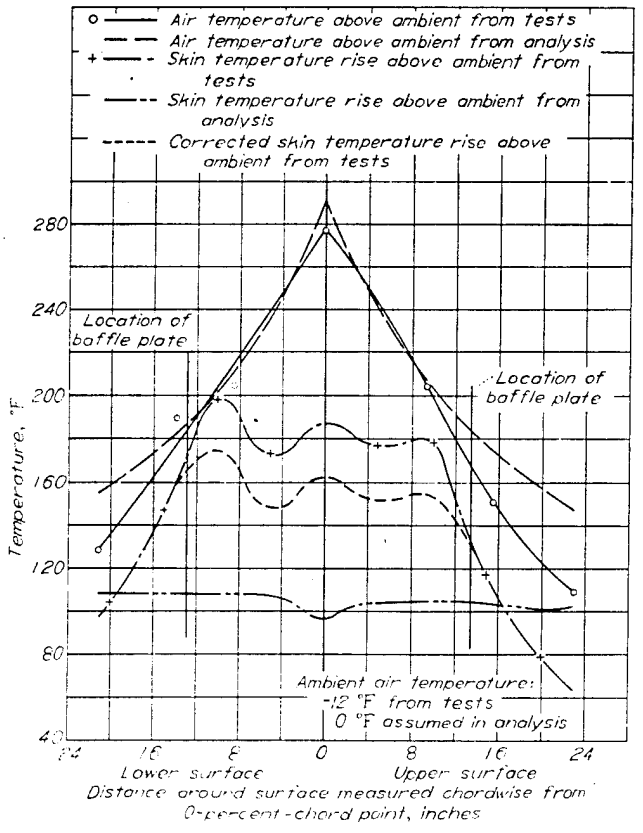

FIGURE 16.—Comparison of analytical and experimental test results of air- and skin-temperature rises above ambient-air temperature for wing station 84.

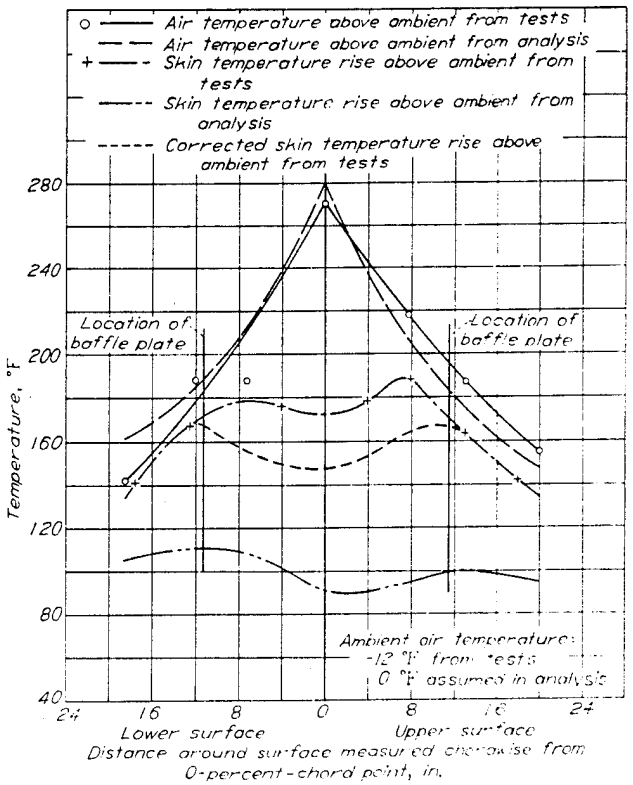

FIGURE 17.—Comparison of analytical and experimental test results of air- and skin-temperature rises above ambient-air temperature for wing station 159.

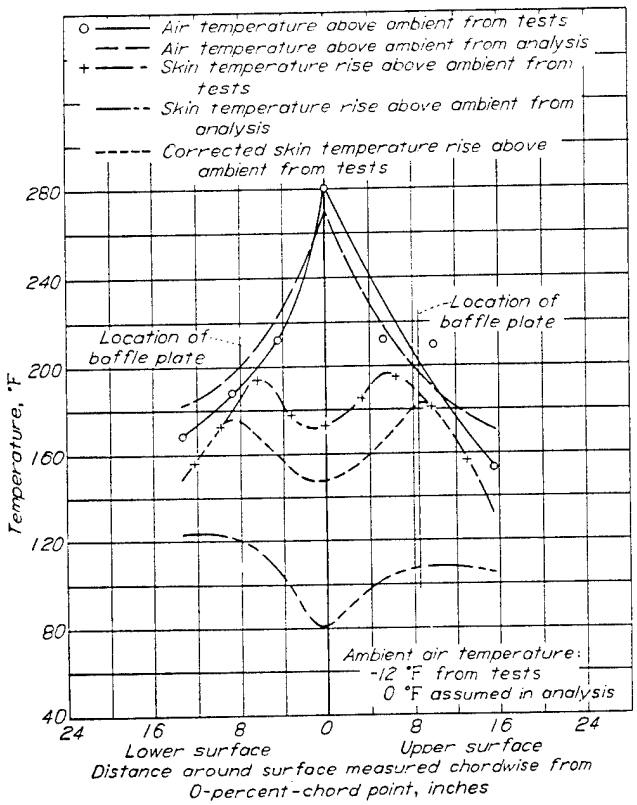

FIGURE 18.—Comparison of analytical and experimental test results of air- and skin-temperature rises above ambient-air temperature for wing station 290.

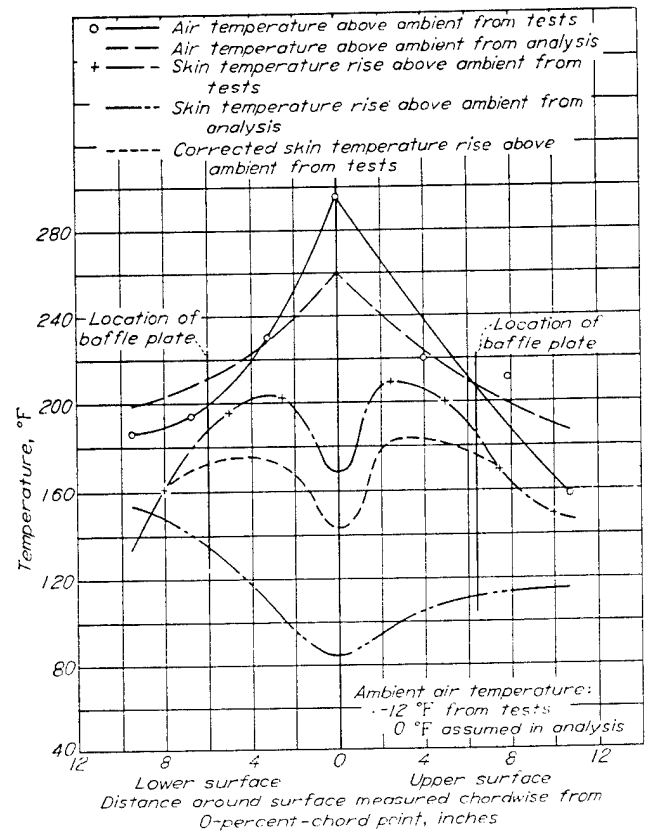

FIGURE 19.—Comparison of analytical and experimental test results of air- and skin temperature rises above ambient-air temperature for wing station 380.

16, 17, 18, and 19. The skin-temperature correction shown in these figures was based on the washer-surface thermocouple tests previously discussed. The test results are taken from data recorded during flight 61, run 5 (table I), which approximated the analytical design conditions. During this run the total heated-air-flow rate was 4,015 pounds per hour to the left-wing outer panel, as compared with an analytic flow rate of 4,130 pounds per hour, and the temperatures of the air entering the corrugations agreed closely with the assumed air temperatures. The air-temperature rise through the exchanger was 369° F (69° F above the temperature rise of the analysis), resulting in a thermal output of 362,000 Btu per hour. This is 20 percent higher than the anticipated value of 300,000 Btu per hour. Nevertheless, the air-temperature change from the exchanger outlet to the corrugation inlets was sufficient to give approximately the corrugation air-inlet temperatures of the analysis at all but one station (380). Furthermore, the temperature of the air entering the corrugation at station 380 was higher than at any other station. These two facts, together with a consideration of the leading-edge construction (fig. 12), indicate that some of the heat was transferred from the air in passing between the nose-rib liner and the corrugations to the corrugation inner surfaces, and ultimately to the outer skin, causing a decrease in heated-air temperature from the leading-edge duct to the corrugation inlets. Since the nose-rib liner ends at station 292, this effect would not prevail at station 380, and the temperature of the air at the corrugation entrance would be substantially the same as in the leading-edge duct at this point.

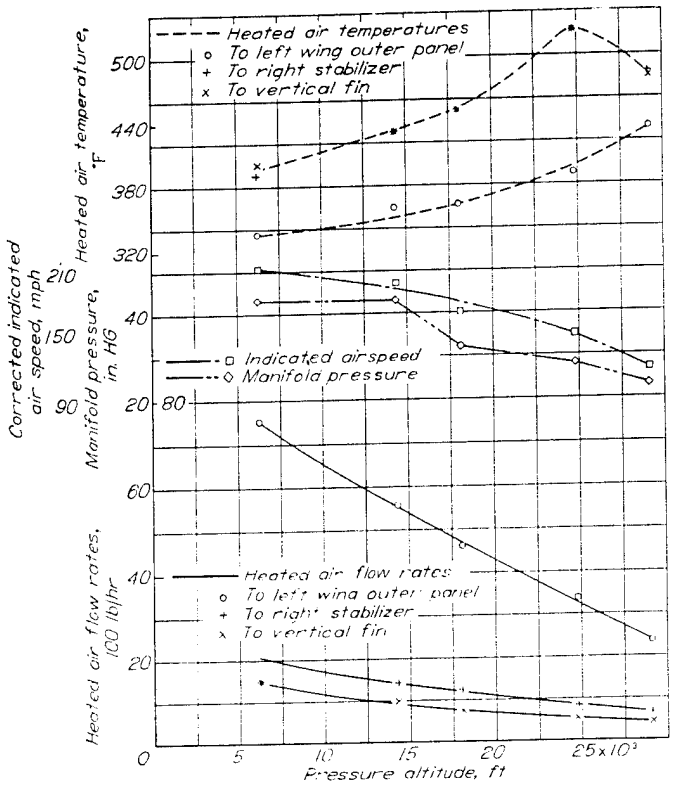

FIGURE 20.—Variation of heated air flow rates and temperatures, indicated airspeed and manifold pressure with pressure altitude test condition 3: Full throttle; twin engine operation.

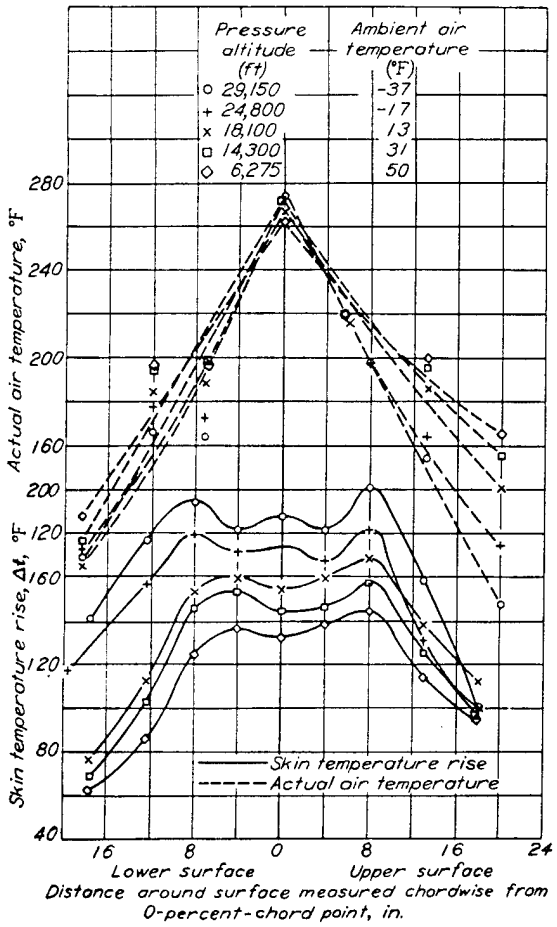

FIGURE 21.—Left wing outer panel station 159 chordwise skin- and air-temperature distributions at various altitudes. Test condition 3: Full throttle; twin engine operation.

The indicated air-temperature drops through the corrugations at stations 84, 159, and 290 recorded during the test flight were in fairly close agreement with the calculated values from the analysis, but the air-temperature change through the corrugations at station 380 was considerably greater than calculated. Thus, at all points the total heat transferred from the heated air to the skin was higher than calculated. It should be realized, then, that the average heat flow through the heated surface, shown in table I and calculated from the air-temperature change through the corrugations, is not the total heat flow through the surface. Further evidence of these facts is exemplified in the results of the skin-temperature indications from the tests. The average corrected skin-temperature rises obtained from the flight-test data were approximately 60° F higher than calculated, indicating that a greater amount of heat had been transferred from the heated air to the skin than had been calculated in the analysis. Conduction and radiation effects from the corrugation walls to the heated surfaces were conservatively neglected in the analysis, and this fact probably accounts in part for the lower calculated skin temperatures.

The rapid decrease in skin-temperature rise shown in figures 16, 17, 18, and 19 in the region immediately aft of the baffle plate is probably a result of two effects. The first and most important effect is the location of the transition region. In the analysis, the point of transition from laminar to turbulent flow was calculated to be well aft of the heated region. This was for an aerodynamically smooth wing. It is indicated from the decrease in skin-temperature rise in the region from about 5 to 10 percent chord that transition actually occurred in this area. Such a condition could conceivably prevail in view of the relatively rough surface and waviness of the wing. The second effect is the location of the baffle plate. Aft of this point, the skin received no heat from the air in the D-duct before entering the corrugations. For this reason, the surface temperature would tend to decrease aft of about 5 percent chord.

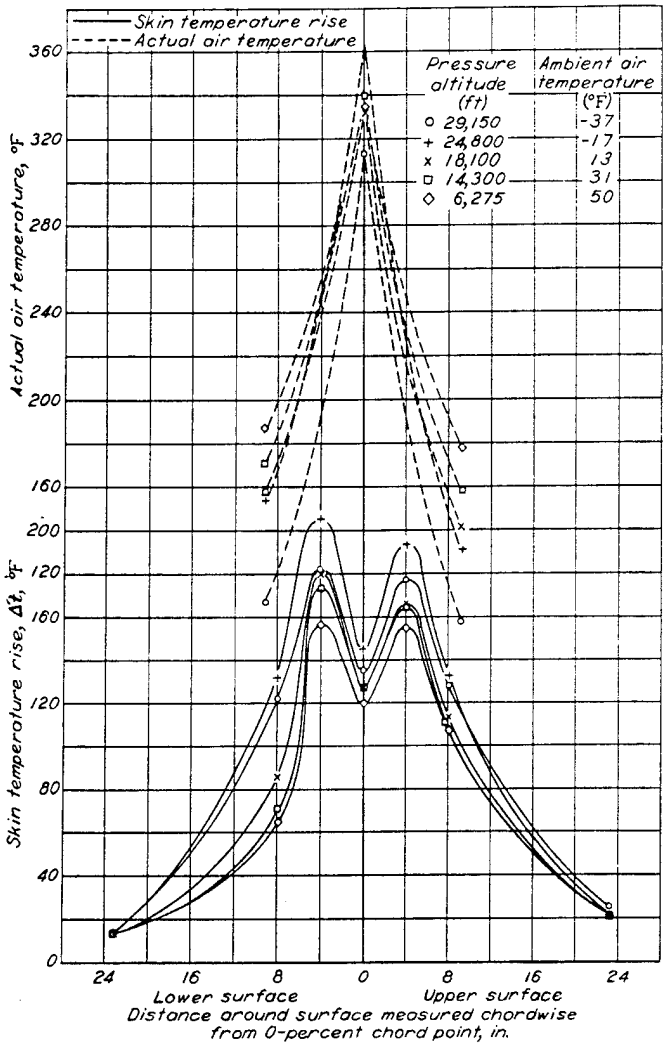

FIGURE 22.—Right stabilizer station 125 chordwise skin- and air-temperature distribution at various altitudes. Test condition 3: Full throttle; twin engine operation.

The effects of altitude on the thermal performance of the ice-prevention system during level twin-engine flight are shown in figures 20 to 24. For level flight at any of the test altitudes below 25,000 feet, the temperature rise of the leading-edge skin of the wing and empennage was approximately the same for all of the engine operating conditions employed. The curves of figures 20 to 24, therefore, have

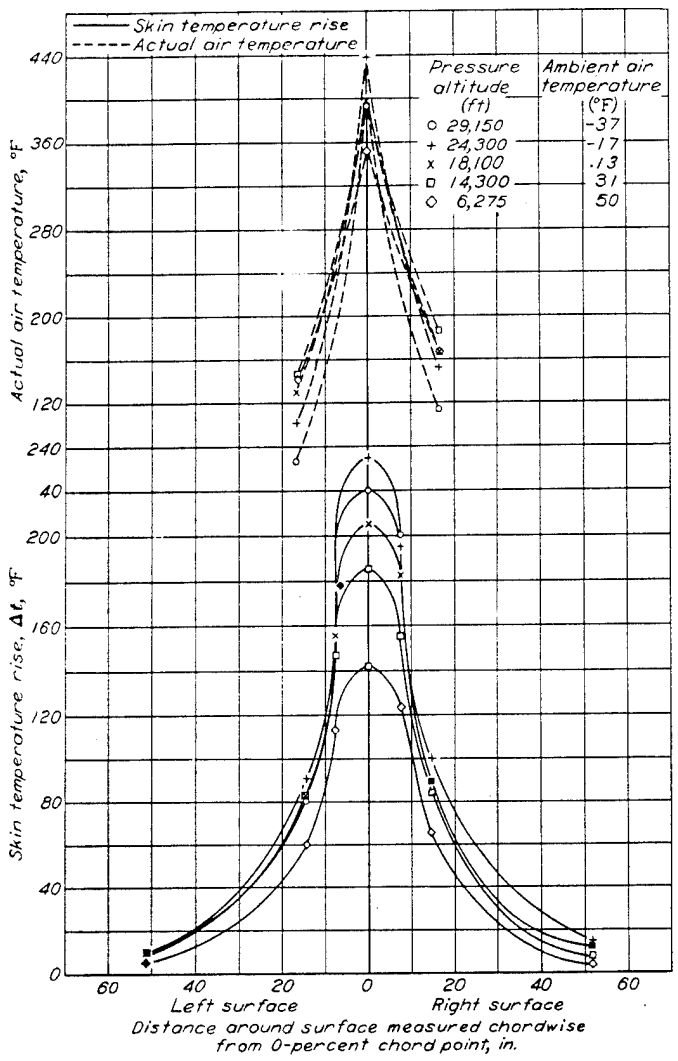

FIGURE 23.—Vertical fin station 124 chordwise skin- and air-temperature distribution at various altitudes. Test condition 3: Full throttle; twin engine operation.

been presented for condition 3 of table I only. Figure 20 illustrates the variation with altitude of the flow rates and temperatures of the air delivered to the left-wing outer panel, the right stabilizer, and the vertical fin, and also the variation with altitude of manifold pressure and indicated airspeed. Figures 21 through 23 present, respectively, the chordwise skin- and air-temperature distribution at wing station 159, stabilizer station 125, and fin station 124. Figure 24 illustrates the variation with altitude of the average skin temperature forward of the baffle plates for the left-wing outer panel, the right stabilizer, and the vertical fin. The ambient-air-temperature variation with altitude for the full-throttle tests is also included in figure 24.

The change with altitude of the average actual skin temperatures of the leading-edge regions of the wing, stabilizer,

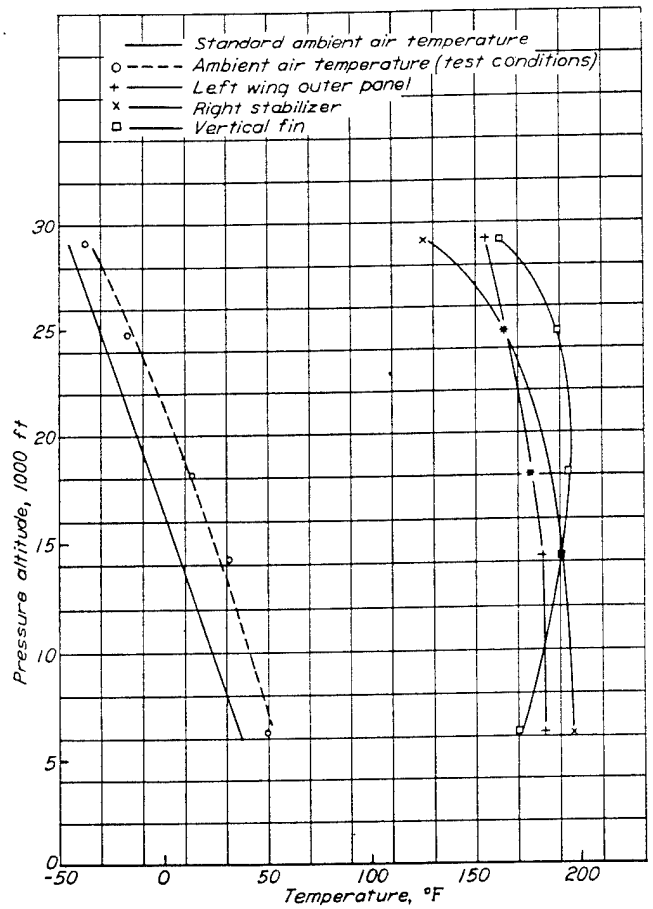

FIGURE 24.—Variation with altitude of average skin temperatures forward of baffle plates for left wing outer panel, right stabilizer and vertical fin. Test condition 3: Full throttle; twin engine operation.

and fin heated surfaces forward of the baffle plates (fig. 24) was less than 30° F for the altitude range below 25,000 feet pressure altitude. The rapid decrease of these average temperatures above 25,000 feet pressure altitude is of little concern, since the normal operating altitude range of the test airplane is well below 25,000 feet pressure altitude. The ambient-air temperatures for these tests, plotted in figure 24, did not correspond to standard ambient-air temperature; however, the ambient-air-temperature gradient which prevailed did correspond closely to the standard ambient-air-temperature gradient (0.00356° F/ft). Thus, for the altitude range below 25,000 feet pressure altitude, the actual leading-edge skin temperatures would vary little at any of the test flight conditions and altitudes if a standard ambient-air-temperature gradient prevailed.

Considering next the single-engine tests, the chordwise air- and skin-temperature variations at wing station 380 are presented in figure 25 for the flights conducted at 10,000 feet pressure altitude.

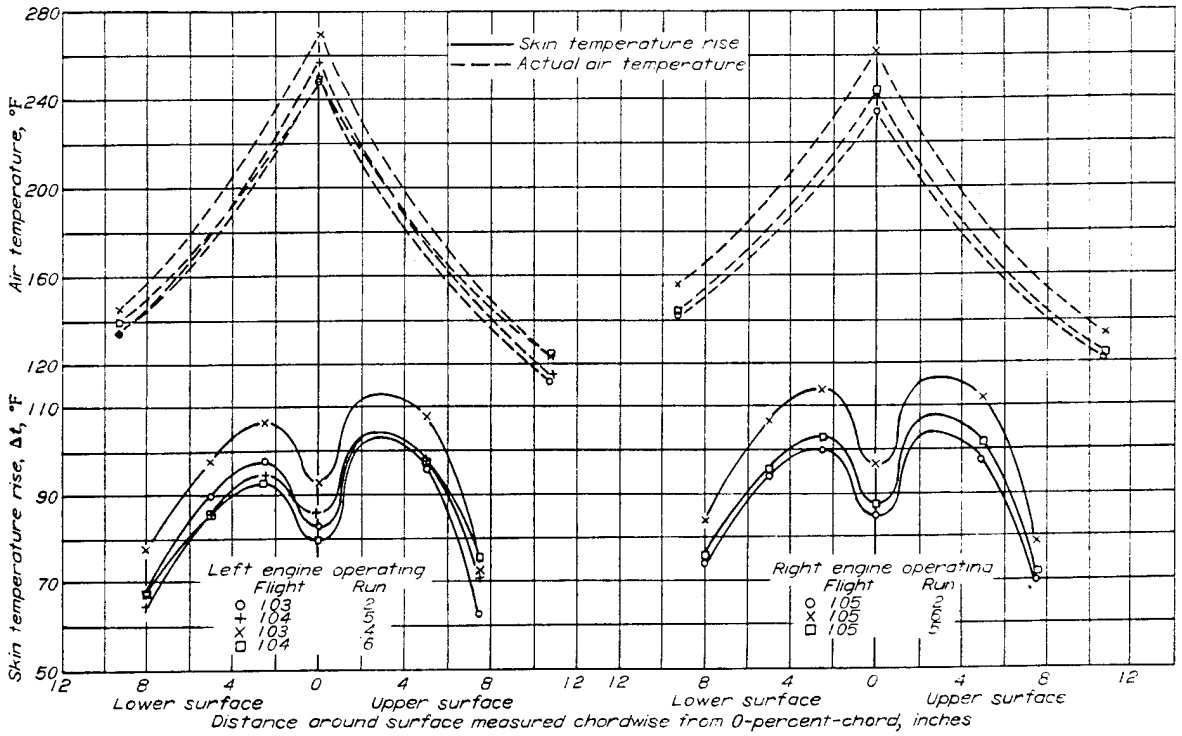

FIGURE 25.—Left wing outer panel station 380 skin- and air-temperature distribution for right and left single engine operation at 10,000 feet pressure altitude.

The skin-temperature rises (above ambient-air temperature) were about the same, irrespective of test altitudes and flight conditions and irrespective of which engine was operated. Thus, if the actual skin temperatures were referred to a standard ambient-air-temperature gradient, they would decrease at approximately the same rate as the standard ambient-air temperatures decrease with altitude. The adequacy of the temperature rises presented in figure 25 for the prevention of the accretion of ice will be discussed after the icing test results have been presented.

RESULTS OF THE ICING TESTS

The test results obtained in natural-icing conditions for the wing and the empennage are presented in tables III and IV for full- and reduced-heated-air-flow rates, respectively. The thermal data for the secondary heat exchanger and the windshield are presented in table V, which also includes one flight in clear air. The severity of icing (light, moderate, and heavy) noted in part 1 of tables III and IV was arbitrarily selected to provide a means for comparing flights. The degree of severity assigned to each condition was based on the past experience of the pilots and the flight test engineers, utilizing the following approximate criteria. The light icing conditions would probably permit flight without any means of ice protection. The heavy icing conditions would probably cause an unprotected airplane to descend in a short time. Those conditions designated as moderate are representative of intermediate conditions.

The thermal ice-prevention system was operated 173 hours in flight, 30 hours of which were in natural-icing conditions. Any ice accumulations on the wings, empennage, and windshield surfaces were slight, and did not noticeably affect the operational performance of the airplane. On the basis of the observed performance, the thermal system could be said to provide satisfactory protection to these heated areas.

TABLE III.—PERFORMANCE OF THE THERMAL ICE-PREVENTION SYSTEM DURING FULL-HEAT-FLOW TESTS IN NATURAL-ICING CONDITIONS

PART 1—OPERATING CONDITIONS

Date of flight	Flight No.	Run No.	Pressure altitude (ft.)	Corrected indicated airspeed (mph)	Ambient air (°F.)	Engine conditions		Severity of icing	Type of icing
						Manifold pressure (in. Hg)	Rpm		
Jan. 30, 1944	29	1	6,500	172	30	31	1,900	Moderate	Glaze.
Feb. 7, 1944	34	1	4,920	163	22	31	1,900	Moderate	Glaze and rime.
Feb. 14, 1944	41	5	3,260	184	20	31.5	1,900	Moderate	Glaze.
Feb. 23, 1944	49	1	13,160	143	6	30	1,900	Heavy ice and snow	Glaze and snow
Mar. 1, 1944	50	4	5,600	162	25	31	1,900	Heavy	Rough glaze.
Mar. 2, 1944	51	1	4,750	170	29	31	1,900	Moderate	Glaze.
Mar. 13, 1944	57	1	8,000	160	32	30	1,900	Moderate	Glaze.
Mar. 15, 1944	59	1	2,825	167	28	31.5	1,900	Light	Glaze.
Mar. 22, 1944	63	1	3,925	158	27	31.5	1,900	Light	Glaze.
Mar. 22, 1944	65	1	4,000	171	26	31.5	1,900	Light	Glaze.
Jan. 30, 1944	29	2	5,520	149	30	26.5	1,600	Moderate	Glaze.
Feb. 7, 1944	34	2	4,300	132	22	27	1,600	Light	Glaze and rime.
Feb. 14, 1944	41	6	3,500	162	20	27.5	1,600	Moderate	Glaze.

[1]Right inboard heat exchanger off.

NOTE.—All flights were conducted within 500 miles of Minneapolis, Minn., except flight 49 which was a ferry flight from Moffett Field, Calif. to Minneapolis, Minn.

TABLE III.—Continued

PART 2.—HEAT DISTRIBUTION

Flight No.	Run No.	Exchanger heat flows (1,000 Btu/hr)			Heat flows to heated surfaces (1,000 Btu/hr)			
		Left outboard	Left inboard	Right inboard	Left wing outer panel	Right stabilizer	Fin	To secondary exchanger
29	1	349	419	143	349	78	129	80
34	1	348	266	171	348	77	126	87
41	5	397	471	161	397	88	145	95
49	1	340	308	163	340	79	126	89
50	4	423	399	189	423	96	158	101
51	1	414	415	187	414	96	157	109
57	1	300	338	140	300	88	145	81
59	1	414	402	173	414	119	158	97
63	1	420	449	0	420	61	97	64
65	1	415	387	151	415	89	148	91
29	2	267	267	143	267	60	135	68
34	2	271	278	143	271	64	100	67
41	6	236	359	154	236	73	119	73

PART 3.—SURFACE HEATING VALUES

Flight No.	Run No.	Average heat delivered per square foot of double-skin leading-edge surface (Btu/hr)			Average heat flow through heated skin surface per square foot of double-skin surface (Btu/hr)			Ratio of heat flow through heated skin surface to heat delivered			Average temperature rise of wing outer panel, 0% chord (° F.)
		Left wing outer panel	Right stabilizer	Vertical fin	Left wing outer panel [1]	Right stabilizer [2]	Vertical fin [3]	Left wing outer panel	Right stabilizer	Vertical fin	
29	1	3,390	3,670	7,180	1,490	1,440	3,580	0.45	0.39	0.50	66.0
34	1	3,280	3,570	7,040	1,510	1,930	3,480	.46	.54	.50	69.8
41	5	3,760	4,100	8,100	1,690	2,160	3,880	.42	.53	.48	85.8
49	1	3,220	3,670	7,000	1,380	1,830	3,390	.43	.50	.48	96.6
50	4	4,000	4,470	8,790	1,830	2,290	4,610	.46	.51	.53	82.4
51	1	3,920	4,500	8,750	1,780	2,540	4,530	.46	.56	.52	80.8
57	1	2,840	4,110	8,060	1,810	2,070	4,300	.64	.50	.53	73.6
59	1	3,920	5,580	8,800	1,670	2,170	4,620	.48	.39	.53	95.8
63	1	3,980	2,830	5,400	1,530	1,250	2,930	.38	.44	.54	135.0
65	1	3,920	4,150	8,280	1,570	1,970	4,340	.40	.43	.52	113.4
29	2	2,520	2,800	7,510	1,170	1,420	2,840	.46	.51	.38	86.4
34	2	2,570	3,000	5,580	1,070	1,310	2,770	.42	.44	.50	92.4
41	6	2,240	3,400	6,650	1,480	1,680	3,340	.66	.49	.50	85.8

[1] Calculated on basis of average temperature drop of the heated air in the corrugations at stations 24, 84, 159, 290, and 380 and the total air-flow rate from left outboard exhanger.
[2] Calculated on basis of average temperature drop of the heated air in the corrugations at stations 69, 125, and 171, and the total air-flow rate to the right stabilizer.
[3] Calculated on basis of average temperature drop of the heated air in the corrugations at stations 124 and 170 and the total air-flow rate to the vertical fin.

TABLE IV.—PERFORMANCE OF THE THERMAL ICE-PREVENTION SYSTEM DURING REDUCED-HEAT-FLOW TESTS IN NATURAL-ICING CONDITIONS

PART 1.—OPERATING CONDITIONS

Date of flight	Flight No.	Run No.	Pressure Altitude (ft)	Corrected indicated airspeed (mph)	Ambient air (°F)	Engine conditions		Severity of icing	Type of icing
						Manifold pressure (in. Hg)	Rpm		
Jan. 30, 1944	29	3	5,500	162	30	31	1,900	Moderate	Glaze.
Feb. 7, 1944	34	3	4,620	159	21	31	1,900	Moderate	Glaze and rime.
Feb. 14, 1944	41	3	2,760	182	23	31.5	1,900	Light	Glaze.
Mar. 1, 1944	50	5	5,500	153	26	31	1,900	Heavy	Rough glaze.
Mar. 2, 1944	51	2	5,200	164	28	31	1,900	Moderate	Glaze.
Mar. 15, 1944	59	3	5,250	162	28	31	1,900	Light	Glaze.
Mar. 17, 1944	60	4	3,450	163	17	31.5	1,900	Light	Rime.
Mar. 22, 1944	63	2	3,900	165	27	31	1,900	Light	Glaze.
Mar. 24, 1944	65	2	4,050	170	27	31	1,900	Light	Glaze.

PART 2.—HEAT DISTRIBUTION

Flight No.	Run No.	Exchanger heat flows (1,000 Btu/hr)			Heat flows to heated surfaces (1,000 Btu/hr)			
		Left outboard	Left inboard	Right inboard	Left wing outer panel	Right stabilizer	Fin	To secondary exchanger
29	3	57	.....	.....	57	.....	.....	.....
34	3	.....	.....	.....	155	.....	.....	.....
41	3	89	.....	.....	89	.....	.....	.....
50	5	179	200	115	179	59	93	61
51	2	142	151	78	142	54	74	53
59	3	108	128	62	108	45	66	44
60	4	53	138	40	53	41	53	34
63	2	.....	0	300	.....	55	84	55
65	2	.....	450	0	.....	63	100	63

TABLE IV.—Concluded

PART 3.—SURFACE HEATING VALUES

Flight No.	Run No.	Average heat delivered per square foot of double-skin leading edge surface (Btu/hr)			Average heat flow through heated skin surface per square foot of double-skin surface (Btu/hr)			Ratio of heat flow through heated skin surface to heat delivered			Average temperature rise of wing outer panel percent chord (° F)
		Left wing outer panel	Right stabilizer	Vertical fin	Left wing outer panel [1]	Right stabilizer [2]	Vertical fin [3]	Left wing outer panel	Right stabilizer	Vertical fin	
29	3	540	.....	.....	250	.....	.....	0.48	.....	.....	39.5
34	3	1,460	.....	.....	760	.....	.....	.52	.....	.....	56.5
41	3	840	.....	.....	440	.....	.....	.52	.....	.....	47.5
50	5	1,690	2,760	5,050	830	1,230	2,880	.49	0.45	0.57	61.5
51	2	1,340	2,500	4,110	640	970	2,300	.47	.39	.56	63.0
59	3	1,020	2,110	3,660	470	840	1,970	.46	.40	.54	71.0
60	4	490	1,890	2,930	240	700	1,650	.48	.37	.56	94.0
63	2	.....	2,560	4,680	.....	1,130	2,560	.....	.44	.55	.....
65	2	.....	2,940	5,560	.....	1,370	2,920	.....	.47	.52	.....

[1] Calculated on basis of average temperature drop of the heated air in the corrugations at stations 21, 84, 159, 290, and 380, and the total air-flow rate from left outboard exchanger.

[2] Calculated on basis of average temperature drop of the heated air in the corrugations at stations 69, 125, and 171, and the total air-flow rate to the right stabilizer.

[3] Calculated on basis of average temperature drop of the heated air in the corrugations at stations 124 and 170 and the total air-flow rate to the vertical fin.

TABLE V.—PERFORMANCE OF SECONDARY HEAT EXCHANGER AND WINDSHIELD THERMAL ICE-PREVENTION SYSTEM

Flight No.	61	64	64	65
Run No.	4	1	2	3
Pressure altitude, feet	18,000	5,300	5,000	4,500
Correct indicated airspeed, mph	143	165	164	159
Airplane operating conditions	31 in. Hg. manifold pressure—1,900 rpm			
Meteorological conditions	(1)	(2)	(2)	(2)
Ambient air temperature °F	−12	21	21	29
Air flow from primary exchanger, lbs/hr	725	716	1,088	1,049
Heat removed from primary air, Btu/hr	26,400	20,400	34,700	30,000
Temperature of primary air discharged over windshield, °F	151	119	146	164
Secondary air flow, lbs/hr	386	650	604	589
Temperature of secondary air entering exchanger, °F	38	48	54	63
Temperature of secondary air leaving exchanger, °F	208	131	168	189
Temperature of air entering windshield gap at bottom, °F	167	124	147	172
Temperature of air discharged from windshield gap to cockpit, °F	92	96	111	114
Heat delivered to windshield referred to ambient air, Btu/hr	19,900	17,400	21,600	22,900

[1] Clear air.
[2] Light ice.

Wing outer panel.—The thermal ice-prevention system essentially prevented the formation of ice on the wing outer panels when operated with full-heated-air-flow rates. The full-heated-air-flow rates, in natural-icing conditions, provided average heat flows through the left-wing leading edge (table III, pt. 3) of approximately 1,100 to 1,800 Btu per hour per square foot of double-skin leading-edge surface, and the average 0-percent-chord surface temperatures above ambient (table III, pt. 3) ranged from 66° to 113° F. The lowest 0-percent-chord temperature recorded was 82° F at station 380. Slight runback, defined as the freezing of water which runs back from the leading edges, was noted on flight 34 in the 30- to 35-percent-chord region of the right-wing outer panel. These accretions were intermittently removed with constant wing outer-panel heating.

During flight 49, a severe inclement weather condition was encountered over the Sierra Nevada Mountains between Sacramento, Calif., and Salt Lake City, Utah. This condition can best be described as a very heavy snow combined with a heavy natural-icing condition. Snow and ice formed in the stagnation-pressure region along the entire wing span and remained for approximately 10 minutes. The thermal data of flight 49, run 1, were taken during this period and indicate that the left-wing outer-panel 0-percent-chord skin temperature was approximately 100° F. Evidently, the rapid rate at which the snow and ice accumulated and the low ambient-air temperature (6° F) were factors that permitted the accretions on the wing leading edge.

The reduced-heat tests (table IV) show the effects of decreasing the heat flow to the wing outer panel. The average heat flows through the left-wing leading edge (table IV, pt. 3) during these tests ranged from 240 to 830 Btu per hour per square foot of double-skin leading-edge surface, and the average 0-percent-chord temperatures above ambient (table IV, pt. 3) ranged from about 40° to about 95° F. The lowest 0-percent-chord temperature recorded was 50° F at station 380.

A comparison of the reduced-heat data (table IV) with the single-engine-operation data (table II) permits an estimate to be made of the degree of ice protection that would be obtained during flight in natural-icing conditions when one engine has failed. The average heat supplied to each wing outer panel during the single-engine tests was about 140,000 Btu per hour at an average temperature rise above ambient-air temperature of about 330° F. The heat flows to the left-wing outer panel given in table IV, which provided protection in natural-icing conditions, ranged from slightly above this amount to considerably below, and the heated-air-temperature rises above ambient-air temperature were lower. The indicated airspeeds at which the reduced heat-flow data were taken were considerably higher than those used during the single-engine-operation tests. Thus, a lower external heat-transfer coefficient would prevail during single-engine operation, and a smaller quantity of heat would be required for protection. Therefore, it is evident that limited protection would be realized in natural-icing conditions when one engine has failed. This limited protection would be adequate for icing conditions similar to those encountered during the natural icing (tables III and IV); however, it probably would not be sufficient to protect the airplane in icing conditions of greater severity. This comparison, and the conclusions drawn therefrom, are specifically for the wing outer panels; however, since the characteristics of the empennage systems are similar, the conclusions are probably valid for the entire airplane.

Run 3 of flight 29 was taken after the left-wing outer-panel leading edge had been allowed to collect a band of ice throughout the span and the heated-air-flow rate was

slowly increased until the ice was removed, with runback taking place. The average heat flow through the wing leading edge during this test was 250 Btu per hour per square foot of double-skin leading-edge surface, and the resulting average 0-percent-chord temperature above ambient was 40° F. After the test, the heated-air-flow rate was increased to full and the runback was removed.

During flight 41, run 3 was taken after the heated-air-flow rate to the left-wing outer panel was decreased until the protection was considered marginal. The average heat flow through the wing leading edge was 440 Btu per hour per square foot of double-skin leading-edge surface, and the resulting 0-percent-chord leading-edge temperature above ambient was 48° F. The lowest 0-percent-chord temperature recorded was 50° F at station 380. Small accretions of ice had collected on the left-wing outer panel 2 or 3 inches forward of the front spar from midspan outboard. During the other reduced-heated-air-flow-rate tests presented in table IV, the thermal ice-prevention system apparently supplied the same protection to the wing outer panels as did the full-heated-air-flow-rate tests taken in the same natural-icing conditions.

Wing tips.—The protection realized at the wing tips with full heat flow was not sufficient to prevent ice in the heavy-icing condition and in several of the moderate-icing conditions encountered. The most common ice formations in this region were on the extreme wing-tip leading edges. During the full-heat-flow heavy-icing condition, flight 50, table III, and during the reduced-heat tests in the heavy icing, table IV, and in some of the moderate-icing conditions, the formation of ice was continuous along the leading edge from the wing tips to the wing-tip splices. No photographic data were taken of these ice accumulations, since they could not be adequately photographed in flight, and since they never remained on the surface after landing. The internal structure does not provide a sufficiently high heat-transfer coefficient at the leading edges of the wing tips.

Wing center panel.—The wing center panels were for the most part adequately protected. A very small patch of ice was noted to accumulate on the flange of the heat-exchanger outlet-duct fairing where the ducting enters the center-panel wing leading edge. It was also noted that snow would pack on this flange. During some of the more severe icing conditions, slight accumulations of runback were noted to form on the upper surface of the wing center panel. The conditions of the wing center panels were the same as those of the wing outer panels during flight 49. Temperature data presented in reference 11 indicate that the protection was sufficient at all times. The temperature in natural-icing conditions at the 0-percent-chord leading edge, indicated at station 90, never dropped below 104° F, even during the reduced-heated-air-flow-rate tests. It is believed that a better design could be realized, however, by revising the heated-air corrugations so that the heated air enters the corrugations at the leading edge of the wing instead of at the underside end of the corrugations.

Horizontal stabilizers.—With the thermal ice-prevention system directing full-heated-air-flow rates to the horizontal stabilizers, ice formed on the leading edges of the stabilizer tips. These accumulations were similar to those observed on the wing tips, and, in general, formed in the same manner and in these same icing conditions. During flight 34 at the time data were taken, slight runback was noted on the underside of the right stabilizer panel at about 10 percent chord. No observations of the stabilizers were made during flight 49. The thermal data for the horizontal stabilizer indicate that the temperatures realized were sufficient to prevent ice. The average heat flow through the stabilizer leading edge in natural-icing conditions ranged from about 1,250 to about 2,150 Btu per hour per square foot of double-skin leading-edge surface during the full-heated-air-flow-rate tests (table III, pt. 3), and from about 700 to about 1,400 Btu per hour per square foot of double-skin leading-edge surface during the reduced-heated-air-flow-rate tests (table IV, pt. 3). The lowest 0-percent-chord temperature recorded for the stabilizer, exclusive of the tip, was 51° F at station 69 during the reduced-heated-air-flow-rate tests.

Vertical fin.—The entire surface of the vertical fin including the tip was clear of ice during both the full- and reduced-heated-air-flow-rate operations of the thermal ice-prevention system. The temperatures of the skin surfaces presented in reference 11 indicate that the quantity of heat supplied was more than adequate for complete protection in the test icing conditions. The average heat flows through the vertical-fin leading edge, in natural-icing conditions, ranged from approximately 2,700 to 4,600 Btu per hour per square foot of double-skin leading-edge surface during the full-heated-air-flow-rate tests (table III, pt. 3), and from approximately 1,600 to 2,900 Btu per hour per square foot of double-skin leading-edge surface during the reduced-heated-air-flow-rate tests (table IV, pt. 3). The lowest 0-percent-chord temperature recorded was 81° F at station 205 during the reduced-heated-air-flow-rate tests.

Windshields.—The pilot's and copilot's windshields were protected from ice accumulations in all the natural-icing-test conditions. The external heating system offered thorough windshield ice prevention in all the natural-icing conditions except the heavy-icing condition encountered during flight 50. During this flight with only the external heating system in operation, the pilot's and copilot's windshields collected ice at a fast rate and the ice almost completely covered the windshields. After the windshields had collected ice, as shown in figure 26, the internal secondary air-heating system

was placed in operation without inserting the double-panel windshields. Figure 27 shows the partial ice removal effected after 15 minutes. It was noted that when the double-panel windshields were inserted, the rate of ice removal was increased. The values given in table V were taken during later flights and provide the thermal data for maximum protection which was never required to remove or prevent ice in any of the natural-icing conditions encountered.

These tests indicate that windshield ice prevention may be realized by the passage of heated air over the outer surface of the windshields. Before any specific design criteria for this method of windshield ice prevention can be established, however, further information is required regarding the relationships of the following: Temperature and flow rate of the heated air delivered, temperature rise above ambient-air temperature of the outer surface of the windshield, pressure and temperature distribution of the heated air flowing in the windshield boundary layer, and area and shape of the windshield.

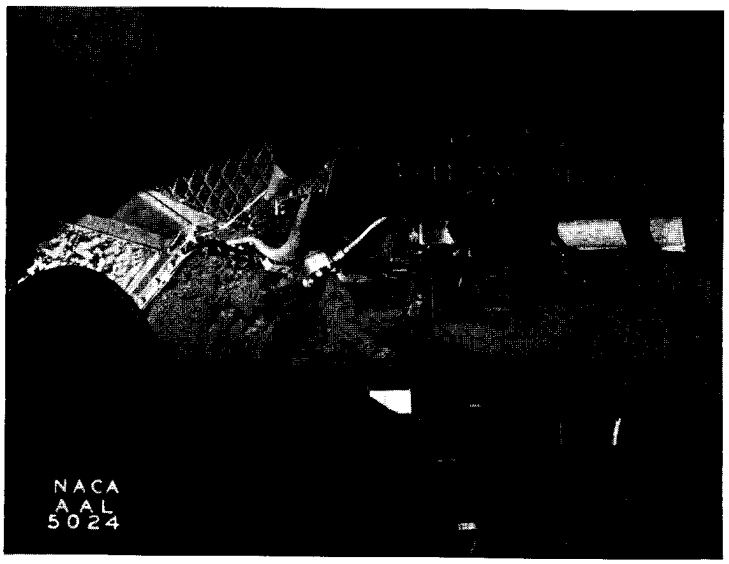

FIGURE 26.—Ice accumulation on pilot's and copilot's windshields after 45 minutes in heavy-icing conditions with only primary heated air directed over outside surfaces of windshields. Photograph taken in flight.

Ice-removal tests.—In order to establish the effectiveness of the system in removing ice on the heated surfaces prior to take-off, tests were conducted in which artificial ice was applied to stations 159 of the wing outer panels as previously discussed. The tests were conducted at a ground ambient-air temperature of 6° F. After the engines had been started and normal engine warm-up had taken place for 5 minutes, water drops started forming on the left-side ice application. While the airplane was taxied out of the runway for take-off, water drops were forming on both the strips of ice, but no substantial change in over-all appearance was evident. Take-off was conducted 14 minutes after the engines had been started and ice removal immediately began to take place. The leading edges of stations 159 were clear of ice, as shown in figure 28, before the airplane left the ground.

Natural frost was removed from the wings, the empennage, and the windshields of the airplane on cold mornings (−10° to 15° F) while the airplane was warmed up for flight. The frost on these heated surfaces could be almost completely removed after conducting engine warm-up for not more than one-half hour.

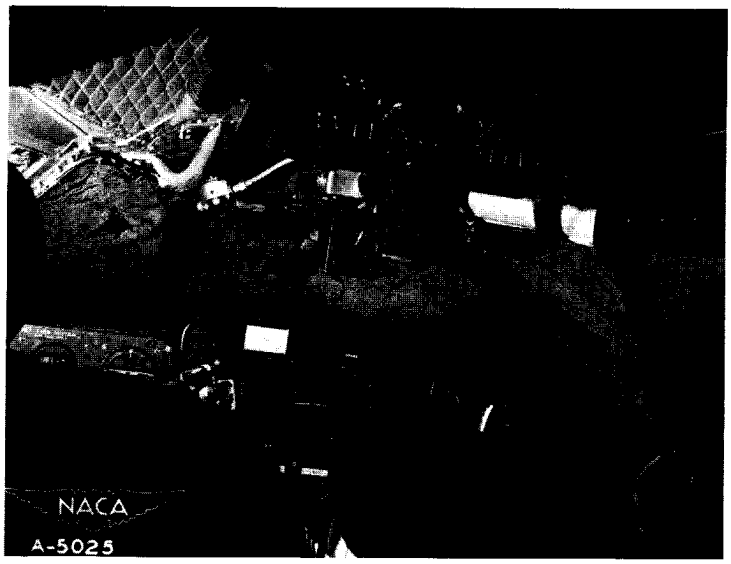

FIGURE 27.—Partial ice removal from pilot's and copilot's windshields with secondary heated air directed over the inside of the windshields without inserting double panels. Photograph taken in flight.

During flight, in many of the natural-icing conditions, the leading edge of the left-wing outer panel was allowed to collect ice. The outboard panel was always cleared of the ice accumulations in less than 1 minute after full-heated-air-flow rate to the left outer wing was employed.

The frost-removal and artificial-ice-removal test indicate that frost or ground ice collections can be removed sufficiently for flight by the thermal ice-prevention system. The flight-test removal of natural ice indicates that protection is realized almost immediately in flight upon placing the heating equipment in operation.

Unprotected surfaces.—The unprotected surfaces which accumulated ice in nearly all the natural-icing conditions encountered were the engine cowling, the carburetor air inlets, the heat-exchanger air scoops, the stabilizer splices, the stabilizer and wing-tip splices, the antennas, the antenna masts, the airspeed masts, the free-air thermometer, and the

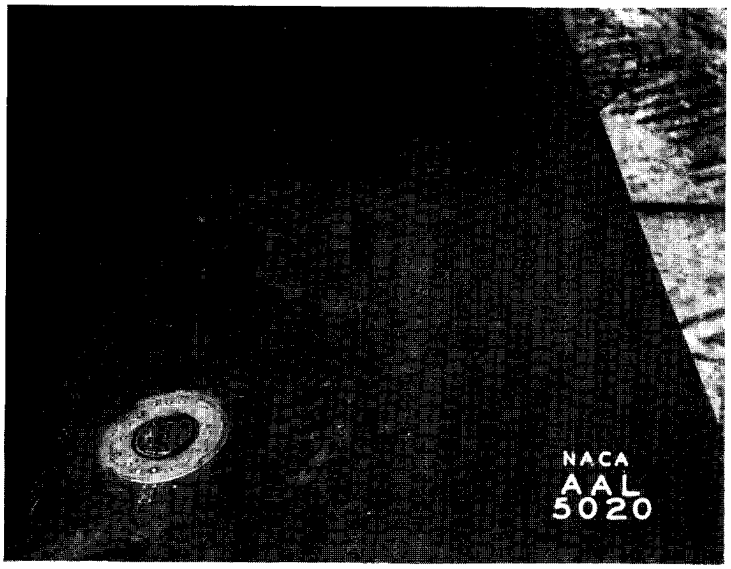

FIGURE 28.—Ice removed by engine warm-up and take-off in simulated icing tests.

dome on top of the fuselage. After flight 60, inspection of the airplane revealed slight rime-ice accretions on the underside of the ailerons near the hinge region and on the underside inboard ends of the elevators. These ice accretions were evidently caused by air flow through the aileron gap and through the gap between the inboard ends of the elevators and the fuselage fairing. Ice formations on some of the unprotected surfaces are shown in figures 29 to 32. The largest ice formations were realized during flight 50 in heavy-icing conditions. Figures 31 and 32 are photographs taken after landing of some of the ice accumulations resulting from this flight. These ice formations were much larger in flight. The temperature of the ambient air before landing in Minneapolis was 38° F and the ice was melting and falling off at the time the pictures were taken. During flight, the ice on the cowling (fig. 32) had extended 2 to 3 feet rearward along the nacelle sides and the ice on the nose of the airplane (fig. 31) had extended rearward over the windshields.

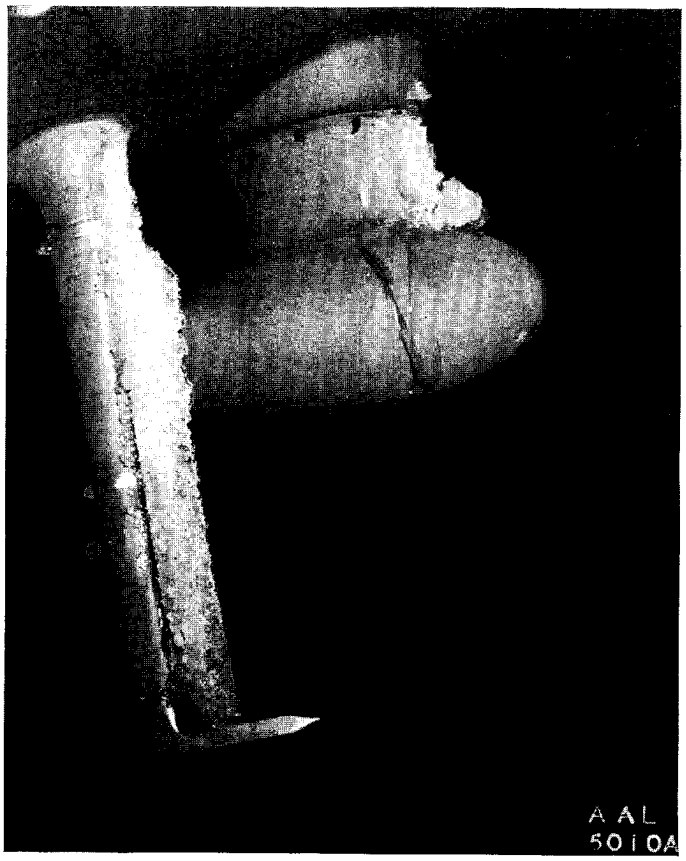

FIGURE 29.—Ice accumulations on the right airspeed mast and loop antenna of the test airplane after flight 29. Photograph taken after landing.

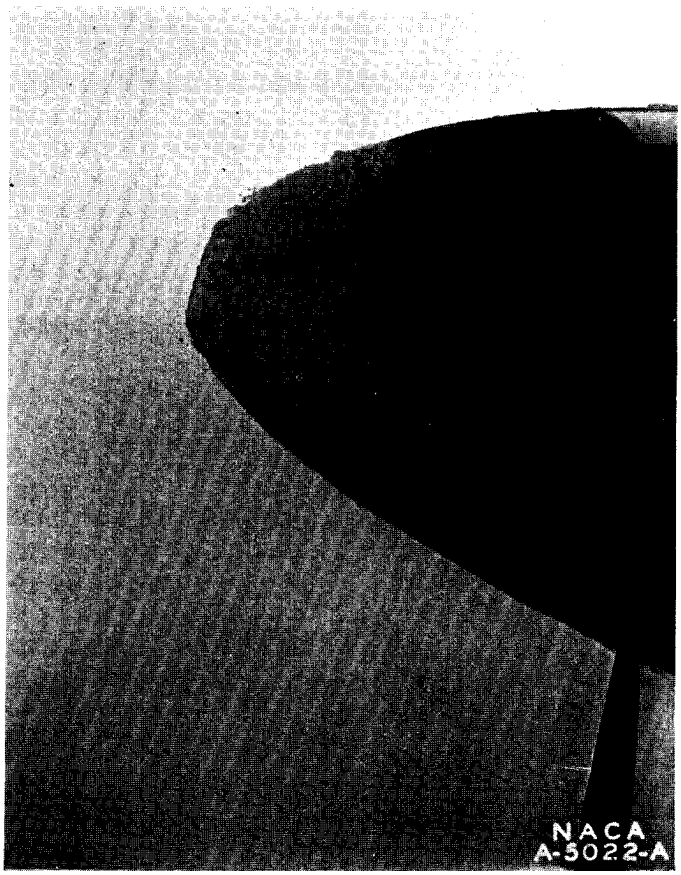

FIGURE 31.—Nose of test airplane after flight 50. Rearward extension of the accretion had fallen off.

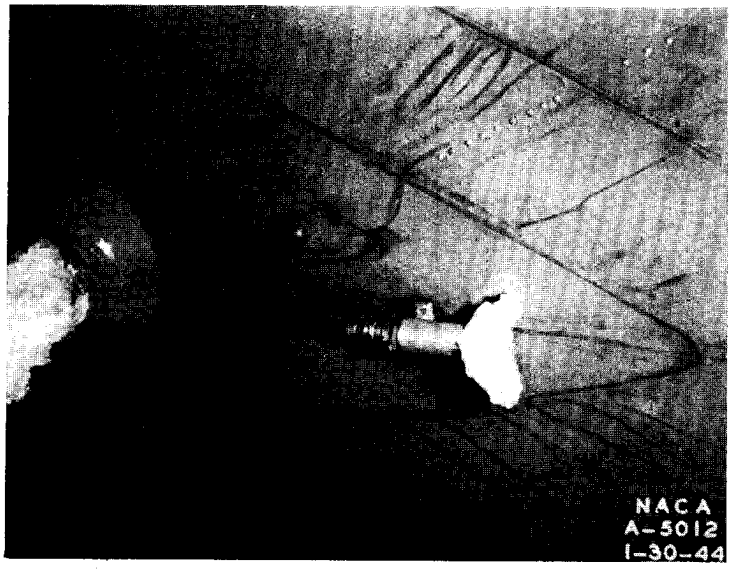

FIGURE 30.—Ice accumulation on pilot's free-air temperature thermometer after flight 29. Photograph taken after landing.

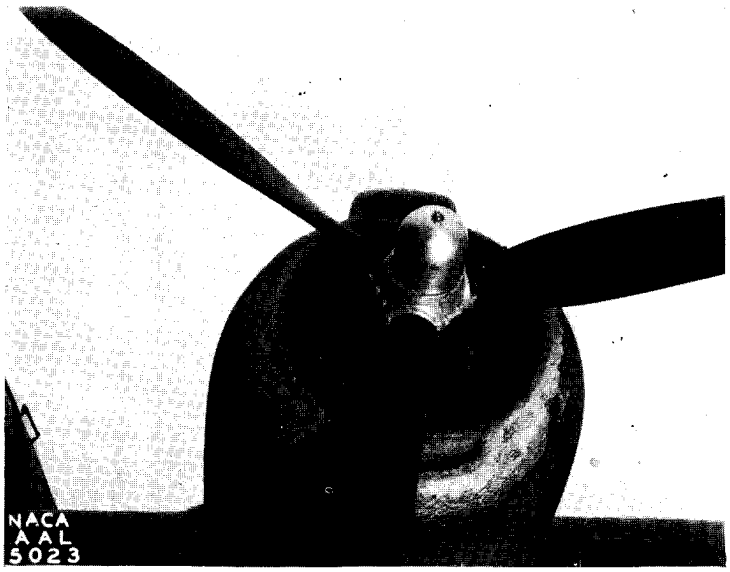

FIGURE 32.—Ice accretion on the eft engine cowl after flight 50.

EFFECT OF THE THERMAL SYSTEM ON THE AIRPLANE PERFORMANCE AND SAFETY

The foregoing portion of this report has discussed the development and testing of the thermal ice-prevention system which was undertaken with the principal objective of obtaining satisfactory protection in icing conditions. These tests revealed that satisfactory protection was provided by the system and, therefore, attention was next directed toward an investigation of any deleterious effects the thermal ice-prevention system might have upon the airplane performance and safe operation. Four separate investigations were conducted to evaluate any detrimental effects; namely (1) measurements of the effect of the thermal system on the airplane cruise performance, (2) a consideration of the effect of the temperatures encountered during operation of the thermal system on the strength of the airplane structure, (3) measurement of the change in wing structure stresses caused by operation of the thermal system, and (4) a metallurgical examination of the wing leading-edge structure for effects of corrosion after 225 hours of flight operation of the thermal system. The results of investigations (1) and (3) are presented in detail in references 12 and 14, which will be abstracted in the following. Investigations (2) and (4) have not been previously reported, and will be presented briefly herein.

EFFECT OF THE THERMAL SYSTEM ON THE AIRPLANE CRUISE PERFORMANCE

The objectives of the first of the four investigations were (1) to determine the effect of the system on the airplane cruise performance, (2) to establish, if possible, the factors contributing to any change in performance, and (3) to evaluate the amounts of such contributions. The factors which were selected for investigation as possible contributors to any change in performance were: (1) the increase in exhaust-gas back pressure resulting from the heat exchangers, (2) the internal drag of the thermal ice-prevention system, (3) the weight of the thermal ice-prevention system, and (4) the external drag of the heat-exchanger installations.

Description of equipment.—For these tests the airplane and instrumentation were in the same condition as previously described, except as noted hereafter. Three different configurations of primary heat-exchanger installation were tested: (1) exchanger installed, no fairings (fig. 10), (2) exchangers installed with fairings (fig. 11), and (3) exchangers replaced by the original exhaust stack (fig. 33).

Tests.—The effect of the thermal ice-prevention system on the performance of the airplane was measured in flight in terms of indicated airspeed while maintaining constant manifold pressure on the engines, and in terms of manifold pressure while maintaining a constant indicated airspeed. All tests were conducted at 10,000 feet density altitude, with the engines operating at 1,900 rpm and low blower, and at an airplane gross weight of approximately 38,000 pounds.

The tests were conducted under the following four conditions:

1. Heat exchangers in place, heated air discharged overboard, engine manifold pressure maintained constant at 30 inches of mercury

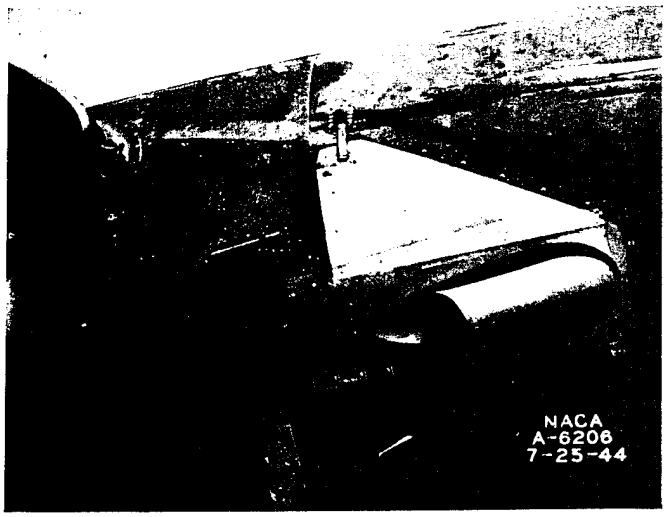

FIGURE 33.—Standard production exhaust stack installation for the test airplane.

2. Heat exchangers in place, heated air delivered to the surface-heating system, engine manifold pressure maintained constant at 30 inches of mercury

3. Heat exchangers removed, standard production exhaust stacks installed, engine manifold pressure maintained constant at 30 inches of mercury

4. Heat exchangers removed, standard production exhaust stacks installed, indicated airspeed maintained constant at values previously established by tests of condition 1

These conditions provide the change in performance caused by the thermal system in terms of airspeed (conditions 1, 2, and 3) and in terms of manifold pressure (conditions 1, 2, and 4). The effect of the heat-exchanger fairings (fig. 11) upon the performance of the airplane was established by flights with the fairings in place and removed, with the airplane operating under conditions 1 and 2.

For conditions 4, three test runs were made at the same engine speed as conditions 1 and 2, and at approximately the same indicated airspeed and density altitude as those conditions. The resultant manifold pressures were 28.8, and 28.5 inches of mercury. For conditions 1 and 2 the manifold pressure was 30 inches of mercury.

Data during each test were recorded manually at intervals of approximately 1 minute for a sufficient length of time after equilibrium conditions had been established to assure attainment of representative results.

Over-all performance change.—The results of the flight tests are presented in terms of airspeed in figure 34. The values of pressure altitude and indicated airspeed presented in the figure are the averages of the recorded data for each test condition. The variation of individual readings of these variables from the average values presented did not exceed 50 feet and 3 miles per hour, respectively. Since the relationship of indicated airspeed to pressure altitude for conditions 1 and 2 was substantially identical, only one curve has been drawn through the experimental points for those two conditions.

The curves of figure 34 indicate that the performance change resulting from the installation of the thermal system amounted to approximately 6 miles per hour indicated air-

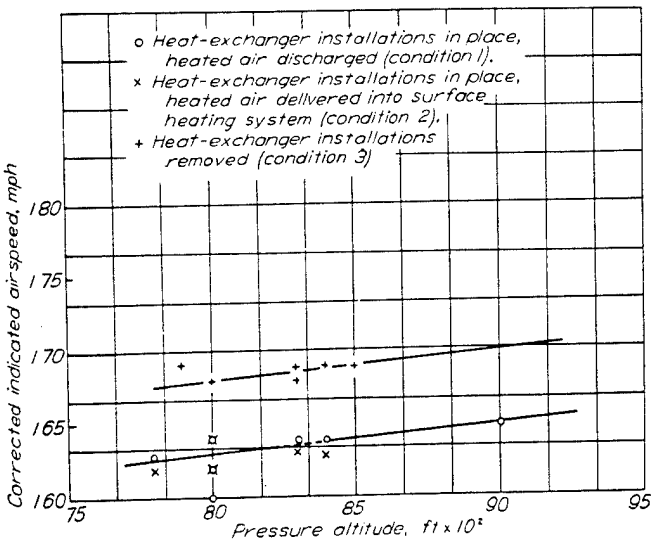

FIGURE 34.—Variation of indicated airspeed with pressure altitude for the test airplane with and without the heat exchanger installations in place. Flight conditions: 10,000-feet density altitude; 30 inches of mercury manifold pressure and 1,900 rpm.

speed, or 1.4 inches of mercury manifold pressure at the test conditions. Sufficient performance data are available for the test airplane to interpret these performance changes in terms of brake horsepower. The calculations are presented in reference 12 and indicate that the airspeed loss expressed in terms of equivalent horsepower loss was 96 thrust horsepower, and computed from the manifold pressure data was 88 thrust horsepower. The experimental data used for computing these two values were taken independently of each other, and the methods provide reasonable agreement. Therefore, the performance change in terms of thrust horsepower caused by the installation of the thermal system may be considered as 92 thrust horsepower, which is an average of the values obtained by the two methods.

Power loss attributed to exhaust gas back Pressure.—An estimate of the reduction of power caused by the heat-exchanger exhaust-gas back pressure may be made on the basis of general data available. This estimate is presented in reference 12 and shows that, for 8,000-foot pressure-altitude test conditions, the effect of heat-exchanger back pressure is a loss of about 4 brake horsepower per engine, which is equivalent to 6.4 thrust horsepower for the test airplane. The values of thrust horsepower reduction attributed to exhaust-gas back pressure, as derived in reference 12, are not more than 0.6 percent of the total power developed by the engines, and would cause a decrease in indicated airspeed of about one-half mile per hour.

Reduction of power attributed to internal drag of the thermal system.—As indicated in figure 34, there was no measurable difference between the performance of the airplane when the heated air was discharged (condition 1) and when the heated air was delivered into the surface-heating system (condition 2).

If it is assumed, in either case of operation, that the same amount of air enters the heat exchangers and all the kinetic energy of the air is expended, a maximum value of $(\text{thp})_{\text{int}}$ may be calculated. From the data of table I, the heated-air-flow rate through all the heat exchangers at the 8,000-foot pressure-altitude conditions may be approximated as 14,000 pounds of air per hour. The indicated airspeed, given in figure 34, for this condition is 163 miles per hour and the total kinetic energy of the 14,000 pounds of air per hour would amount to about 8½ thrust horsepower. In any actual case, the horsepower loss caused by internal drag would be less.

Additional airplane gross weight attributed to the thermal system.—The performance tests were all conducted with the airplane at approximately the same weight and, therefore, the test measurements did not include data on the effects of the additional weight contributed to the airplane by the thermal system.

Based on weight studies made of previous thermal systems similar to that installed in the test airplane, the weight added to the bare airplane (i. e., without any form of ice-prevention equipment) by the installation of the thermal system has been approximated to be 500 pounds. The 1,900-rpm cruise charts for the airplane indicate that at 8,000 feet pressure altitude, and a constant manifold pressure of 30.2 inches of mercury, a change in airplane gross weight from 35,000 to 40,000 pounds (an increase in weight equal to 10 times the estimated weight of the thermal system) produces a corresponding change in indicated airspeed of 2 miles per hour. Thus, the installation weight evidently has a negligible effect on the performance of the airplane at the test conditions. Further calculations, presented in reference 12, show that the additional fuel weight which must be carried by the airplane at the test conditions to overcome the effects of the heat-exchanger installations would be in the order of 45 pounds of fuel per hour.

Reduction of power attributed to the external drag of the thermal system.—It has been established that the exhaust-gas back pressure, the internal-drag effects, and the weight of the thermal system contribute only slightly to the total performance difference measured. These effects are estimated to total less than 15 thrust horsepower. The remainder, approximately 77 thrust horsepower, is attributed to the external drag of the heat-exchanger installations. It is evident from figure 10 that the external drag would be large.

Considerable external drag, however, is not necessarily inherent to heat-exchanger installations. If the heat exchangers were located within the nacelles and the air inlet scoops in the stagnation region of the cowling, the external drag could be reduced considerably. The installation on the test airplane was installed for the purpose of investigating the surface-heating system, and the available time was not sufficient to permit complicated nacelle alterations to be made for submerging the exchangers within the nacelles.

EFFECT OF TEMPERATURES ENCOUNTERED ON THE STRENGTH OF THE AIRPLANE STRUCTURE

The major effects on the strength of an aluminum alloy structure resulting from exposure to elevated temperatures are (1) reduction of the yield and ultimate strength while at elevated temperatures, (2) creep [2] of the structure while at

[2] Creep is dependent on the structure temperature, the time interval that a member is subjected to the temperature, and the stress imposed on the member during the time interval.

high temperatures even when the stress is below the yield point, and (3) artificial aging [3] of the structure.

Instrumentation and tests.—The instrumentation of the ice-prevention system which was provided for the thermal performance tests included a few thermocouples in the left wing at locations where high structural temperatures were anticipated. These thermocouples were located at two stations on the nose ribs, on the web of the 30-percent-chord spar, and on the stringer immediately aft of the corrugated inner skin on the upper surface. Subsequent to the performance tests, additional thermocouples were placed in the left wing on the nose ribs, baffle plate, nose rib liner, corrugated inner skin, 30-percent-chord spar cap and web, and several spanwise stringers. Temperature data to augment that already obtained in the performance tests were obtained during ground warm-up, take-off, and during flight in clear air at approximately 5,000, 10,000, and 15,000 feet pressure altitude, with the airplane flown at various normal operating conditions. Variations in the rate of heated-air flow to the wing were obtained by manipulation of the valve after the heat exchanger. The heated-air temperature was varied by control of the power of the left engine and adjusting the power of the right engine to provide the airspeed desired.

Results and discussion.—The maximum temperatures recorded during the performance tests of the thermal system were: nose ribs, 294° F, and stringer and spar web, 134° F. In the later, more extensive tests, the maximum structure temperature rises (above ambient-air temperature) were: nose rib liner, 393° F; baffle plate, 356° F; nose rib, 335° F; inner skin, 317° F; and outer skin, 235° F. These temperatures were recorded during a climb at 15,000 feet.

By assuming that operation of the thermal system could be limited to a maximum free-air temperature of 32° F, the actual temperatures of the structural components just listed would be 425° F, 388° F, 367° F, 349° F, and 267° F, respectively. An indication of the effect of temperatures of this magnitude on the yield and ultimate strength of 24S–T Alclad is obtainable from reference 20. In this reference, the strength reduction is shown to be a function of both maximum temperature and time. For a duration of 15 minutes at the temperatures previously listed, the reduction of yield and ultimate strength in percent of the values at 75° F for the wing components would be: nose rib liner, 16 percent (yield) and 29 percent (ultimate); baffle plate, 15 and 22 percent; nose rib, 14 and 18 percent; inner skin, 13 and 16 percent; and outer skin, 6 and 10 percent. For times longer than 15 minutes up to at least 10 hours, the yield strength remains constant or increases and the ultimate strength remains constant or decreases, depending on the temperature considered (reference 20).

It should be pointed out that the airplane tested had no provisions for automatically controlling the heat flow to the wing. Consequently, at low-speed high-power conditions such as the test climb at 15,000 feet, the heated-air temperatures which prevailed (an average air-temperature rise of 424° F at station 37) were considerably in excess of those that provided satisfactory ice prevention during tests of the thermal system in natural-icing conditions. If the maximum heated-air temperature in the wing were regulated to that required for ice prevention under any normal flight conditions of the airplane, the structure temperatures would be considerably lower. Reference 11 indicates that the maximum actual temperature of the heated air leaving the heat exchangers for the wings was approximately 340° F during the tests in natural-icing conditions. The maximum temperature in the wing duct would be below this value. If the heated-air temperature in the wing duct did not exceed a maximum of 320° F in a 32° F atmosphere, the maximum structure temperature rises that would prevail would be approximately: nose rib liner, 266° F; baffle plate, 240° F; nose rib, 225° F; inner skin, 212° F; and outer skin, 155° F. These values were approximated from the relationship of heated-air temperature to structure temperature as established by these tests. They can be accepted as valid for any flight condition within the test range wherein the air temperature in the wing duct is 320° F in a 32° F atmosphere. If the structure were subjected to these temperature rises for 15 minutes in a 32° F atmosphere, the reduction in the yield strength in percent of the value at 75° F would be approximately 3 percent for the outer skin and 4 to 9 percent for the baffle plate, nose rib liner, nose rib, and inner skin (reference 20). The corresponding ultimate strength reductions would be approximately 6 percent and 9 to 11 percent, respectively

The effects of creep and artificial aging of Alclad 24S–T aluminum alloy are discussed in references 21 and 22, respectively. The data of references 21 and 22 indicate that the effects of creep and artificial aging are negligible for Alclad 24S–T aluminum alloy at temperatures below 300° F. At temperatures above this value, the design of stressed members may require the consideration of these factors. Data presented later in this report show that artificial aging was present in the section of the wing of the test airplane where the heated air impinged upon the baffle plate on entering the wing.

CHANGE IN WING STRESSES RESULTING FROM OPERATION OF THE THERMAL SYSTEM

A consideration of the thermal stresses which might be generated in the wing as the result of uneven temperature distribution suggested two possible effects: (1) Increases in stress in the heated leading edge because of restrained thermal expansion, and (2) increases in stresses in the remainder of the wing, which is relatively unheated, caused by expansion of the leading-edge region. A flight investigation, was undertaken, therefore, to establish the location, nature, and magnitude of the stress changes incurred in the wing of the test airplane resulting from operation of the thermal system. This investigation is presented in detail in reference 14.

Description of equipment.—The details of construction of the left wing outer panel of the test airplane, in which the stress measurements were obtained, are shown in figures 12 and 35. The wing is of all metal stressed-skin construction with spars at 30 and 70 percent of the chord. The skin is reinforced with spanwise hat sections and extruded stringers.

The changes in stress were measured with standard commercial wire resistance-type strain gages. In determining

[3] Artificial aging may produce a change in physical properties which will remain after the structure cools, and the extent of aging is dependent on the temperatures reached and the length of time that the member is subjected to these temperatures.

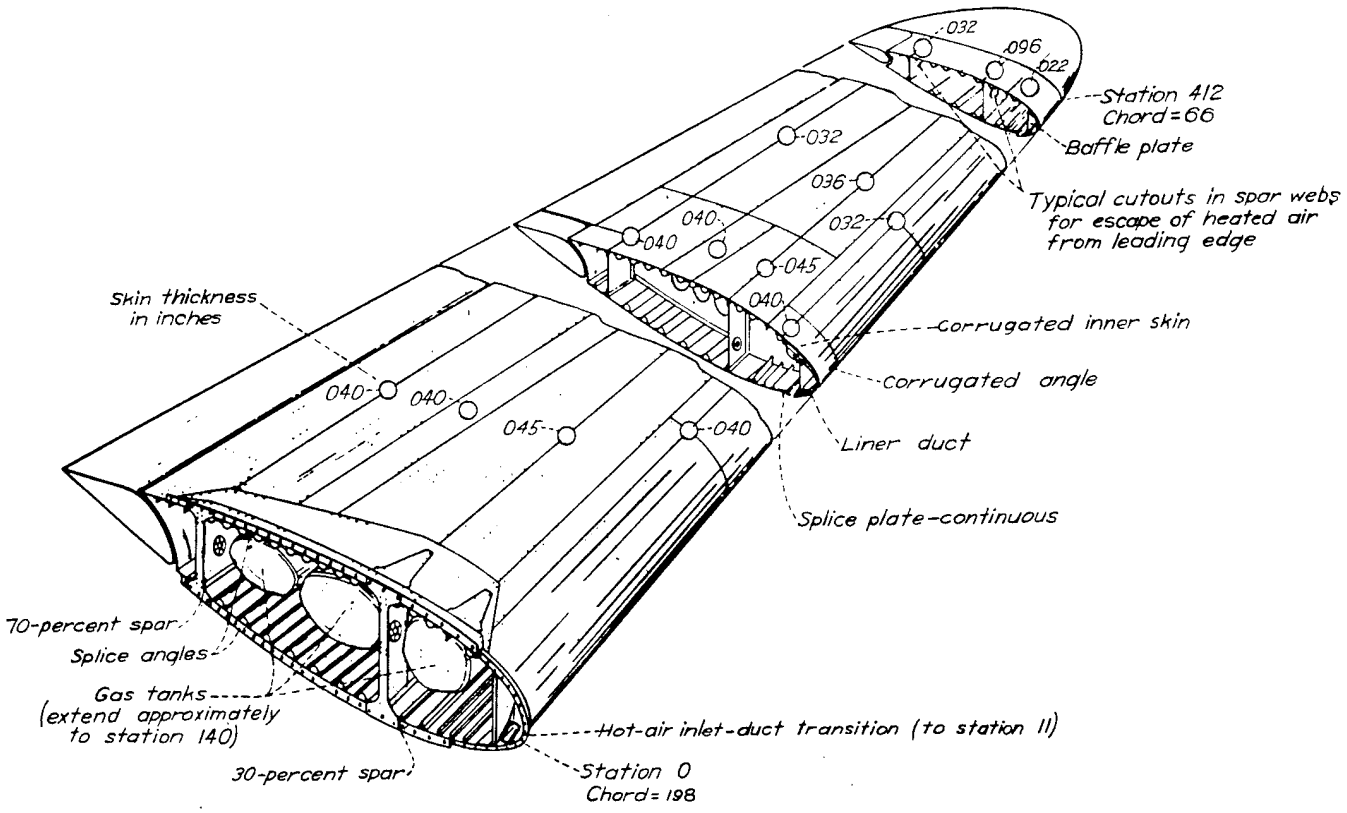

FIGURE 35.—Structural details of the left-wing outer panel of the test airplane with leading-edge revised for thermal ice prevention

the location of the gages, consideration was given to the stress reports for the unheated wing and the measured temperature distribution in the wing as presented in references 11 and 13. The stress reports showed that the margins of safety were appreciably lower at the wing root than near the tip; while the temperature data indicated that, in general, the spanwise distribution of temperature rise for a given chord location was approximately constant. The assumption was made that, for a given chord location, the stress change along the span would be substantially constant with the application of heat, and, therefore, the gages were located at two stations relatively near the root (47 and 137 in. from station 0).

The individual locations of the strain gages and thermocouples are shown in figures 36 and 37. Two general types of gages were employed; namely, plain (single-element) gages on structural members such as hat sections and spar caps where the direction of stress was known, and rosette (triple-element) gages on the wing skin where the direction, as well as the magnitude, of the maximum stress had to be established. The discontinuities in the strain-gage numbering system are the result of omitting from figures 36 and 37 those gages which failed.

The plain gages were installed with their strain-sensitive axes parallel to the longitudinal axes of the structural members. The rosette gages were oriented as shown in figure 38, which also gives the designation for the three strain elements. Aft of the double-skin region, the rosette gages were mounted in pairs, back to back, and connected in series in order to eliminate strain indications caused by possible local skin buckling. This procedure was not feasible in the double-skin region but was considered unnecessary because of the stabilizing effect of the inner corrugations. The strain gages were connected to a recording oscillograph which provided a continuous record of any 12 gages at one time.

Surface-type iron-constantan thermocouples, rolled to a thickness of 0.002 inch, were cemented to the aluminum surface with the junctions within one-quarter of an inch of the strain-gage elements. The thermocouples are designated by the same number as the corresponding strain gage and are prefixed with the letter T. (See figs. 36 and 37.) A thermocouple designation shown in figures 36 and 37 which is not accompanied by a corresponding gage number indicates the gage failed.

Standard NACA instruments were installed to record airspeed and normal acceleration. An NACA timer was used to synchronize the airspeed, accelerometer, and oscillograph records. The accelerometer was installed on the floor of the airplane at the center of gravity and oriented to record accelerations normal to the wing chord at station 0. The airspeed recorder was connected to the service airspeed-head installation and the error in static-pressure reading was determined in flight for all the test conditions with a trailing static pressure head.

Stress measurement technique.—When employing strain gages to measure stress changes in a structural member which is subjected to a temperature, as well as a stress variation, a question arises concerning the differentiation between movement due to stress and that due to thermal expansion. Superimposed on this complication is the unknown effect of elevated temperatures on the resistance of the strain-

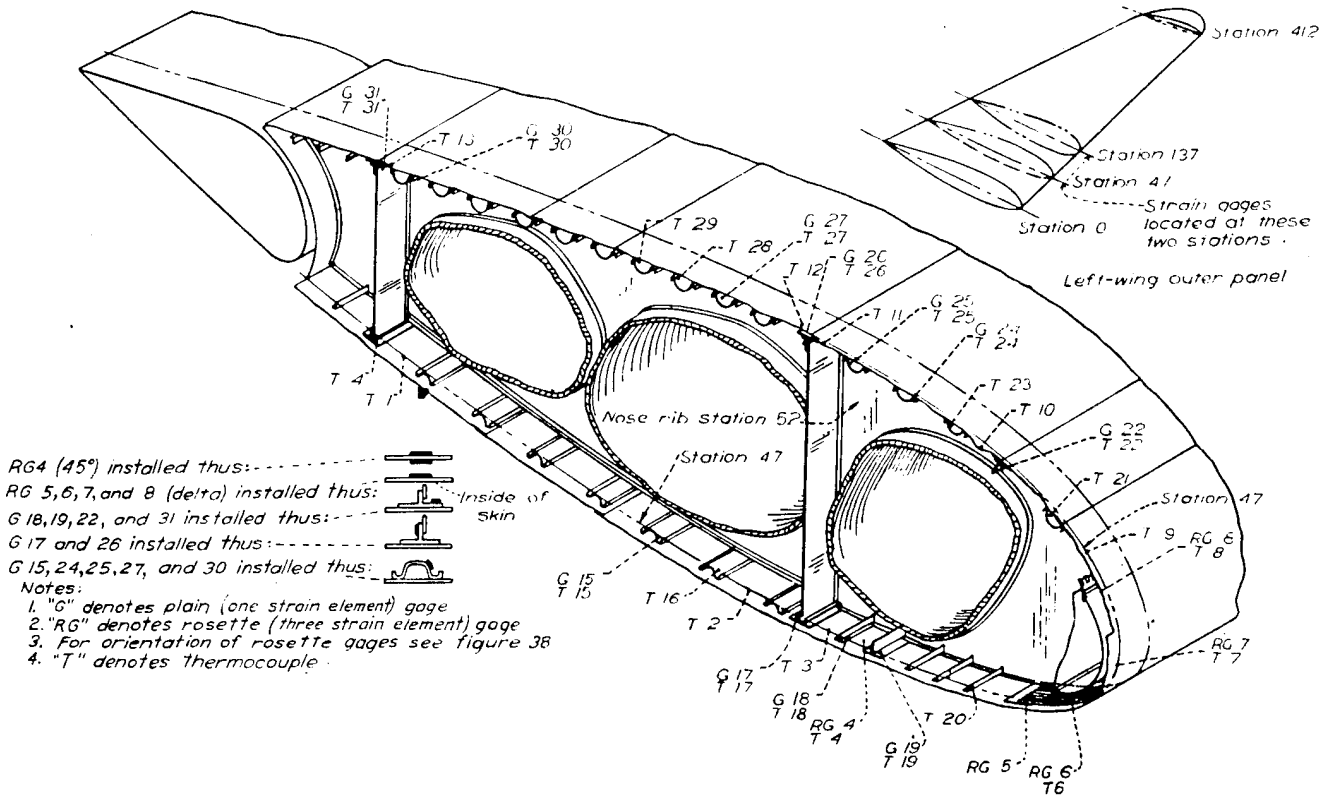

FIGURE 36.—Location of strain gages and thermocouples at wing outer-panel station 47.

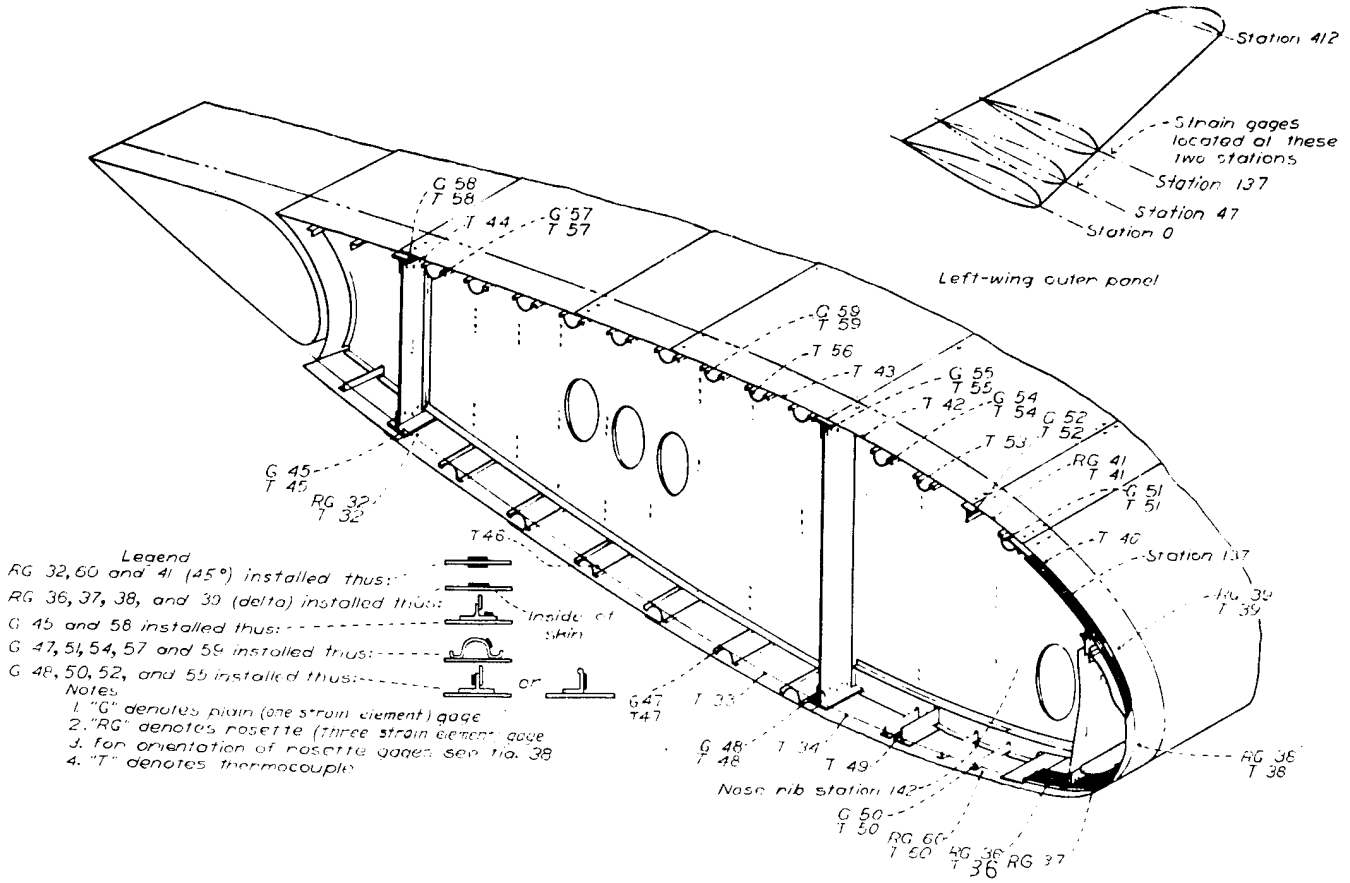

FIGURE 37.—Location of strain gages and thermocouples at wing outer-panel station 137.

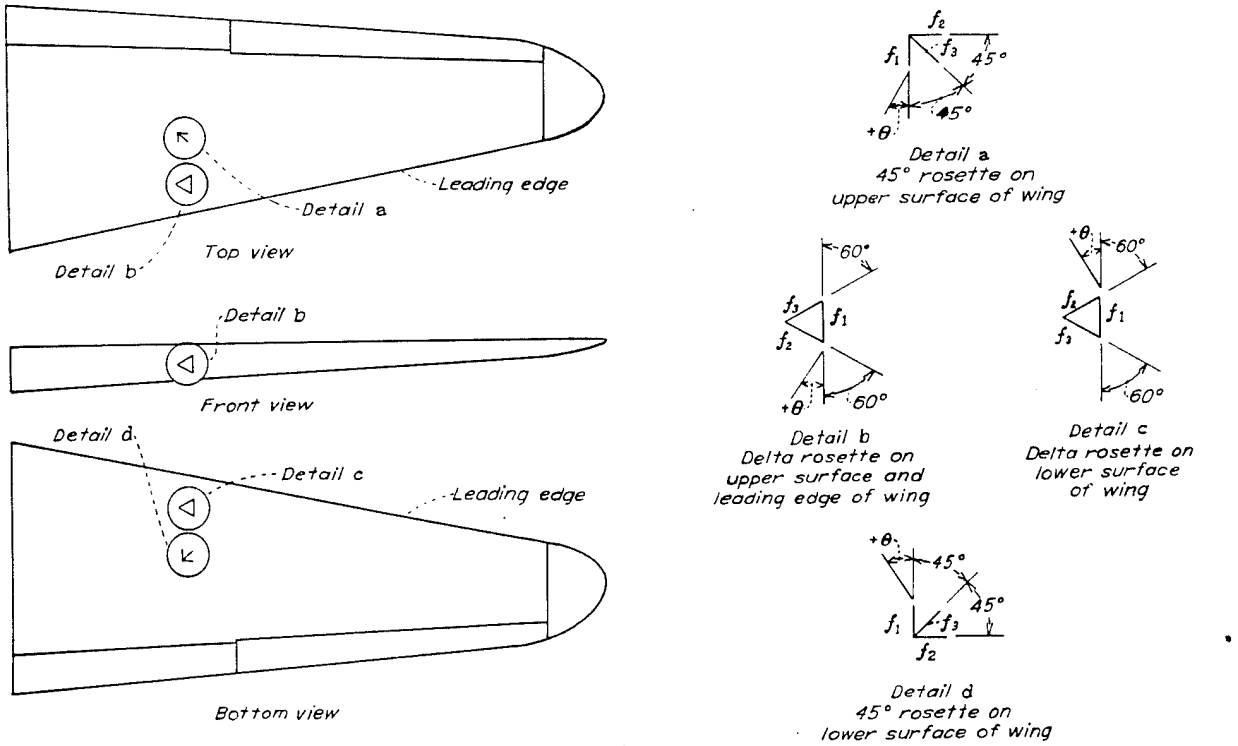

FIGURE 38.—Orientation of rosette gages on the left-wing panel of the test airplane.

gage material. One installation method commonly used to overcome these problems consists of locating a dummy strain gage beside the active gage but cemented to a small piece of the structure metal which is free to expand. The compensation is based on the assumption that the piece of metal to which the dummy gage is attached will assume the same temperature as the surface upon which the active gage is installed. This method was considered unreliable in the case of the wing of the test airplane.

Laboratory calibrations were made to investigate the stress-strain curves which would result if the dummy gage were maintained at a constant temperature while the aluminum calibration specimen and the active gage were subjected to various stresses at different temperatures. The results of this calibration for a typical strain gage used in the investigation are presented in figure 39. The important fact to note in figure 39 is that the calibration curves form a series of parallel straight lines. This means that the sensitivity factor of the gage (ratio of unit change in resistance to unit strain causing this change) is independent of the initial stress and temperature throughout the calibration range.

The method of applying the calibration curves of figure 39 to the determination of stress changes in the heated wing was as follows: Assume that point a of figure 39 represents the stress and temperature conditions at a gage in the wing before the wing heat was applied. The temperature of point a was known but the stress was not; however, since only stress changes were to be evaluated, the strain-recording equipment was adjusted to zero reading (or balanced). The heat was then directed to the wing and the changes in temperature and strain-gage reading were recorded. If the temperature change had been 30° F and the strain-gage reading agreed with point b, pure expansion and no change in stress would be indicated. If the strain-gage reading corresponded

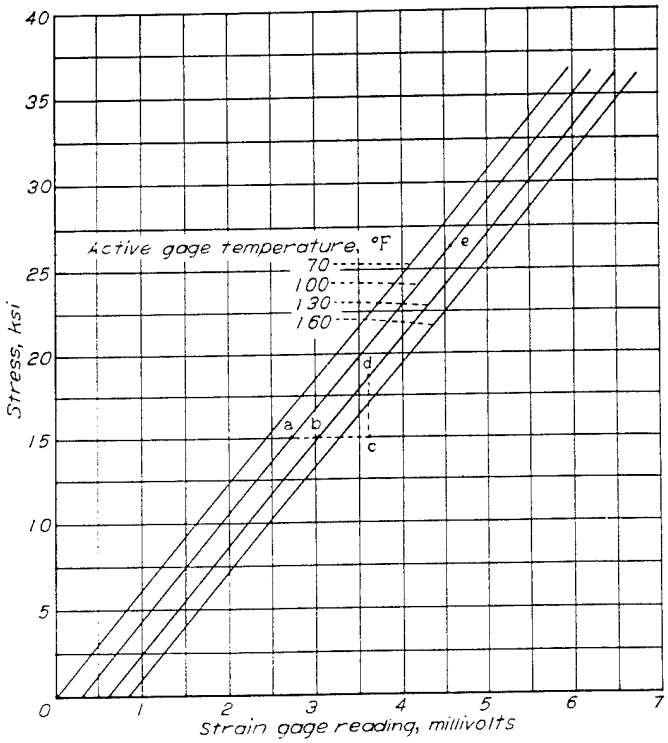

FIGURE 39.—Typical laboratory calibration of strain gage showing effect of temperature on gage reading. Dummy gage temperature constant at 70° F.

to point e, however, a change in stress equal to the distance between points e and d (or an increase in tension) was indicated. It is evident that the same result would be obtained for any other initial point of e instead of a, since the curve slopes were all equal. Hence the absolute value of the stress at the time of balancing the strain equipment had no bearing on the result.

Flight test procedure.—All the flight tests were made at a pressure altitude of 10,000 feet and a take-off gross weight of 45,700 pounds. Data were obtained at two airspeeds (110 and 135 mph, indicated) in level flight and at 155 to 165 miles per hour in a $2g$ bank at constant altitude. The airspeed in the $2g$ bank was calculated to give the same lift coefficient as that existing in the level-flight condition at 110 miles per hour in order that the two wing-loading conditions would be directly comparable with respect to chordwise pressure distribution.

The detailed flight test procedure was rather involved and is presented in reference 14. Stated briefly, temperature and strain data were recorded for 12 gages with the thermal system inoperative, and then repeated about 4 minutes after the thermal system had been started.

Results.—The maximum and minimum changes in normal stress, the maximum change in shear, and the direction of action of these stress changes were computed from the rosette-gage data and are presented in table VI. The terms "maximum normal" and "minimum normal" are used here in their algebraic sense. The Poisson ratio correction has been applied, and the data presented in table VI represent actual stress changes. The angle θ in the table gives the direction of the line of action of the maximum change in normal stress and is measured from the wing chord with the positive direction as shown in figure 38. The line of action of the minimum change in normal stress is at right angles to that of the maximum normal stress, and the maximum change in shear is at an angle of 45° to either of these axes. The rosette-gage stresses were also resolved in the spanwise and chordwise directions, and these data are presented in table VII. The chordwise variation of temperature and stress change at the two test stations for the three flight conditions are presented in figure 40.

TABLE VI.—MAXIMUM AND MINIMUM CHANGES IN NORMAL STRESS AND MAXIMUM CHANGE IN SHEAR STRESS AT ROSETTE-STRAIN-GAGE LOCATIONS IN WING OUTER PANEL OF THE TEST AIRPLANE RESULTING FROM OPERATION OF THE THERMAL ICE-PREVENTION SYSTEM

High-temperature delta rosettes at station 47

Flight condition \ Gage	RG5				RG6				RG7				RG8			
	Maximum normal	Minimum normal	Maximum shear	θ [1] (deg)	Maximum normal	Minimum normal	Maximum shear	θ [1] (deg)	Maximum normal	Minimum normal	Maximum shear	θ [1] (deg)	Maximum normal	Minimum normal	Maximum shear	θ [1] (deg)
110 mph correct I. A. S. level flight	+8,960	+6,150	1,420	+20¼	+3,410	−3,660	3,540	−1¾	+5,480	−4,210	4,840	+3½	+4,750	−3,100	3,930	+¼
135 mph correct I. A. S. level flight	+9,560	+5,340	2,110	+21¼	+3,200	−3,260	3,230	−2¾	+4,610	−4,430	4,520	+3½	+4,480	−3,750	4,120	−3½
155 to 165 mph correct I. A. S. $2g$ bank	+9,010	+5,490	1,760	+15	+3,290	−3,900	3,590	−6¼	+5,040	−6,010	5,520	+5¾	+3,600	−4,020	3,810	+1

High-temperature delta rosettes at station 137

Flight condition \ Gage	RG36				RG37				RG38				RG39			
	Maximum normal	Minimum normal	Maximum shear	θ [1] (deg)	Maximum normal	Minimum normal	Maximum shear	θ [1] (deg)	Maximum normal	Minimum normal	Maximum shear	θ [1] (deg)	Maximum normal	Minimum normal	Maximum shear	θ [1] (deg)
110 mph correct I. A. S. level flight					+5,400	−3,570	4,480	−1	+3,250	−6,950	5,100	+2½	+3,280	−5,210	4,250	−6
135 mph correct I. A. S. level flight	+4,500	+520	1,990	−33	+5,300	−2,210	3,750	−¼	+3,000	−6,170	4,580	+2¼	+2,260	−4,810	3,540	+¾
155 to 165 mph correct I. A. S. $2g$ bank	+4,570	+1,740	3,150	−34¼	+7,880	−1,650	4,760	−½	+3,200	−7,900	5,540	+3	+700	−3,340	2,020	+¼

Low-temperature 45° rosettes at stations 47 and 137

Flight condition \ Gage	RG4				RG32				RG41				RG60			
	Maximum normal	Minimum normal	Maximum shear	θ [1] (deg)	Maximum normal	Minimum normal	Maximum shear	θ [1] (deg)	Maximum normal	Minimum normal	Maximum shear	θ [1] (deg)	Maximum normal	Minimum normal	Maximum shear	θ [1] (deg)
110 mph correct I. A. S. level flight	+1,870	+580	640	+65	+310	−580	440	+3½	+2,110	+90	1,010	−93½	+900	−330	620	−17
135 mph correct I. A. S. level flight	+1,550	+530	510	+59	+400	−430	420	+4	+2,000	−50	1,020	−97¼	+910	+210	370	−15

[1] For designation of positive θ see fig. 38.
+Denotes tension stress, pounds per square inch.
−Denotes compression stress, pounds per square inch.
Data corrected for Poisson ratio effect.

TABLE VII.—SPANWISE AND CHORDWISE STRESS CHANGES AT ROSETTE STRAIN-GAGE LOCATIONS IN WING OUTER PANEL OF THE TEST AIRPLANE RESULTING FROM OPERATION OF THE THERMAL ICE-PREVENTION SYSTEM

High-temperature delta rosettes at station 47

Flight condition \ Gage	RG5		RG6		RG7		RG8	
	Spanwise	Chordwise	Spanwise	Chordwise	Spanwise	Chordwise	Spanwise	Chordwise
110 mph correct I. A. S. level flight	+6,390	+8,550	−3,660	+3,410	−4,180	+5,470	−3,100	+4,750
135 mph correct I. A. S. level flight	+5,890	+8,980	−3,250	+3,190	−4,400	+4,580	−3,720	+4,460
155 to 165 mph correct I. A. S. 2g bank	+5,710	+8,750	−3,820	+3,250	−5,900	+4,900	−4,020	+3,600

High-temperature delta rosetts at station 137

Flight condition \ Gage	RG36		RG37		RG38		RG39	
	Spanwise	Chordwise	Spanwise	Chordwise	Spanwise	Chordwise	Spanwise	Chordwise
110 mph correct I. A. S. level flight			−3,570	+5,400	−6,940	+3,230	−5,040	+3,180
135 mph correct I. A. S. level flight	+1,700	+3,310	−2,210	+5,300	−6,170	+2,990	−4,810	+2,260
155 to 165 mph correct I. A. S. 2g bank	+2,630	+3,665	−1,650	+7,880	−7,880	+3,180	−3,340	+700

Low-temperature 45° rosettes at stations 47 and 137

Flight condition \ Gage	RG4		RG32		RG41		RG60	
	Spanwise	Chordwise	Spanwise	Chordwise	Spanwise	Chordwise	Spanwise	Chordwise
110 mph correct I. A. S. level flight	+1,630	+830	−570	+310	+2,080	+120	−230	+700
135 mph correct I. A. S. level flight	+1,280	+810	−420	+390	+1,960	−30	+260	+890

+ denotes tension stress, pounds per square inch.
− denotes compression stress, pounds per square inch.
Data corrected for Poisson ratio effect.

Discussion.—The anticipated effect of heating the wing leading edge on the chordwise wing stress distribution was (1) an increase in compression for the double-skin region as a result of resistance to thermal expansion, (2) an increase in tension in the region between the double skin and the 30-percent spar caused by the expanded leading edge pulling on the relatively cool afterbody, and (3) an increase in compression at the 70-percent spar caused by the two spars and the wing skin acting as a box beam to resist the moment imposed by the expanding leading edge. This general trend is evident in all the curves showing the chordwise distribution of stress change. (See fig. 40.) These curves are based on the values of stress change normal to the chord. The chordwise temperature distribution has been added to the stress-distribution curves in order to facilitate the interpretation and explanation of the test data.

A comparison of the stress changes for the three flight conditions is presented in figures 40 (g) and 40 (h). Although the increased heat supplied to the wing in the 2g bank is evidenced by increased compression at the leading edge and some deviation of the 2g curve from the level-flight curves at other chord positions, the over-all agreement between the stresses for the three conditions is considered sufficient to allow them to be discussed as one general trend.

The expected compression at the leading edge and 70-percent spar is evident in figure 40. From 10- to 30-percent chord, however, considerable variation in the data is noted. This apparent discrepancy at first appears to refute the anticipated general trend, but on further examination is seen to be the result of local conditions superimposed upon the over-all pattern. An example of this effect is shown by the data presented for gages 41, 51, and 52 in figure 40 (d). The expansion of the leading edge would be expected to pull on the hat section containing gage 51 and exert tension similar to gage 36 on the lower surface. Apparently, however, the heated air discharging from the double skin heated the hat section considerably (note temperature distribution) and the restrained expansion induced compressive stresses which were larger than the induced tension. The expansion forces of the hat section, in turn, placed the colder skin in tension as signified by the indication of gage 41. At the location of gage 52 the stress has again reversed, the actual value at gage 52 being the result of the combined effects of several factors of unknown magnitude.

Because local conditions in some cases caused large stress differences at a given chord location (the actual deviation depending upon whether the strain gage was mounted on the skin or on a longitudinal stiffener), the stress curves presented for station 137 represent some mean values of stress for the region from 10- to 30-percent chord. Although the same local heating existed at station 47 (note temperature distribution for upper surface, figures 40 (a), 40 (b), and 40 (c)), the scatter of data was not obtained because all the gages in the local heating region were mounted on the stiffeners. The stress curve for the upper surface is, therefore, more representative of stress in the stiffeners than in the skin.

The belief that the scatter of data between 10- and 30-percent chord is largely attributable to localized heating rather than inaccurate measurements is verified by an inspection of figures 40 (g) and 40 (h). These curves show consistency of the data between the three flight conditions

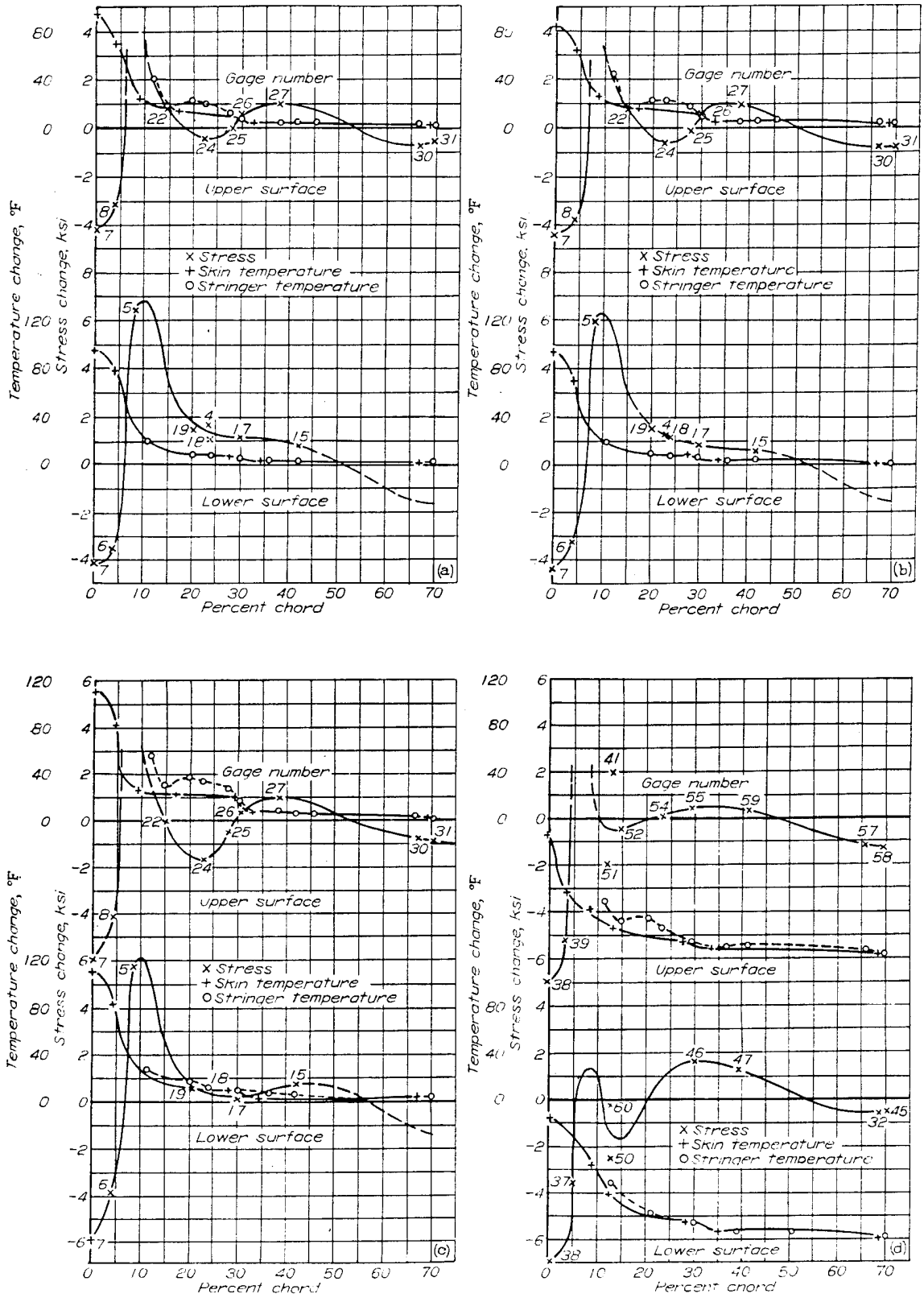

(a) Station 47, level flight, 110 mph.
(b) Station 47, level flight, 135 mph.
(c) Station 47, 2g bank, 155 to 165 mph.
(d) Station 137, level flight, 110 mph.

FIGURE 40.—Chordwise distribution of stress change in the wing resulting from operation of the thermal ice-prevention system.

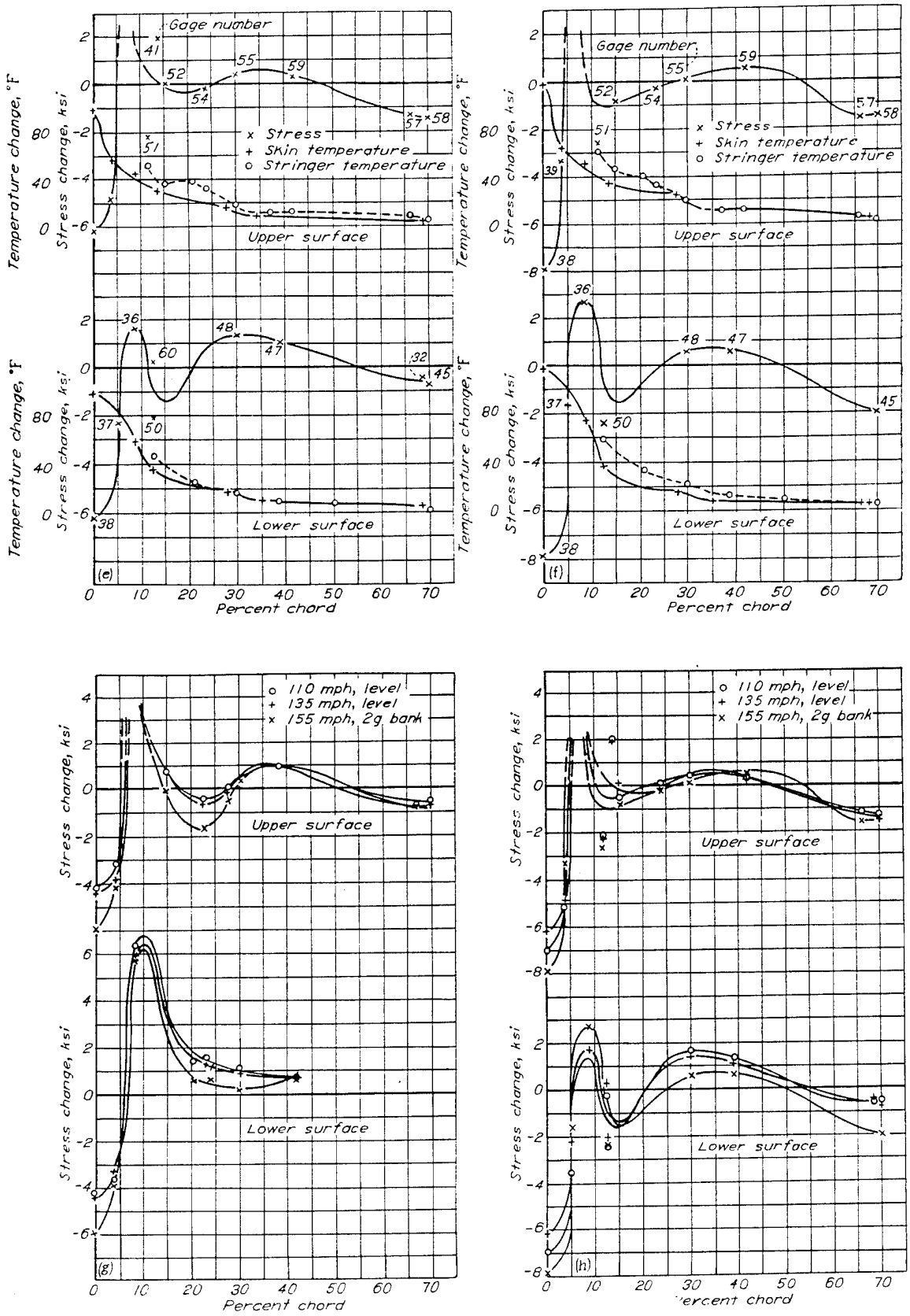

(e) Station 137, level flight, 135 mph.
(g) Comparison of three flight conditions, station 47.

(f) Station 137, 2g bank, 155 to 165 mph.
(h) Comparison of three flight conditions, station 137.

FIGURE 46.—Concluded.

for the regions where temperature gradients between the internal structure and skin were negligible. Further examples of this local heating effect between 10- and 30-percent chord could be cited; however, the purpose of this report is to determine, in general, the magnitude and importance of the stress changes rather than to present a detailed investigation of the wing of the test airplane.

In order to obtain some indication of the seriousness of the stress changes, the test data were compared with the critical values as specified in the wing outer-panel stress analysis as prepared by the airplane manufacturer. The largest changes in stress were measured at the wing leading edge, but are particularly difficult to interpret because of the lack of data on the allowable leading-edge stresses. Some test data are available which can be reasonably applied to the wing leading-edge construction, prior to revisions to incorporate the thermal system, but information on the double-skin type of construction did not appear to be available. In order to obtain some indication of the seriousness of the measured leading-edge stress changes, the stresses from the wing design analysis were combined with the thermal stresses and the final result compared with a calculated allowable value for combined loading of the unaltered leading edge. This analysis is presented in reference 14 and indicated that the thermal system did not produce a critical stress condition for the test airplane. Because of the specific nature of the problem, and also the lack of information on the treatment of combined stresses from aerodynamic loads and thermal expansion in sheet metal structures, no conclusion can be made regarding the probability of thermal stresses of serious magnitude occurring in other airplanes.

METALLURGICAL EXAMINATION OF THE WING LEADING-EDGE STRUCTURE FOR EFFECTS OF CORROSION

The possibility of corrosion is always present in aircraft structures and this possibility assumes greater importance when the corrosion resistance of the structure may have been reduced by over-heating. The probability of corrosion is increased in the case of a wing incorporating a thermal ice-prevention system with free-stream air as the heat-transfer medium because of the corrosive media which may be inducted into the wing interior. In such a system the free-stream air, containing supercooled waterdrops and possibly snow, passes through a heat exchanger located in the engine exhaust-gas stream and then circulates through the wing interior.

The passage of this hot, moist air over surfaces of Alclad 24S–T would not be expected to cause appreciable corrosion were it not for the fact that condensation may occur and that the condensation invariably contains dissolved substances. Cloud drops usually contain dissolved oxygen along with other substances common to certain regions (e. g., chlorides from sea water). The water resulting from condensation acts as an electrolyte, allowing galvanic action, which is especially difficult to combat in such a complex structure as an airplane wing. If there is any leakage of exhaust gas into the system, sulphides, bromides, and carbonates may be introduced. The acids which may result from the combination of these radicals with the condensation are corrosive to aluminum alloys.

As a result of the foregoing considerations, a metallurgical examination of the structural material in the wing leading edge of the test airplane was undertaken to determine whether the high temperatures existing had produced any evidences

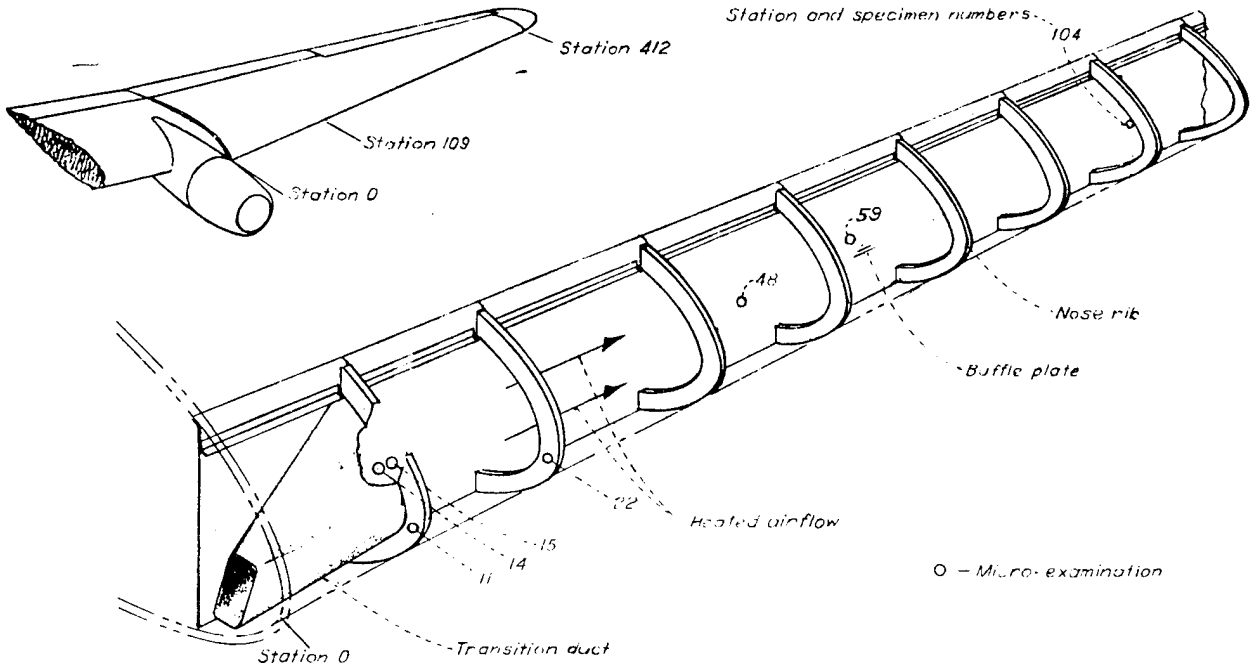

FIGURE 41.– Leading edge of the left wing outer panel showing location of specimens taken for micro-examination.

of corrosive action which could be attributed to the thermal system.

Selection of specimens.—Representative specimens were removed from the wing after about 225 hours of flight operation of the thermal system. The locations at which the specimens were removed were selected by a visual examination for pitting or any other indication of corrosive action. Samples were taken from the baffle plate at stations 14, 15, 48, 59 and 104, from the nose ribs at stations 11 and 22, and from the nose outer skin at station 11, as shown in figure 41.

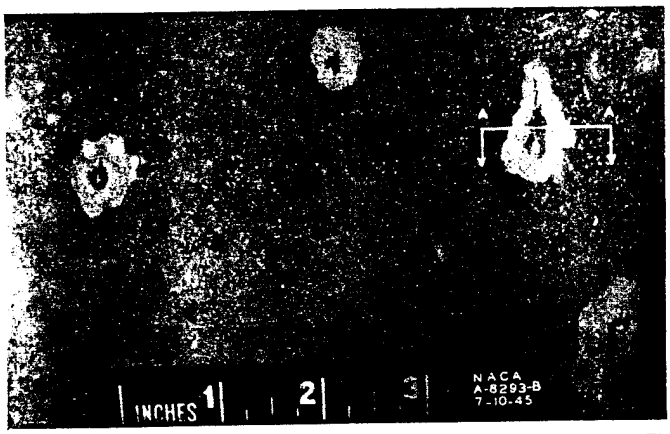

FIGURE 42.—Corrosion and soil deposit on baffle plate between stations 56 and 60. The large black spots are particles from a synthetic sponge-rubber gasket.

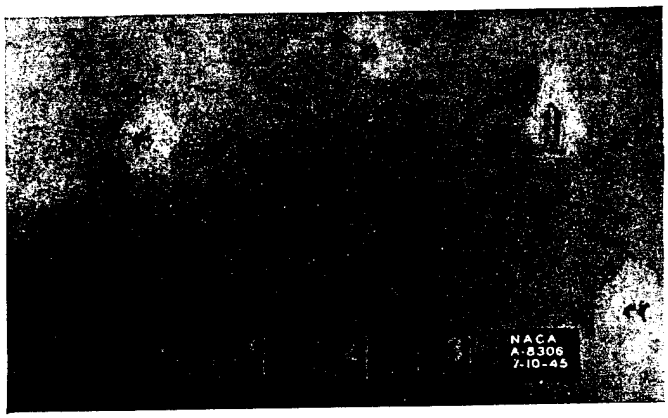

FIGURE 43.—Area of baffle plate shown in figure 42 after cleaning with acetone.

Results and discussion.—Visual examination of the baffle plate revealed a slightly dirty surface accompanied by an appearance of slight pin-point corrosion as shown in figure 42. After removal of the dirt, the positive presence of corrosion was established and is shown in figure 43. The large black lumps adhering to the sheet (fig. 42) were identified as particles from a synthetic sponge-rubber gasket which was located at the inboard end of the transition duct (station 0, fig. 41). The heat had disintegrated a portion of the gasket and the hot air had carried the particles into the ducting where they had deposited and hardened on the surface of the baffle plate. Beneath these black lumps of synthetic rubber a severe corrosion was noted. Examination of a cross section of the baffle plate, indicated by the line A–A on figure 42, revealed a marked pitting of the cladding, but a normal core (fig. 44). Microexamination of a cross section beneath another particle at station 14 showed a definite attack of the core along the grain boundaries (fig. 45). The fact that the synthetic rubber particles set up intercrystalline corrosion at station 14 and not at station 59 may be attributed to the probably higher baffle-plate temperature at station 14 and thus a greater susceptibility to intercrystalline corrosion at that station.

A further examination of the cross section of the baffle plate at station 14 revealed a decidedly aged core structure. Heavy precipitation at the grain boundaries and within the

FIGURE 44.—Cross section of baffle-plate cladding and core beneath the synthetic rubber particle at section A–A, figure 42. Magnification, 200X; Keller's etch. Pitting is severe but has not penetrated the cladding.

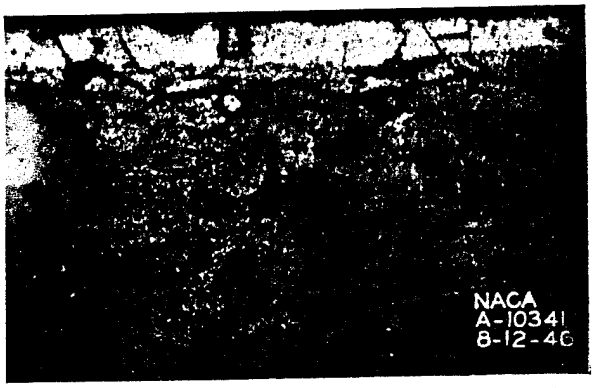

FIGURE 45.—Cross section of baffle-plate cladding and core at station 14, showing intercrystalline corrosion. Magnification, 250X; Keller's etch, and hot 25-percent solution of nitric acid.

grains was observed. Long periods of heating had instigated a coalescence of the precipitation resulting in relatively large rounded particles. Also, a considerable decrease in grain contrast was noted. Aluminum alloys exhibiting such a structure are reported in reference 23 to be quite susceptible to intercrystalline corrosion. The baffle-plate specimens at stations 48 and 104 revealed a normal 24S–T aluminum alloy core structure, indicating that the overheating of the baffle plate and attendant reduction in resistance to corrosion did not extend to station 48.

Microexamination of the section of the web of the nose rib at station 11 evidenced minute amounts of precipitation at the grain boundaries, but it is not believed that any excessive temperature effects were indicated. The microstructures of the leading-edge outer skin at station 11 and in the web of the nose rib at station 22 were comparable to that of normal 24S–T aluminum alloy.

CONCLUSIONS

As the result of a comprehensive investigation of a thermal ice-prevention system for a typical twin-engine transport airplane, the following conclusions which are applicable to systems similar to that tested may be stated:

1.) A comparison of the surface temperature rise experienced in flight (130° to 150° F above ambient-air temperature) with that specified in the design analysis (100° F) indicates that the analysis procedure for calculating the necessary heated-air flow-rates is conservative and requires further refinement.

2.) The thermal performance of the ice-prevention system permitted operation in all natural-icing conditions encountered without the loss of functional efficiency of the heated surfaces.

3.) The installation of an ice-prevention system similar in thermal performance to that tested could be effected with a negligible loss in the airplane cruise performance, provided the heat-exchanger installation was given consideration in the early stages of the nacelle design.

4.) In order to avoid unnecessary and possibly dangerous reduction in strength of the thermal ice-prevention structure while at elevated temperatures, control of the heated-air temperature to provide only that heat required for ice-prevention may be desirable in some installations. Even with such control the reduction in yield and ultimate strength of some structural members in the leading-edge region can be of the order of 5 to 10 percent.

5.) The operation of a wing leading-edge thermal ice-prevention system may (depending upon the unheated wing margins of safety) result in stress changes requiring consideration in the wing stress analysis.

6.) No corrosive effects were noted which could be attributed to the basic principle of employing free-stream air, heated by an exhaust-gas-to-air heat exchanger, as the heat transfer medium in an internal circulatory system.

AMES AERONAUTICAL LABORATORY,
NATIONAL ADVISORY COMMITTEE FOR AERONAUTICS,
MOFFETT FIELD, CALIF.

REFERENCES

1. Theodorsen, Theodore, and Clay, William C.: Ice Prevention on Aircraft by Means of Engine Exhaust Heat and a Technical Study of Heat Transmission from a Clark Y Airfoil. NACA Rep. No. 403, 1931.
2. Rodert, Lewis A.: A Preliminary Study of the Prevention of Ice on Aircraft by the Use of Engine-Exhaust Heat. NACA TN No. 712, 1939.
3. Rodert, Lewis A.: An Investigation of the Prevention of Ice on the Airplane Windshield. NACA TN No. 754, 1940.
4. Rodert, Lewis A., and Jones, Alun R.: A Flight Investigation of Exhaust-Heat De-Icing. NACA TN No. 783, 1940.
5. Rodert, Lewis A., Clousing, Lawrence A., and McAvoy, William H.: Recent Flight Research on Ice Prevention. NACA ARR, Jan. 1942.
6. Jones, Alun R., and Rodert, Lewis A.: Development of Thermal Ice-Prevention Equipment for the B-24D Airplane. NACA ACR, Feb. 1943.
7. Jones, Alun R., and Rodert, Lewis A.: Development of Thermal Ice-Prevention Equipment for the B-17F Airplane. NACA ARR No. 3H24, 1943.
8. Neel, Carr B., Jr.: An Investigation of a Thermal Ice-Prevention System for a C-46 Cargo Airplane. I—Analysis of the Thermal Design for Wings, Empennage, and Windshield. NACA ARR No. 5A03, 1945.
9. Jackson, Richard: An Investigation of a Thermal Ice-Prevention System for a C-46 Cargo Airplane. II—The Design, Construction, and Preliminary Tests of the Exhaust-Air Heat Exchanger. NACA ARR No. 5A03a, 1945.
10. Jones, Alun R., and Spies, Ray J., Jr.: An Investigation of a Thermal Ice-Prevention System for a C-46 Cargo Airplane. III—Description of Thermal Ice-Prevention Equipment for Wings, Empennage, and Windshield. NACA ARR No. 5A03b, 1945.
11. Selna, James, Neel, Carr B., Jr., and Zeiller, E. Lewis: An Investigation of a Thermal Ice-Prevention System for a C-46 Cargo Airplane. IV—Results of Flight Tests in Dry-Air and Natural-Icing Conditions. NACA ARR No. 5A03c, 1945.
12. Selna, James: An Investigation of a Thermal Ice-Prevention System for a C-46 Cargo Airplane. V—Effect of Thermal System on Airplane Cruise Performance. NACA ARR No. 5D06, 1945.
13. Selna, James, and Kees, Harold L.: An Investigation of a Thermal Ice-Prevention System for a C-46 Cargo Airplane. VI—Dry-Air Performance of Thermal System at Several Twin- and Single-Engine Operating Conditions at Various Altitudes. NACA ARR No. 5C20, 1945.
14. Jones, Alun R., and Schlaff, Bernard A.: An Investigation of a Thermal Ice-Prevention System for a C-46 Cargo Airplane. VII—Effect of the Thermal System on the Wing-Structure Stresses as Established in Flight. NACA ARR No. 5G20, 1945.
15. Corson, Blake W., Jr.: The Belt Method for Measuring Pressure Distribution. NACA RB, Feb. 1943.
16. Allen H. Julian, and Look, Bonne C.: A Method for Calculating Heat Transfer in the Laminar Flow Region of Bodies. NACA Rep. No. 764, 1943.
17. Kushnick, Jerome L.: Thermodynamic Design of Double-Panel, Air-Heated Windshields for Ice Prevention. NACA RB No. 3F24, 1943.
18. Jackson, Richard, and Hillendahl, Wesley H.: Flight Tests of Several Exhaust-Gas-to-Air Heat Exchangers. NACA ARR No. 4C14, 1944.
19. Boelter, L. M. K., Martinelli, R. C., Romie, F. E., and Morrin, E. H.: An Investigation of Aircraft Heaters. XVIII—A Design Manual for Exhaust Gas and Air Heat Exchangers. NACA ARR No. 5A06, 1945.
20. Flanigan, A. E., Tedsen, L. F., and Dorn, J. E.: Final Report on Study of the Forming Properties of Aluminum Alloy Sheet at Elevated Temperatures: Part X—Tensile Properties After Prolonged Times at Temperature. Serial W-146, NDRC Research Project NRC-548, WPB 128, Oct. 20, 1944. (Available from Dept. of Commerce as PB 15934.)
21. Flanigan, Alan E., Tedsen, Leslie F., and Dorn, John E.: Final report on Study of the Properties of Aluminum Alloy Sheet at Elevated Temperatures. Part XII—Stress Rupture and Creep Tests in Tension at Elevated Temperatures. Serial W-216, NDRC Research Project NRC-548, WPB 128, June 11, 1945. (Available from Dept. of Commerce as PB 15924.)
22. Kotanchik, Joseph N., Woods, Walter, and Zender, George W.: The Effect of Artificial Aging on the Tensile Properties of Alclad 24S-T and 24S-T Aluminum Alloy. NACA RB No. 3H23, 1943.
23. Keller, F., and Brown, R. H.: The Heat Treatment of 24S and Alclad 24S Alloy Products. Aluminum Co. of America, Aluminum Research Laboratories, Tech. Paper 9, 1943.

U. S. GOVERNMENT PRINTING OFFICE: 1945

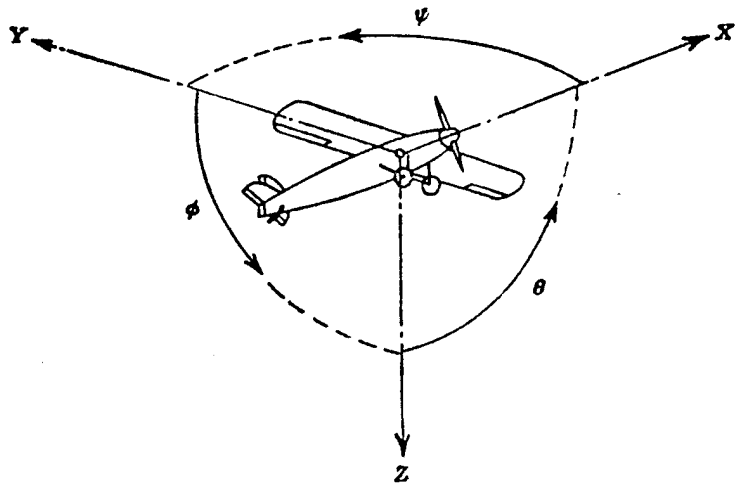

Positive directions of axes and angles (forces and moments) are shown by arrows

Axis		Force (parallel to axis) symbol	Moment about axis			Angle		Velocities	
Designation	Symbol		Designation	Symbol	Positive direction	Designation	Symbol	Linear (component along axis)	Angular
Longitudinal	X	X	Rolling	L	$Y \longrightarrow Z$	Roll	φ	u	p
Lateral	Y	Y	Pitching	M	$Z \longrightarrow X$	Pitch	θ	v	q
Normal	Z	Z	Yawing	N	$X \longrightarrow Y$	Yaw	ψ	w	r

Absolute coefficients of moment

$C_l = \frac{L}{qbS}$ (rolling) $\quad C_m = \frac{M}{qcS}$ (pitching) $\quad C_n = \frac{N}{qbS}$ (yawing)

Angle of set of control surface (relative to neutral position), δ. (Indicate surface by proper subscript.)

4. PROPELLER SYMBOLS

D Diameter

p Geometric pitch

p/D Pitch ratio

V' Inflow velocity

V_s Slipstream velocity

T Thrust, absolute coefficient $C_T = \frac{T}{\rho n^2 D^4}$

Q Torque, absolute coefficient $C_Q = \frac{Q}{\rho n^2 D^5}$

P Power, absolute coefficient $C_P = \frac{P}{\rho n^3 D^5}$

C_s Speed-power coefficient $= \sqrt[5]{\frac{\rho V^5}{P n^2}}$

η Efficiency

n Revolutions per second, rps

Φ Effective helix angle $= \tan^{-1}\left(\frac{V}{2\pi r n}\right)$

5. NUMERICAL RELATIONS

1 hp = 76.04 kg-m/s = 550 ft-lb/sec

1 metric horsepower = 0.9863 hp

1 mph = 0.4470 mps

1 mps = 2.2369 mph

1 lb = 0.4536 kg

1 kg = 2.2046 lb

1 mi = 1,609.35 m = 5,280 ft

1 m = 3.2808 ft